공학박사학위논문

Calibration of Resistance Factors for Drilled Shafts considering Lower-Bound Resistance

지지력의 하한을 고려한 현장타설말뚝의 저항계수 보정

2014년 8월

서울대학교 대학원

건설환경공학부

김 석 중

Calibration of Resistance Factors for Drilled Shafts considering Lower-Bound Resistance

지도 교수 김 명 모

이 논문을 공학박사 학위논문으로 제출함

2014 년 7 월

서울대학교 대학원

건설환경공학부

김 석 중

김석중의 공학박사 학위논문을 인준함

2014 년 6 월

위 원 장 _____ (인)

부위원장 _____ (인)

위 원 _____ (인)

위 원 _____ (인)

위 원 _____ (인)

Abstract

Calibration of Resistance Factors for Drilled Shafts considering Lower-Bound Resistance

Kim, Seok Jung

Department of Civil & Environmental Engineering

The Graduate School

Seoul National University

Recently, the Load Resistance Factor Design (LRFD) has been substituted for the Allowable Stress Design (ASD) or Working Stress Design (WSD) for the design of foundations around the world. This was introduced into Korea about a decade ago. However, the resistance factors suggested by AASHTO (2007, 2010) represent the characteristics of bedrocks defined in the US, which may differ from the bedrocks in Korea. Therefore, it is necessary to determine the accurate resistance factors for drilled shafts based on reliable load test results, considering the discrepancy of rocks between the US and Korea. Also, there is a general belief that the calculated probabilities of failure from conventional reliability analyses are not realistic, because of the conservative bias used when predicting the resistance and tails of probability distributions for load and resistance. The existence of a lower bound of resistance affects the reliability and resistance factors, even though

the lower bound of the resistance is small. Therefore, it is necessary to calibrate the resistance factors considering the lower-bound resistance.

In this thesis, the accurate resistance factor for drilled shafts was determined based on thirteen sets of drilled shaft load test data with strain gauges. With the mixed log-normal distribution of resistance, reliability analysis for the determination of reliability index and resistance factor was performed using the AFOSM (Advanced First Order Second Moment method). The target reliability indices were determined as 2.5, 3.0, and 3.5. For the target reliability index of 3.0 (the AASHTO recommended value), the resistance factors were determined in the range of 0.13-0.32 for shaft resistance, 0.19-0.29 for base resistance, and 0.28-0.42 for the total resistance.

Also, the lower bounds of resistance for each resistance (shaft, base and total) and different bearing capacity equation were determined based on the Hoek-Brown failure criteria (2002) and GSI downgrading. Considering the lower bound of resistance, resistance factors were increased by about 0~8% for the shaft resistance factor, 0~13% for the base resistance factor, and 0~2% for the total resistance factor.

Keywords : Load Resistance Factor Design (LRFD), Drilled Shaft, Load Transfer Analysis, Resistance Factor, Lower-bound Resistance,

Student Number : 2008-22974

TABLE OF CONTENTS

LIST OF TABLES

LIST OF FIGURES

1. Introduction

1.1 Background

Recently, the Load Resistance Factor Design (LRFD) has been substituted for the Allowable Stress Design (ASD) or Working Stress Design (WSD), for the design of foundations around the world. The Load Resistance Factor Design (LRFD) method was introduced into Korea about a decade ago. The LRFD method considers the uncertainty of the resistance, based on reliability analysis. Therefore, the probability of failure can be quantitatively estimated. Consequently, consistent and reliable designs of geotechnical structures are possible. However, to ensure coherent reliability, representative resistance and load factors should be estimated. AASHTO (2007, 2010) suggested resistance factors for the design of a drilled shaft socketed in bedrock as 0.50~0.55 for the shaft resistance, and 0.50 for the base resistance.

However, the resistance factors suggested by AASHTO (2010) should represent the characteristics of bedrocks defined in the US, which may differ from the bedrocks in Korea. The resistance factors suggested by AASHTO (2010) are determined only for the intact rock condition. In contrast, in the case of bedrocks in Korea, the representative rock types are granite and gneiss; and these rocks are classified by the strength criteria as moderate or hard rock. However, there are many discontinuities and much weathering, so rocks are

classified by the weathering degree criteria as weathered rock or soft rock. Therefore, there are discrepancies in the rock conditions between the US and Korea, and the direct application of the AASHTO resistance factors for domestic design is not appropriate.

Many previous researches have been conducted for the resistance factors in Korea. In 2008, the Korea Institute of Construction Technology (2008) suggested the total resistance factors for driven steel pipe piles and drilled shafts; and Jung (2010) suggested the total, shaft, and base resistance factors for drilled shafts, using numerical analysis. Also, Park (2011) updated the total resistance factors for driven steel pipe piles, based on Bayesian theory, to incorporate the results of proof tests. However, most previous researches are limited to the suggestion of total resistance factors. Also, the shaft and base resistance factors by Jung (2010) are doubtful, due to the fact that the resistance factors are results based on numerical analysis. Therefore, it is necessary to determine accurate resistance factors for drilled shafts based on reliable load test results, considering the discrepancies of rocks between the US and Korea.

Also, there is a general belief that the calculated probabilities of failure from conventional reliability analysis are not realistic, because of the conservative bias used when predicting resistance and tails of probability distributions for the load and resistance. A general log-normal distribution of resistance, with a lower tail that extends to zero, does not capture the realistic possibility. There is a physical limit to the smallest possible capacity for a pile foundation. This limit is greater than zero, and is defined as the lower bound

for the resistance.

Previous researches by Najjar (2005) investigated the possibility of a lower bound capacity for driven steel pipe piles in cohesive and cohesionless soils, and indicated strong evidence for the existence of a lower bound capacity. In geotechnical engineering applications, the left-hand tail of the resistance distribution governs the probability of failure. As a result, the existence of a lower bound of resistance affects the reliability and resistance factors, even though the lower bound of the resistance is small. Therefore, it is necessary to calibrate the resistance factors considering the lower bound resistance.

1.2 Objectives

The main objectives of this thesis are to:

(i) Determine accurate resistance factors for drilled shafts, based on load test results in Korea; and,

(ii) Calibrate the determined resistance factors, considering the lower bound of resistance.

Most previous researches in Korea are limited to the suggestion of total resistance factors. This is because the selected load test data were not able for load transfer analysis. Therefore, it was not possible to determine the shaft and base resistance of each test pile. Also, the shaft and base resistance factors

by Jung (2010) are doubtful, due to the fact that the resistance factors are results based on numerical analysis.

For this thesis, 13 sets of drilled shaft load test data with strain gauges were collected, and load transfer analysis was performed to determine accurate shaft and base resistances. In the cases of bi-directional load tests, the equivalent load-displacement curves were drawn, to determine the total resistance. Also, calibration of the elastic modulus of concrete drilled shafts and equivalent load-displacement curves considering the axial load and elastic settlement were conducted, for more accurate resistances.

After the determination of accurate resistances, reliability analysis was performed for the determination of target reliability index and resistance factors, using the AFOSM.

The lower bound of resistance for each resistance (shaft, base and total) and different bearing capacity equation were determined. For the determination of the lower bound of resistance, the Hoek-Brown failure criteria (1988, 2002) and GSI downgrading were adopted, to calculate the unconfined compressive strength of rock masses. Calculated unconfined compressive strengths of rock masses were applied to each bearing capacity equation, and the lower bounds of resistance were determined as the ratio of predicted resistance by bearing capacity equations.

Considering the lower bound of resistance, resistance factors were calibrated, to overcome the conservative bias of conventional reliability analysis. From the calibrated resistance factors for each bearing capacity equations, the influence of the lower bound of resistance could be discussed.

1.3 Dissertation Organization

This dissertation focuses on the calibration of resistance factors for drilled shafts considering the lower-bound of resistance, and consists of six chapters.

Chapter 1. Introduction

Chapter 1 includes the background, research objectives, and organization of the dissertation.

Chapter 2. Literature Review

Chapter 2 presents previous studies on resistance factors in Korea, and reviews the limitations of previous research. Also, this chapter introduces the concept of the lower bound of resistance, and the application of lower bound information on the calibration of resistance factors.

Chapter 3. Evaluation of Resistance for Drilled Shaft

Chapter 3 evaluates the resistance for drilled shafts. Data from drilled shaft load test conducted in Korea were collected, and it was possible to conduct load transfer analyses for shaft and base resistances, because strain gauges were installed in the test piles. For more accurate resistance, the elastic modulus of drilled shafts and equivalent load-displacement curves were calibrated. Measured resistances were determined based on load tests, and

predicted resistances were calculated, using the bearing capacity equations suggested by many researchers.

Chapter 4. Determination of Resistance Factor

Chapter 4 determines the target reliability index and resistance factors for each resistance (shaft, base, and total), and different bearing capacity equation. The reliability analysis method was selected as the AFOSM. Determined resistance factors are presented, and compared with AASHTO (2007, 2010) suggested values.

Chapter 5. Calibration of Resistance Factor considering Lower-Bound Resistance

Chapter 5 includes the determination of the lower bound of resistance for each resistance and bearing capacity equation. Based on the Hoek-Brown failure criteria (1988, 2002) and GSI downgrading, the unconfined compressive strengths of rock mass were determined, and applied to calculate the lower bound of resistance. Resistance factors were calibrated considering the lower bound of resistance. The influence of the lower bound of resistance is discussed.

Chapter 6. Summary and Conclusions

Chapter 6 summarizes the results of this study, and presents the conclusions.

2. Literature Review

2.1 Load and Resistance Factor Design (LRFD)

2.1.1 Introduction

The design of pile foundation depends upon the applied load and the resisting capacity of pile. Both loads and resistance have various sources of uncertainties. These uncertainties can be quantified using reliability based design (RBD). RBD is a design concept that purposes at maintaining the probability of reaching limit states lower than some limiting values. Therefore, a direct measurement of risk is possible with RBD. LRFD is design methodology that is similar to existing allowable strength design (ASD), but has been developed using reliability based design concepts. LRFD enables identification and separation of different uncertainties in loading and resistance and recommends appropriate partial factor or reliability indices to ensure the margin of safety based on probability theory. Therefore, it is more rational to apply factors which are developed by reliability analysis to both resistance and loads than using the factor of safety which is determined arbitrarily. The LRFD criterion can be expressed as:

$$\phi R_n \geq \sum \gamma_i Q_i \tag{2.1}$$

Where, γ_i : load factor, Q_i : load, ϕ : resistance factor, and R_n : nominal resistance.

The load factors are usually greater than one and account for uncertainties in loads. The resistance factors are less than one and account for variabilities in geotechnical parameters and model the associated uncertainties when calculating geotechnical resistances.

The advantages of the LRFD method are as follows:

i. It accounts for variability in both resistance and load.

ii. It achieves relatively uniform levels of safety based on the strength of soil and rock for different limit states and foundation types.

iii. It provides more consistent levels of safety in the superstructure and substructure as both are designed using the same loads for predicted or target probabilities of failure.

The disadvantages and limitations of the LRFD method are as follows:

i. The most rigorous method for developing and adjusting resistance factors to meet individual situations requires availability of statistical data and probabilistic design algorithms.

ii. Resistance factors vary with design methods and are not constant.

iii. Implementation requires a change in design procedures for engineers accustomed to ASD.

2.1.2 Calibration method for reliability analysis

The reliability theory provides a valuable tool to compute the level of probability of failure in the existing or new design codes. Three level of sophistication exist in the calibration by the reliability theory (Withiam et al., 1998). The ***Level Ⅰ*** method is referred to as the First-Order Second Moment (FOSM) method, which uses simple statistical characteristics of the load and resistance variables to describe the probability distributions. It is assumed that the load and the resistance are statistically independent random variables.

The ***Level Ⅱ*** method is referred to as the Advanced First-Order Second Moment (AFOSM). When the AFOSM method is used, the limit state function is linearized at the design point on the nonlinear failure surface rather than at the mean value of the random variables. For the AFOSM method, an iterative procedure is needed in the process of finding the value of reliability index. The process is repeated until the difference in the calculated value of the reliability index on successive iteration is within an acceptable level. This iterative procedure was first developed by Rackwitz and Fiessler (1978) and was based on normal approximations to the nonnormal distributions at the design point. The resistance factors used in the AASHTO LRFD (2007) for drilled shafts were developed using the nonlinear AFOSM method. Therefore,

the ***Level I, Ⅱ*** method, mainly due to its convenience and simplicity, forms the basis of most design codes that utilize or are based on probabilistic methods. The ***Level Ⅲ*** is the most complex and requires knowledge of the probability distributions of load and resistances and the correlations between the variables. Because of its complexity, ***Level Ⅲ*** may not be used in calibrating the AASHTO LRFD Specification (2007). In this study, reliability analysis was performed by the MVFOSM and AFOSM method.

2.1.3 Load and resistance factor design method in several countries

■ **Canada**

The province of Ontario in Canada adopted for bridge design in the 1st and 2nd editions of the Ontario Highway Bridge Design Code (OHBCD). This code was developed based on reliability index of 3.5 for superstructure elements. But the foundation elements generally became larger and the design became more conservative. In the 3rd edition of the OHBDC (MOT, 1992), an overall factored resistance approach was used and yielded more reasonable results but was still more conservative than the previous ASD method. In recent years, the specified geotechnical resistance factors in National Building Code of Canada (NBCC) (NRC, 2010) and Canadian Highway Bridge Design Code (CHBDC) (CSA, 2006) were adopted in design of foundations and resistance factors in each design code were summarized in Table 2.1 to Table

2.3, respectively:

Table 2.1 Resistance factors for deep foundations in OHBDC (MOT, 1992)

Description	Resistance factors
Static analysis, compression	0.4
Static analysis, tension	0.3
Static test, compression	0.6
Static test, tension	0.4
Dynamic analysis, compression	0.4
Dynamic analysis, compression field measurements and analysis	0.5

Table 2.2 Resistance factors for shallow and deep foundations in NBCC (NRC, 2010)

Description	**Resistance factor**
1.Shallow foundation	
(a) Vertical bearing resistance from semi-empirical analysis using laboratory and in-situ test data	0.5
(b) Sliding	
(ⅰ) based on friction (c=0)	0.8
(ⅱ) based on cohesion/adhesion (tanφ=0)	0.6
2. Deep foundation	
(a) Resistance to axial load	
(ⅰ) semi-empirical analysis using laboratory and in-situ test data	0.4
(ⅱ) analysis using static loading test results	0.6
(ⅲ) analysis using dynamic monitoring results	0.5
(ⅳ) uplift resistance by semi-empirical analysis	0.3
(ⅴ) uplift resistance using loading test results	0.4
(b) Horizontal load resistance	0.5

Table 2.3 Geotechnical resistance factors in CHBDE (CSA, 2006)

Application	Resistance factor
Shallow foundations	
Bearing resistance	0.5
Passive resistance	0.5
Horizontal resistance (sliding)	0.8
Ground anchors (soil or rock)	
Static analysis-tension	0.4
Static test-tension	0.6
Deep foundations-piles	
Static analysis	
Compression	0.4
Tension	0.3
Static test	
Compression	0.6
Tension	0.4
Dynamic analysis-compression	0.4
Dynamic test-compression (field measurement and analysis)	0.5
Horizontal passive resistance	0.5

- **Australia**

AUSTROADS (1992) in Australia suggested the resistance factors for deep foundation, and the resistance factors according to method of assessment of ultimate geotechnical strength were suggested in Australian Standard 2159 (1995). These resistance factors in Australia were known to larger values than different codes, especially for static load test. The resistance factors in Australia codes were summarized in Table 2.4 and Table 2.5.

Table 2.4 Resistance factors for deep foundations in AUSTROADS (1992)

Type	**Resistance factor**
Load tested to failure	0.9
Routine proof load tested	0.8
Piles analyzed by dynamic formulae or wave equation methods based on assumed driving system energy and soil parameters	0.4-0.5
Piles subjected to closed-form dynamic solutions, e.g., Case method	0.5
Piles subjected to closed-form dynamic solutions correlated against static load test or dynamic load tests using measured field parameters in a wave equation analysis (e.g., CAPWAP)	0.6
Piles subjected to dynamic load tests using measured field parameters in a wave equation (e.g., CAPWAP)	0.8

Table 2.5 range of resistance factor for deep foundations in AS-2159 (1995)

Method of Assessment of Ultimate Geotechnical Strength	**Resistance factor**
Static load testing to failure	0.70-0.90
Static proof (not to failure) load testing[1]	0.70-0.90
Dynamic load testing to failure supported by signal matching[2]	0.65-0.85
Dynamic load testing to failure not supported by signal matching	0.50-0.70
Dynamic proof (not to failure) load testing supported by signal matching	0.65-0.85
Dynamic proof (not to failure) load testing not supported by signal matching	0.50-0.70
Static analysis using CPT data	0.45-0.65
Static analysis using SPT data in cohesionless soils	0.40-0.55
Static analysis using laboratory data for cohesive soils	0.45-0.55
Dynamic analysis using wave equation method	0.45-0.55
Dynamic analysis using driving formulae for piles in rock	0.50-0.65
Dynamic analysis using driving formulae for piles in sand	0.45-0.55
Measurement during installation of proprietary displacement piles, using well established in-house formulae	0.50-0.65

- **North America(USA)**

The resistance factors for foundations in the AASHTO LRFD Bridge Code (AASHTO 1997) were derived from NCHRP Report 343 (Barker et al. 1991). The research utilized the rational probabilistic approach towards model variability and the inherent spatial variability of soil properties. However, it did not account for site variability. In 1998, a National Highway Institute (NHI, Withiam et al., 1998) Training Course published by Federal Highway Administration (FHWA). In 2004, the Transportation Research Board (TRB) published NCHRP Report 507 "Load and Resistance Factor Design for Deep Foundations". This report proposed new sets of resistance factors which was developed by nationwide database of the static and dynamic load tests and more comprehensive and reliable. This research was used to calibrate the resistance factors for AASHTO LRFD specifications (2004). In recently, AASHTO LRFD specification (2010) was published. And the specified geotechnical resistance factors of drilled shafts in AASHTO LRFD specification (2010) are summarized in Table 2.6 and Table 2.7

Table 2.6 Resistance factors for geotechnical resistance of drilled shafts (AASHTO, 2010)

Method/Soil/Condition			Resistance Factor
Nominal Axial Compressive Resistance of Single-Drilled Shafts, φ	Side resistance in clay	α-method (O'Neill and Reese, 1999)	0.45
	Tip resistance in clay	Total Stress (O'Neill and Reese, 1999)	0.40
	Side resistance in sand	β-method (O'Neill and Reese, 1999)	0.55
	Tip resistance in sand	O'Neill and Reese (1999)	0.50
	Side resistance in IGMs	O'Neill and Reese (1999)	0.60
	Tip resistance in IGMs	O'Neill and Reese (1999)	0.55
	Side resistance in rock	Horvath and Kenney (1979) O'Neill and Reese (1999)	0.55
	Side resistance in rock	Carter and Kulhawy (1988)	0.50
	Tip resistance in rock	Canadian Geotechnical Society (1985) Pressure Method (Canadian Geotechnical Society, 1985) O'Neill and Reese (1999)	0.50
Block Failure, φ	Clay		0.55
Uplift Resistance of Single-Drilled Shafts, φ	Clay	α-method (O'Neill and Reese, 1999)	0.35
	Sand	β-method (O'Neill and Reese, 1999)	0.45
	Rock	Horvath and Kenney (1979) Carter and Kulhawy (1988)	0.40
Group Uplift Resistance, φ	Sand and clay		0.45
Horizontal Geotechnical Resistance of Single Shaft or Shaft Group	All materials		1.0
Static Load Test (Compression), φ	All Materials		Values in Table 2.7, but no greater than 0.70
Static Load Test (Uplift), φ	All Materials		0.60

Table 2.7 Relationship between number of static load tests conducted pier site and resistance factor (AASHTO, 2010)

Number of Static Load Tests per Site	Resistance Factor, φ		
	Site Variability		
	Low	Medium	High
1	0.80	0.70	0.55
2	0.90	0.75	0.65
3	0.90	0.85	0.75
≥4	0.90	0.90	0.80

2.1.4 Load and resistance factor design method in Korea

LRFD is based on the concept of reliability, and the uncertainties related to the design parameters are quantified in a rational framework of reliability theory. In addition, consistent level of safety of structures can be assured in LRFD through evaluation reliability or probability of failure using consistent standards. The rational determination of load and resistance factors considering uncertainties must precede to develop the LRFD codes for foundation structures. Especially, it is essential to estimate the resistance factors which incorporate local experience and practice since the resistance factors are unique for local geology, design and construction practice, and local experiences.

The resistance factors suggested by AASHTO (2010) should represent the characteristics of bedrocks defined in the US that may differ from the bedrocks in Korea. The resistance factors suggested by AASHTO (2010) are determined for only intact rock condition. Table 2.8 shows the example of site investigation details in Carter & Kulhawy(1988). Almost rock types are sedimentary rock like shale, sandstone, and mudstone. Contrarily, in the case of bedrocks in Korea, representative rock types are granite and gneiss according to Korea geologic map in Korea structure and foundation structure design specification (KSFDS, 2003). Korea geologic map are shown in Figure 2.1. Rock characteristic are different according to rock type. Typical range of unconfined compressive strength (UCS) and elastic modulus of representative

rocks were summarized in Table 2.9 and Table 2.10.

Also, resistance factors suggested by AASHTO (201) are determined for only intact rock condition based on RMR classification shown in Table 2.11. However, rock classification in Korea was based on strength criteria and weathering degree criteria shown in Table 2.12 and Table 2.13. Representative rock types in Korea are granite and gneiss, and these rocks are classified as moderate or hard rock by the strength criteria. However, there are many discontinuities and weathering, so rocks are classified as weathered rock or soft rock by the weathering degree criteria. Therefore, there are discrepancies in rock conditions between the US and Korea, and the direct application of the AASHTO resistance factors for domestic design is not appropriate. Therefore, some researches for resistance factors in Korea were performed.

Table 2.8 Details of axial load tests in Carter & Kulhawy (1988)

Test[a] I.D.	Reference	Rock Type	q_u[b] (MN/m^2)	D (m)	B (m)	S_1 (MN/m)	S_2 (MN/m)	S_3 (MN/m)	ν_r[c] and ν_b	E_r (MN/m^2)
Shear Sockets - Compression Loading										
P1	1	Shale	6.75	1.37	0.71	661	61	-	0.22	378
P3	1	Shale	6.75	1.37	0.71	447	244	-	0.22	256
Bay St.	2	Shale	41.0	0.686	0.838	649	250	-	0.22	426
S3	3	Mudstone	0.33	2.31	1.17	1613	294	-	0.26	535
S5	3	Mudstone	0.59	2.59	1.12	1478	221	-	0.26	491
A2	4	Sandstone	6.0	0.92	0.21	121	8	-	0.25	146
A3	4	Sandstone	6.0	0.40	0.316	119	14	-	0.25	184
Voided Toe	5	Chalk	0.8	8.59	1.146	730	130	-	0.25	113
A3	8	Siltstone	0.3	8.90	0.45	500	23	-	0.25	96
Complete Sockets - Compression Loading										
P2	1	Shale	6.75	1.37	0.71	630	229	172	0.22	360
P4	1	Shale	6.75	1.37	0.71	880	563	194	0.22	392
M3	3	Mudstone	2.0	1.80	0.66	1250	60	60	0.26	613
Solid Toe	5	Chalk	0.8	8.50	1.146	825	236	-	0.25	128#
A1	8	Siltstone	0.3	8.95	0.45	1000	20	-	0.25	176#
Shear Sockets - Uplift Loading										
1A	6	Sandstone	2.5	1.08	0.472	1500	92	-	0.25	1188
1B	6	Sandstone	2.5	1.75	0.45	341	76	-	0.25	208
1C	6	Sandstone	2.5	2.77	0.45	1000	167	-	0.25	451
2B	6	Sandstone	2.5	0.90	0.45	125	8	-	0.25	111
2C	6	Sandstone	2.5	1.30	0.536	208	36	-	0.25	141
2F	6	Sandstone	2.5	1.67	0.464	385	65	-	0.25	239
3B	6	Sandstone	18.0	0.80	0.45	1333	478	-	0.25	1258
3C	6	Sandstone	18.0	1.60	0.45	2400	469	-	0.25	1551
2A-2	7	Limestone	-	1.20	0.60	712	17	-	0.25	468
2A-3	7	Limestone	-	1.32	0.60	356	140	-	0.25	226
A4	8	Siltstone	0.2	3.95	0.45	425	19	-	0.25	150

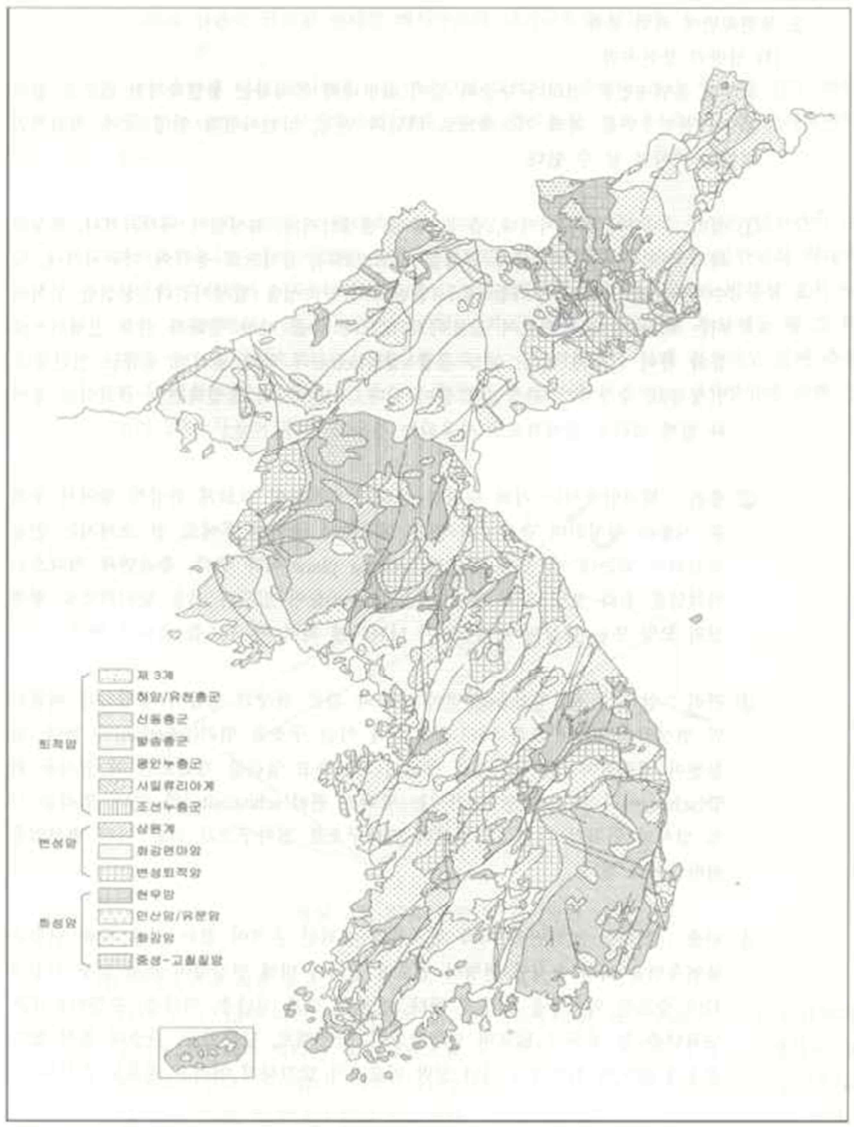

Figure 2.1 Korea geologic map in Foundation structure design specification (KSFDS, 2003)

Table 2.9 Typical range of uniaxial compressive strength as a function of rock category and rock type (Hoek, 1983)

Rock category	General description	Rock type	Uniaxial compressive strength, σ_c (MPa)
A	Carbonate rocks with well-developed crystal cleavage	Dolostone	33.6 - 315
		Limestone	24.5 - 294
		Marble	38.5 - 245
B	Lithified argillaceous rock	Argillite	29.4 - 147
		Claystone	1.4 - 8.4
		Marlstone	53.2 - 196
		Phyllite	24.5 - 245
		Siltstone	9.8 - 119
		Shale	7 - 35.7
		Slate	147 - 210
C	Arenaceous rocks with strong crystals and poor cleavage	Conglomerate	33.6 - 224
		Sandstone	67.9 -175
		Quartzite	63 -385
D	Fine-grained igneous crystalline rock	Andesite	98 -182
		Diabase	21.7 -581
E	Corse-grained igneous and metamorphic crystalline rock	Amphibolite	119 -280
		Gabbro	126 -315
		Gneiss	245 -315
		Granite	147 -343
		Quartzdiorite	9.8 -98
		Schist	9.8 -147
		Syenite	182 -434

Table 2.10 Summary of elastic moduli for intact rock (AASHTO, 2010)

Rock Type	Elastic Modulus, E_i ($MPa \times 10^3$)			Standard Deviation ($MPa \times 10^3$)
	Max.	Min.	Mean	
Granite	100.0	6.410	52.70	24.48
Diorite	112.0	17.100	51.40	42.68
Gabbro	84.1	67.600	75.80	6.69
Diabase	104.0	69.000	88.30	12.27
Basalt	84.1	29.000	56.10	17.93
Quartzite	88.3	36.500	66.10	16.00
Marble	73.8	4.000	42.60	17.17
Gneiss	82.1	28.500	61.10	15.93
Slate	26.1	2.410	9.58	6.62
Schist	69.0	5.930	34.30	21.93
Phyllite	17.3	8.620	11.80	3.93
Sandstone	39.2	0.620	14.70	8.20
Siltstone	32.8	2.620	16.50	11.38
Shale	38.6	0.007	9.79	10.00
Limestone	89.6	4.480	39.30	25.72
Dolostone	78.6	5.720	29.10	23.72

Table 2.11 Rock mass rating (RMR) (AASHTO, 2010)

(a) Geomechanics classification or rock masses

Parameter			Ranges of values						
1	Strength of intact rock material	Point load index (MPa)	> 8	4-8	2-4	1-2	For this low range, uniaxial compressive test is preferred		
		Uniaxial compressive strength (MPa)	> 200	100-200	50-100	25-50	10-25	3.5-10	1.0-3.5
	Relative rating		15	12	7	4	2	1	0
2	Drill core quality, RQD(%)		90-100	75-90	50-75	25-50	< 25		
	Relative rating		20	17	13	8	3		
3	Spacing of joints(mm)		> 3,000	900-3,000	300-900	50-300	< 50		
	Relative rating		30	25	20	10	5		
4	Condition of joints		Very rough surfaces, Not continuous, No separation, Hard joint wall rock	Slightly rough surfaces, Separation <1.25mm, Hard Joint wall rock	Slightly rough surfaces, Separation <1.25mm, Soft Joint wall rock	Slicken-sided surfaces or Gouge <5mm thick or, Joints open 1.25-5mm, Continuous joints	Soft gouge > 5mm thick or, Joints open >5mm, Continuous joints		
	Relative rating		25	20	12	6	0		
5	Ground water	Inflow per 10m tunnel length	None	< 25L/min		25-125 L/min	> 125 L/min		
		Ratio = joint water pressure/ major principal stress	0	0.0-0.2		0.2-0.5	> 0.5		
		General conditions	Completely dry	Moist only (interstitial water)		Water under moderate pressure	Severe water problems		
	Relative rating		10	7		4	0		

(b) Geomechanics rating adjustment for joint orientations

Strike and dip orientations of joints		Very favorable	Favorable	Fair	Unfavorable	Very unfavorable
Ratings	Tunnels	0	-2	-5	-10	-12
	Foundations	0	-2	-7	-15	-25
	Slopes	0	-2	-25	-50	-60

(c) Geomechanics rock mass classes determined from total ratings

RMR rating	100 - 81	80 - 61	60 - 41	40 - 21	< 20
Class no.	Ⅰ	Ⅱ	Ⅲ	Ⅳ	Ⅴ
Description	Very good rock	Good rock	Fair rock	Poor rock	Very poor rock

Table 2.12 Rock classification with unconfined compressive strength (KSFDS, 2003)

Grade	Classification	Unconfined compressive strength(MPa)
A	Extremely hard rock (Very high strength)	≥ 225
B	Hard rock (high strength)	112.5 ~ 225
C	Moderate rock (medium strength)	56 ~ 112.5
D	Soft rock (low strength)	28 ~ 56
E	Extremely soft rock (very low strength)	≤ 28

Table 2.13 Weathering and alteration grades (KSFDS, 2003)

Grade	Term	Description
Ⅰ	Fresh	No visible sign of rock material weathering; perhaps slight discoloration on major discontinuity surface.
Ⅱ	Slightly weathered	Discoloration indicates weathering of rock material and discontinuity surface. All the rock material may be discolored by weathering and may be somewhat weaker externally than in its fresh condition.
Ⅲ	Moderately weathered	Less than half of the rock material is decomposed and/or disintegrated to a soil Fresh or discolored rock is present either as a discontinuous framework or as core stones.
Ⅳ	Highly weathered	More than half of the rock material is decomposed and/or disintegrated to a soil. Fresh or discolored rock is present either as a discontinuous framework or as core stones.
Ⅴ	Completely weathered	All rock material is decomposed and/or disintegrated to soil. The original mass structure is still largely intact
Ⅵ	Residual soil	All rock material is converted to soil. The mass structure and material fabric are destroyed. There is a large change in volume, but the soil has not been significantly transported.

■ **Determination of Resistance Factors for Foundation Structure Design by LRFD (KICT, 2008)**

In 2008, Korea Institute of Construction Technology (KICT) performed the research for resistance factor in Korea. To suggest the resistance factors, database for field surveys, laboratory tests, and static load tests were established. And then, resistance factors for three types of foundation (driven steel pipe piles, drilled shafts, and shallow foundations) were recommended. In this study, resistance factors for total resistance of each foundation types were determined and recommended resistance factors for drilled shafts were summarized in Table 2.14. Target reliability index was 3.0 for redundant piles and 3.5 for nonredundant piles.

Table 2.14 Total resistance factors for drilled shafts in Korea (KICT, 2008)

Method / Target Reliability index	Carter and Kulhawy	AASHTO	FHWA
3.0	0.70	0.51	0.20
3.5	0.54	0.39	0.16

■ **Calibration of Resistance Factors of LRFD for Drilled Shafts Embedded in Weathered Rock (Jung, 2010)**

In this study, the focus is on the calibration of the resistance factors of drilled shafts that are embedded in weathered rock. If a load test which has

rock properties was not carried to failure, this study used a method of extrapolation for the ultimate load. In addition, numerical analysis was conducted to separate the side and end bearing resistances. Consequently, the resistance factors (total, side, and end bearing resistances and the static pile-load test) were calibrated. The recommended resistance factors of the bearing capacity equations and the static pile load test for drilled shafts were summarized in Table 2.15 to Table 2.17

Table 2.15 Recommended resistance factors for drilled shafts (Jung, 2010)

Resistance	**Design method**	**Resistance factor (ϕ)**	
		$\beta_T = 3.0$	$\beta_T = 3.5$
Total resistance	Carter & Kulhawy (1988)	0.80	0.65
	SSHB (2008)	0.55	0.45
Side resistance	CFEM (1992)	0.20	0.15
	Horvath & Kenny (1976)	0.20	0.15
End bearing resistance	Carter & Kulhawy (1988)	0.70	0.60
	Zhang & Einstein (1998)	0.20	0.15
Total resistance (RQD=0)	SSHB (2008)	0.85	0.65
Static load test		Values in Table 2.16	Values in Table 2.17

Table 2.16 Recommended resistance factors of static pile load test for $\beta_T = 3.0$ (Jung, 2010)

φ (Resistance factor)			
No. of Load Tests Per Site	Site Variability		
	Low	Medium	High
1	0.65	0.55	0.40
2	0.80	0.65	0.55
3	0.85	0.75	0.65
≥4	0.90	0.80	0.70

Table 2.17 Recommended resistance factors of static pile load test for $\beta_T = 3.5$ (Jung, 2010)

φ (Resistance factor)			
No. of Load Tests Per Site	Site Variability		
	Low	Medium	High
1	0.60	0.45	0.35
2	0.70	0.60	0.50
3	0.80	0.65	0.55
≥4	0.80	0.70	0.60

■ **Resistance Factor Calibration and Bayesian Implementation for LRFD of Axially-Loaded Driven Steel Pipe Piles (Park, 2011)**

Park (2011) suggested the resistance factors for static bearing capacity of axially-loaded driven steel pipe piles. In addition to suggestion of resistance factors, the framework was modified based on the Bayesian theory so that the resistance factors could be updated reflecting the results of proof pile load tests. The Bayesian theory was implemented to update resistance factors based on the updated distributions of resistance using the results of proof pile load tests which were conducted to failure or not. The distribution of resistance was constructed based on the results of pile load tests conducted to failure by reflecting additional proof pile load test results. The updated resistance factors were fell into the range of 0.27-0.96 and 0.19-0.71 for target reliability index of 2.33 and 3.0, respectively.

2.2 Incorporation of Lower-Bound Resistance into LRFD

2.2.1 Introduction

There is generally a physical limit to the smallest possible capacity for a deep foundation. However, a lower bound on the capacity has rarely been accounted for in performing reliability analyses and developing reliability-based design codes.

In all of the reliability analyses for deep foundations, the foundation capacity is modeled using a lognormal distribution and the coefficient of variation (COV) for the capacity is relatively large, ranging from 0.3 to 1.0. A lognormal distribution, with a lower tail that extends to zero, does not capture the realistic possibility that there is a physical minimum or lower bound for the foundation capacity. Even highly disturbed soil generally has finite shear strength, and there is a physical limit to the smallest possible capacity which is greater than zero for a pile foundation.

The existence of a lower-bound capacity could help to explain why observed failure rates for offshore piles are significantly smaller than calculated probabilities of failure using conventional models. Incorporation of a lower-bound capacity into design for deep foundations is expected to provide a more realistic quantification of reliability for decision-making purposes and therefore a more rational basis for design.

In order to explore the hypothesis of a lower-bound capacity, Najjar

(2005, 2009) analyze the axial load test results of driven pile into normally consolidated to slightly overconsolidated clays and siliceous sands.

In those studies, he compared the various models for the lower-bound resistance to use to relate reliability analysis. Several types of probability distributions were reviewed including conventional probability distribution like normal and lognormal distribution, bounded probability distributions like uniform and beta distribution, and truncated probability distribution. Next, he proposed the realistic probability distribution that can accommodate a lower-bound resistance and used to related reliability. Also, study how a lower-bound capacity could affect the reliability for a pile foundation; and propose an LRFD design-checking format that includes information on the lower-bound capacity in addition to the conventional design information.

2.2.2 Lower-bound resistance

For clays, the predicted axial capacity of driven pipe piles is calculated in the API design method using a variation of the α-method, and lower-bound resistance is calculated using the API method and replacing the undrained shear strength with the remolded shear strength for these normally consolidated to slightly overconsolidated clays. The calculating methods for resistance of test piles in clay are summarized in Figure 2.2.

The reason of replacing the undrained shear strength with the remolded

shear strength for lower-bound calculation is based on the principals of critical state soils mechanics. The remolded shear strength resembles the undrained strength of clays after being subjected to very large strains at a constant void ratio, therefore, replacing shear strength is simple method for lower-bound resistance.

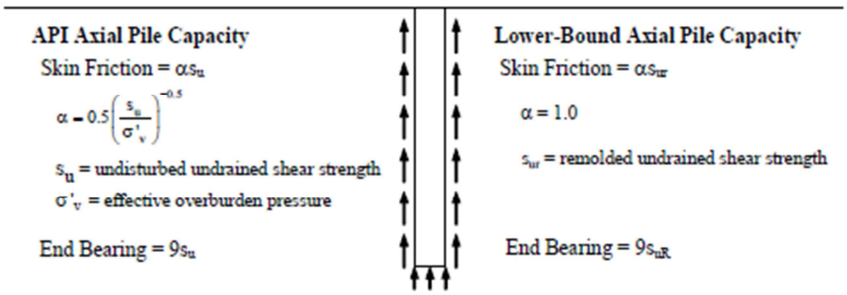

Figure 2.2 Calculating methods for resistance of test piles in clay (Najjar, 2009)

The lower-bound capacity is calculated using the API method and replacing the undrained shear strength with the remolded shear strength for clays, and the ratio of the lower-bound capacity to the predicted capacity ranges from 0.4 to 0.9 and has an average of 0.6.

For siliceous sands, the predicted axial capacity for driven steel pipe piles is calculated in the API design method using a variation of Nordlund's method, and A lower-bound capacity is calculated for each point in the database using the API method with the following modifications: the lateral coefficient of earth pressure is replaced with the at-rest value and the soil-pile friction angle and end-bearing capacity factors are replaced with the values

for one-category less in density (e.g., the values for a “Dense Sand” are replaced with those for a “Medium Sand”). The calculating methods for resistance of test piles in clay are summarized in Figure 2.3.

Likewise in case of clay, lower-bound resistance of pile in sand is calculated by replacing of variance in API method. The lateral coefficient of earth pressure is replaced with the at-rest value because that increases in the effective stress around the pile as a result of pile driving are nonexistent, and that the horizontal effective stresses that act on the pile walls can be represented by free field conditions (at-rest conditions). Also, the soil-pile friction angle and end-bearing capacity factors are replaced with the values for one-category less in density. It is because that downgrade of these factors is the simple model to represent the critical state interface friction angle.

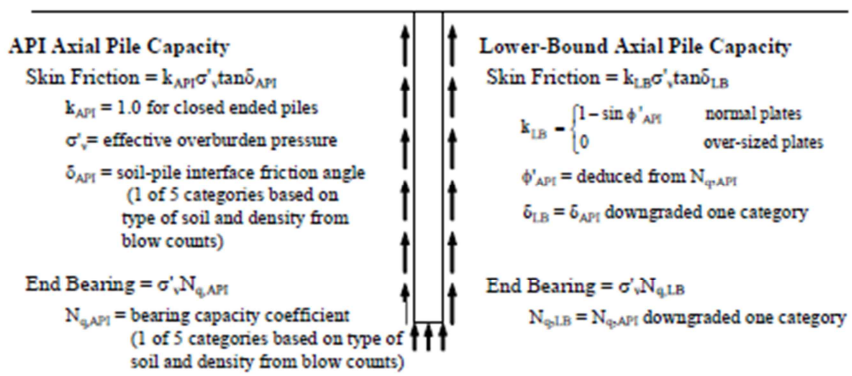

Figure 2.3 Calculating methods for resistance of test piles in sand (Najjar, 2009)

For sands, and the ratio of the lower-bound capacity to the predicted capacity ranges from 0.5 to 0.9 and has an average of 0.7.

2.2.3 Effect of lower-bound resistance on reliability

Most reliability analyses for pile resistance have assumed lognormal distributions for the pile resistance. Contrarily, Najjar (2005) suggested the mixed probability distribution for modeling the resistance shown in Figure 2.4. For capacities greater than the lower bound, the distribution is a continuous probability density function that follows a lognormal distribution, and For capacities at the lower bound, there is a finite probability (that is, a probability mass function) that corresponds to the probability of being less than or equal to the lower bound in the non-truncated lognormal distribution.

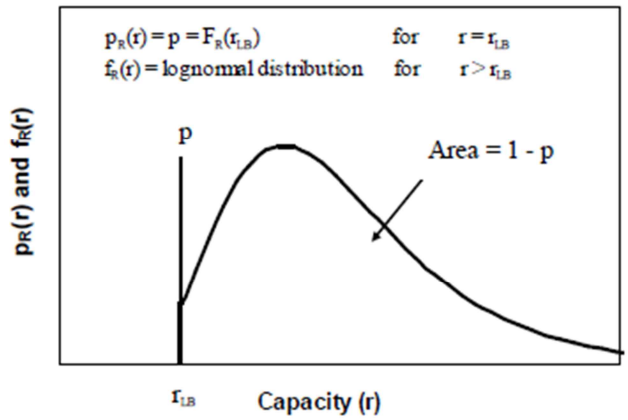

Figure 2.4 Mixed probability distribution for modeling the resistance (Najjar, 2005)

With the probability distribution for resistance as shown in Figure 2.4, the reliability can be calculates as follow equation.

$$\text{Reliability} = P(Q < R) =$$

$$P(Q < R|r = r_{LB})P(R = r_{LB}) + \int_{r_{LB}}^{\infty} P(Q < R|r) f_R(r) dr =$$

$$\Phi\left(\frac{\ln(r_{LB}) - \ln(q_{median})}{\sqrt{\ln(1+\delta_Q^2)}}\right)\Phi\left(\frac{\ln(r_{LB}) - \ln(r_{median})}{\sqrt{\ln(1+\delta_R^2)}}\right) +$$

$$\int_{r_{LB}}^{\infty} \Phi\left(\frac{\ln(r) - \ln(q_{median})}{\sqrt{\ln(1+\delta_Q^2)}}\right)\frac{1}{\sqrt{2\pi}\sqrt{\ln(1+\delta_R^2)}r} e^{\frac{1}{2}\left(\frac{\ln(r) - \ln(q_{median})}{\sqrt{\ln(1+\delta_R^2)}}\right)^2} dr \qquad (2.2)$$

where δ_R is the COV accounting for variations between actual versus predicted resistance, r_{median} is the median resistance, δ_Q is the COV in axial load, q_{median} is the median axial load, and Φ is the standard normal function.

The reliability index is shown in Figure 2.5 as a function of the ratio of the lower-bound resistance to the median resistance. From Figure 2.5, it can be concluded that a lower-bound resistance can have a significant effect on the foundation reliability. Reliability index is linearly increased when the ratio of lower-bound to median capacity exceed the certain value. This results show that the lower-bound resistances have significant effect on the calculated reliability, and this means that resistance factor should incorporate information about lower-bound resistance.

Based on the Figure 2.5, a simple approximation is proposed to relate the reliability to the lower-bound resistance. The model is defined by three points. First, the reliability index with no lower-bound resistance is calculated, and

secondly, a horizontal line is drawn from zero to the most probable failure point. Finally, the reliability index with ratio of lower-bound of 1.0 is calculated and straight line is drawn from the threshold value. The proposed bilinear model is shown in Figure 2.6.

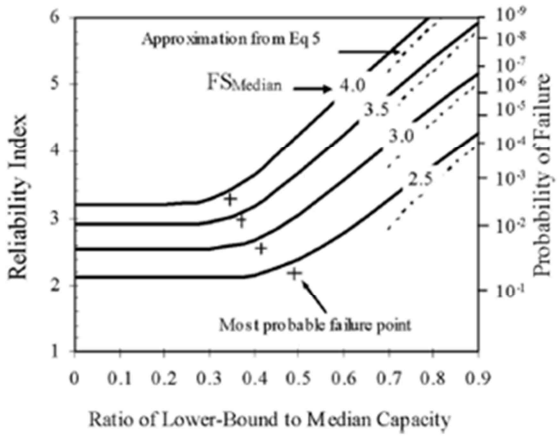

Figure 2.5 Effect of lower-bound resistance on reliability (Najjar, 2009)

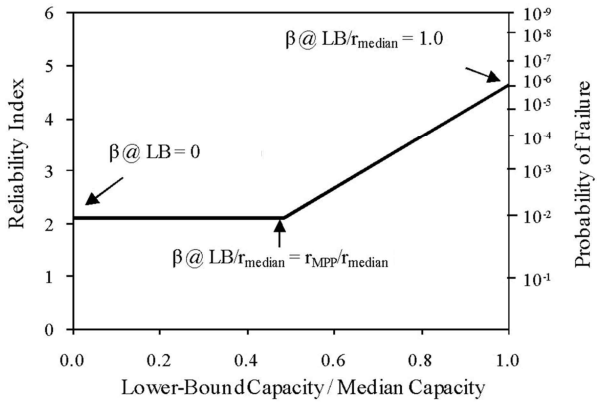

Figure 2.6 Proposed bilinear model for evaluating reliability (Najjar, 2009)

2.2.4 Incorporating lower-bound resistance into LRFD

Since a lower-bound capacity can have a significant effect on the reliability of a design, a reliability-based LRFD design code could include information on the lower-bound resistance. The conventional design checking equation has the following general form as below.

$$\phi_R \cdot r_{nominal} \geq \gamma_S \cdot s_{nominal} \tag{2.3}$$

where, $r_{nominal}$ is nominal resistance calculated using a design method, ϕ_R is resistance factor, $s_{nominal}$ is nominal load for design, and γ_S is load factor. In order to incorporate the effect of a lower-bound resistance, this design checking equation is modified as follows.

$$\phi_{R(LB)} \cdot r_{nominal} \geq \gamma_S \cdot s_{nominal} \tag{2.4}$$

where, $\phi_{R(LB)}$ indicates the resistance factor expressed as the function of the lower-bound capacity. When there is no lower bound and when the load and the resistance follow conventional lognormal distributions, the reliability and resistance factor are calculated from equation (2.5) and equation (2.6).

$$Reliability = \Phi\left(\frac{\ln(FS_{median})}{\sqrt{[(1+\delta_S^2)(1+\delta_R^2)]}}\right) \quad \text{if LB} = 0 \tag{2.5}$$

$$\phi_R = \frac{\gamma_S}{e^{\beta_{target}\sqrt{[(1+\delta_S^2)(1+\delta_R^2)]}}}\left(\frac{\lambda_R}{\lambda_S}\right)\sqrt{\frac{(1+\delta_S^2)}{(1+\delta_R^2)}} \quad \text{if LB} = 0 \tag{2.6}$$

For a nonzero lower-bound capacity, the required median factor of safety will decrease as the lower bound increases, and the required resistance factor when there is a lower-bound resistance, $\phi_{R(LB)}$, can be expressed in terms of the conventional case as follows.

$$\phi_{R(LB)} = \left(\frac{FS_{median(LB=0)}}{FS_{median(LB)}}\right)\phi_R \tag{2.7}$$

The increase in the resistance factor due to an increase in the lower-bound resistance is inversely proportional to the corresponding decrease in the factor of safety. The variation of the ratio of the resistance factor incorporating a lower-bound resistance to the conventional resistance factor, $\phi_{R(LB)}/\phi_R$, is shown as a function of the lower-bound resistance shown in Figure 2.7.

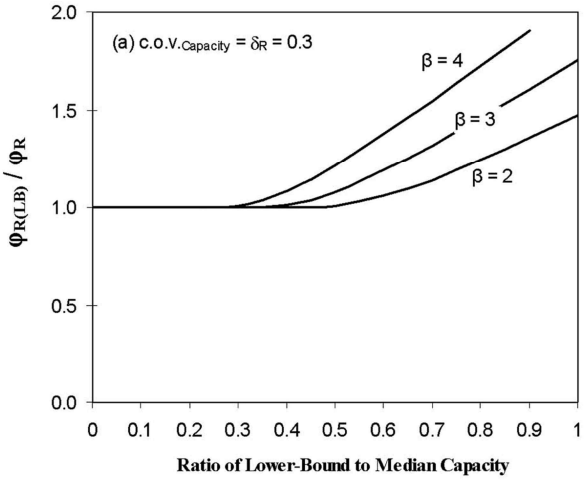

Figure 2.7 Variation of resistance factor with lower-bound resistance (Najjar, 2009)

3. Evaluation of Resistance for Drilled Shaft

3.1 Collected Load Test Data

In recent years, constructions of heavy and large structure construction like super long span bridge or skyscraper have been consistently increased, therefore, large-diameter drilled shafts are more widely used in geotechnical design. According to this trend, first of all, target pile foundation type of this thesis is selected as drilled shafts,

In case of load test of drilled shafts, applied loads are generally very large and need large reaction structure. However, it is possible to remove reaction structure and use self- weight of drilled shafts as reaction load using bi-directional load tests as known as Osterberg Cell Test. Bi-directional load tests have advantage and easy mechanism to calculate accurate shaft and base resistance as well as total resistance. As mentioned above part, introduction and literature review, most previous researches for suggestion of resistance factors in Korea are limited to suggestion of total resistance factors due to absence of information and/or impossibility for determination of shaft and base resistance. Also, shaft and base resistance factor by Jung (2010) have doubtful point due to resistance factors are results based on numerical analysis. Therefore, secondly, bi-directional load test for drilled shafts has been mainly selected for this study.

Also, it is very important to determine accurate resistance. In procedure

for reliability-based resistance factor calibration, the measured resistance can influence the results of reliability analysis and resistance factor calibration significantly. However, most load tests included the bi-directional load tests conducted in Korea are conducted for just total resistance because of economic efficiency, construction period, and additional efforts. So, most load tests do not provide shaft and base resistance, and even if load tests provide shaft and base resistance, reliability of these resistances are not verified and convincible. Therefore, load test data with strain gauge in test piles are collected for accurate measurements of shaft and base resistance. One of the important purposes of this thesis is accurate resistance factors for drilled shafts in Korea. Based on accurate shaft, base and total resistances from load transfer analysis, accurate resistance factors can be determined.

Synthesizing the overall considerations, 13 sets of load test results of drilled shafts are collected for this study. The test pile profile and rock properties from site investigation are summarized in Table 3.1 and detailed site investigation results and pile profiles are shown in Figure 3.1 to Figure 3.3. Most of the piles were socketed into soft rock or weathered rock. Unconfined strengths of bedrock were estimated from point load test and unconfined compressive load test. Also, RQD and TCR were estimated. Also, strain gauges were installed in each test piles to evaluate shaft and base resistance using load transfer analysis.

The test piles of TP 1 to TP 8 were instrumented with strain gauges to load transfer mechanisms. However, the piles of TP 9 to TP 13 were not installed with strain gauges, thus load transfer analysis was not conducted.

Table 3.1 Test pile profile and site investigation results

	Pile length(m)	Embedded depth(m)	Pile diameter(m)	Rock type	Weathering degree[1)]	Load (ton)	Unconfined strength (MPa)	RQD (%)	TCR (%)
TP 1	18.96	38.96	2.35	Gneiss & Schist	WR + SR	10,750	3.1~19.8	0~13	54~100
TP 2	20.61	36.21	1.85		WR + SR	5,000	10.2~25.4	22~78	53~100
TP 3	9.11	33.41	1.35		WR + SR	4,500	5.6~25.0	25~72	80~100
TP 4	35.38	36.38	1.85		WR + SR	3,750	1.8~8.7	4~35	30~100
TP 5	40.14	55.42	3	Biotite granite	WR + SR	21,000	30.4~194	0~68	51~100
TP 6	44.10	56.60	2.4		WR	17,000	5~14	0~36	20~100
TP 7	45.10	51.20	2.4	Biotite granite & Pegmatite	WR + SR	12,000	44~47	0~42	90~100
TP 8	40.01	52.26	2.4	Pegmatite, Gneiss & Aplite	WR + SR	9,000	1~192	0~55	30~100
TP 9	33.5	33.5	1.5	Gneiss	WR	1,950	71.4~87.2	-	-
TP 10	13.5	13.5	1.0		WR(HW)	1,800	38	0	50
TP 11	13.5	13.5	1.0		WR(CW)	1,800	38	0	100
TP 12	13.5	13.5	1.0		WR(MW)	1,800	38	18~42	100
TP 13	13.5	13.5	1.0		WR(MW)	1,800	38	23~61	100

[1)] WR: Weathered Rock, SR: Soft Rock, CW: Completely Weathered, HW: Highly Weathered, MW: Moderately Weathered

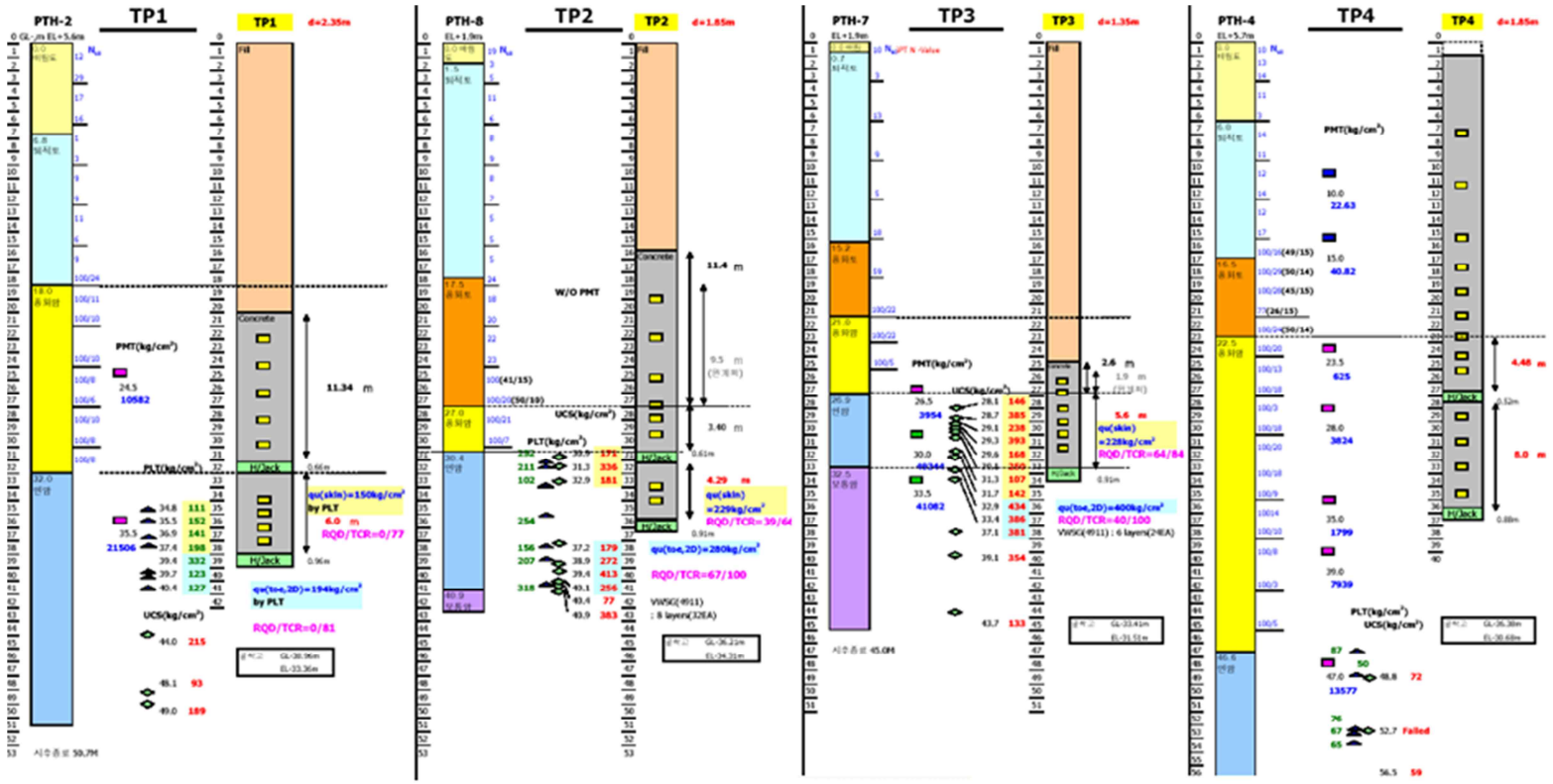

Figure 3.1 Detailed site investigation results and pile profiles of Test pile TP1 to TP4

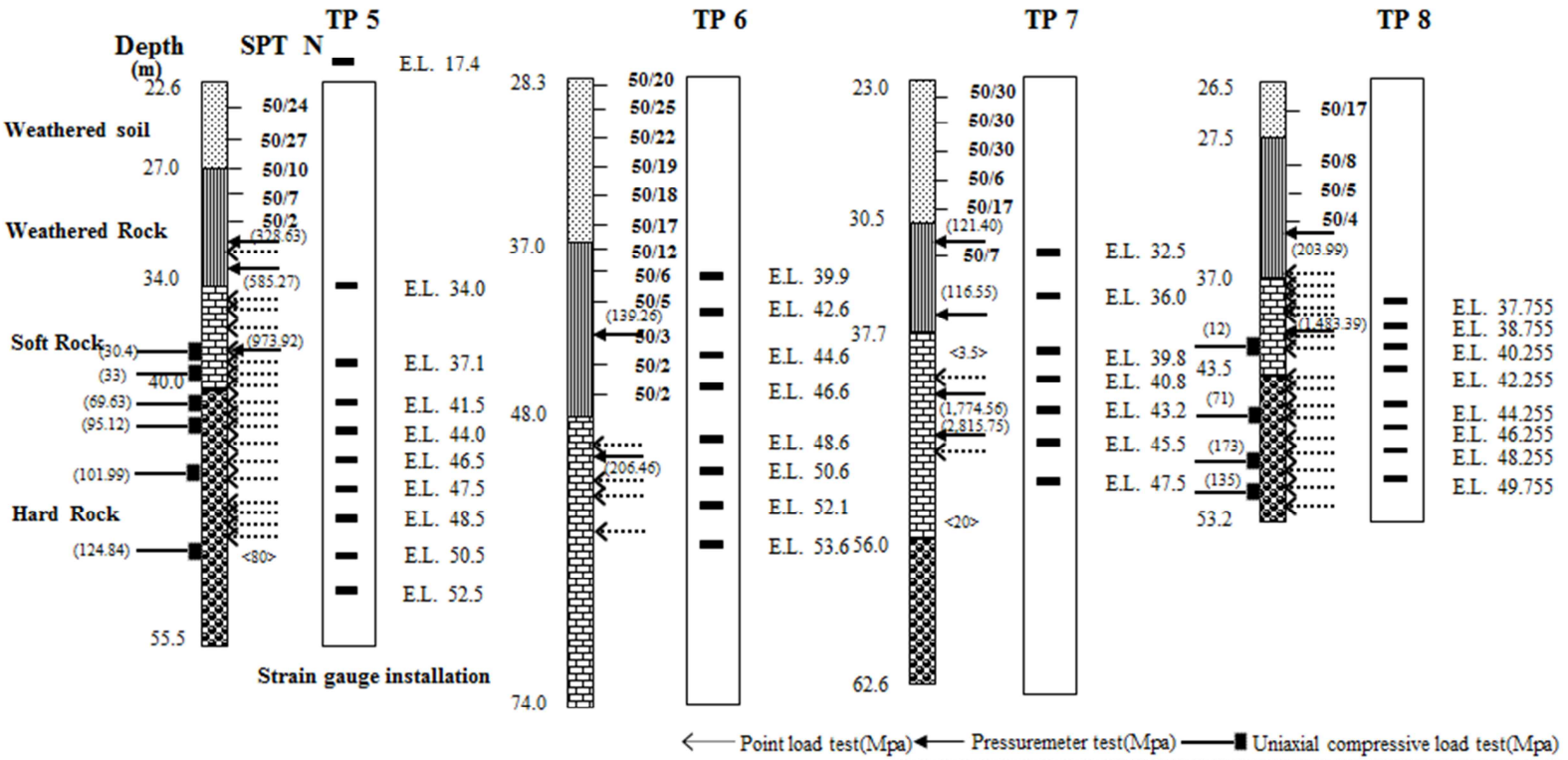

Figure 3.2 Detailed site investigation results and pile profiles of Test pile TP5 to TP8

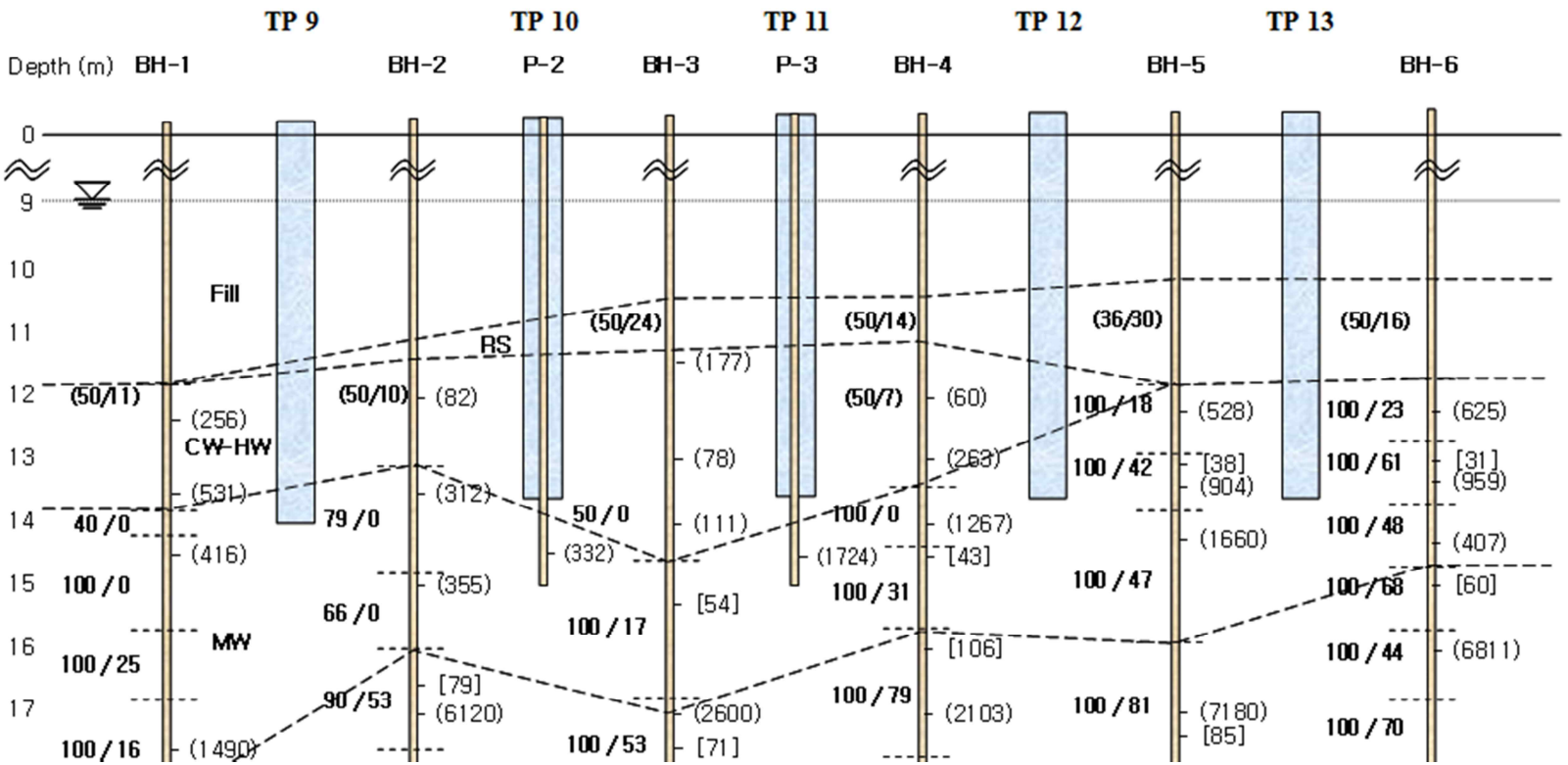

Figure 3.3 Detailed site investigation results and pile profiles of Test pile TP9 to TP13

3.2 Measured Resistance by Load Tests

Measured resistances are determined by load test results. And, ultimate bearing capacity obtained from the load test is called measured resistance. In general cases, measured resistance means just total measured resistance from load-displacement curve for static load tests or equivalent load-displacement curve for bi-directional load tests. However, these results are not accurate. Because that load-displacement curve are generally drawn using applied load and measured displacement in pile head, so load-displacement curves cannot include the detailed ground properties and axial load transfer for drilled shaft in loading stage. Also, to determine the shaft and base resistances in previous researches by Kwon (2004) and Jung (2010), numerical analysis were conducted and the results of numerical analysis were treated as measured shaft and base resistances. However numerical analysis results are not realistic resistance but assumed resistance by finite elements methods. Therefore, in this study, shaft resistances and base resistances are determined through load transfer analysis using measured strain data.

The procedures for calculation of measured resistance are summarized in below.

A. To calculate the shaft and base resistance by load test
   i. Measure the strain for each gauge installed depth
   ii. Calculate axial load for each depth by load transfer analysis
   iii. Evaluate displacement of each depth

iv. Draw the f-w curve(shaft resistance-displacement curve) & q-w curve(base resistance-displacement curve)

v. Determine measured shaft resistance using f-w curve, and base resistance using q-w curve (Jung, 2010)

B. Procedure for calculation of measured total resistance by load test

i. Measure applied load and displacement

ii. Draw the load-displacement curve and determine the total resistance using curve

iii. If load test was conducted by bi-directional load test, draw the equivalent load-displacement curve (Jung, 2010)

In this study, some calibrations are performed to determine the more accurate and realistic resistances. In load transfer analysis steps for shaft and base resistances, elastic modulus of drilled shafts are considered. Also in step of equivalent load-displacement curve for total resistances, the method for equivalent load-displacement curve is modified.

3.2.1 Calibration for load transfer analysis

Axial loads and shaft and base resistances can be calculated by load transfer analysis using strain data with load level. In load transfer analysis, the elastic modulus of concrete is one of the most important parameters to consider. The elastic modulus, E_{50}, suggested by American Concrete Institute (ACI, 1996), has been commonly used. However, elastic modulus of concrete shows nonlinear stress-strain characteristic, so nonlinearity should be considered in load transfer analysis. Fellenius (1989) compared the tangent modulus considering nonlinear stress-strain relationship with the constant elastic modulus. Figure 3.1 shows the typical data from an instrumented static pile loading test on a pile with a constant modulus. Figure 3.4 (a) shows the theoretical elastic line (lower-line) for a pile and Figure 3.4 (b) shows the relationship of tangent modulus with increasing strain. The tangent modulus initially reduces with increasing strain to become constant at a certain account of strain. Contrarily, Figure 3.5 shows the results considering nonlinear stress-strain relationship. In Figure 3.5 (a), the stress-strain relationship of concrete pile shows nonlinear behavior when loaded, therefore, the tangent modulus of the concrete pile is not constant but reducing and the line slopes downward with increasing strain.

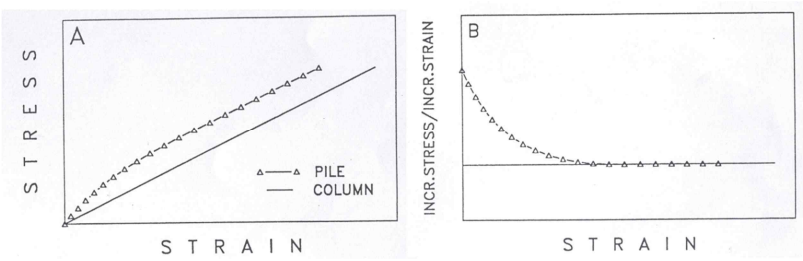

Figure 3.4 Typical data from an instrumented static pile loading test on a pile with a constant modulus

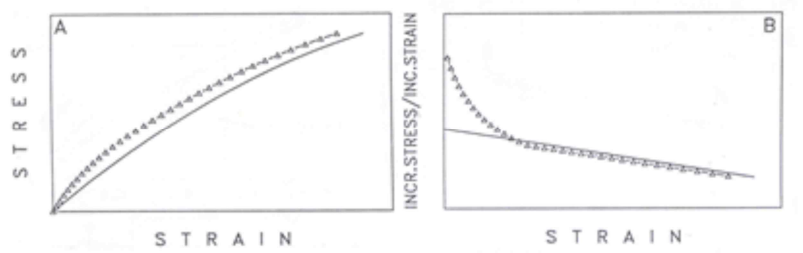

Figure 3.5 Typical data from an instrumented static pile loading test on a concrete pile with a modulus reducing with increasing stress

In this study, elastic modulus was calculated by the Fellenius (1989) method, assuming the stress-strain relation of concrete to be a quadratic function, and then, the calculated elastic modulus was applied to the load transfer analysis. For calibration of elastic modulus, strain data near the load cell is used because of large strain range. The calibrated elastic modulus of test piles (TP 1 ~ TP 8) are shown in Figure 3.6 to Figure 3.13. The solid line means constant elastic modulus and the dotted line means calibrated elastic modulus of test piles.

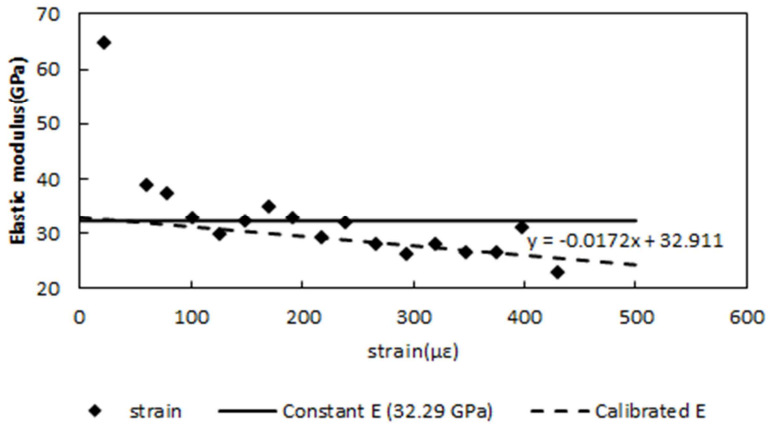

Figure 3.6 Calibrated elastic modulus of TP 1

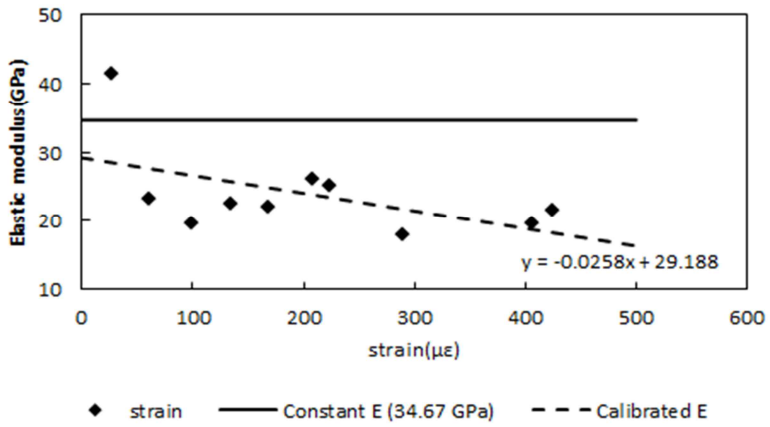

Figure 3.7 Calibrated elastic modulus of TP 2

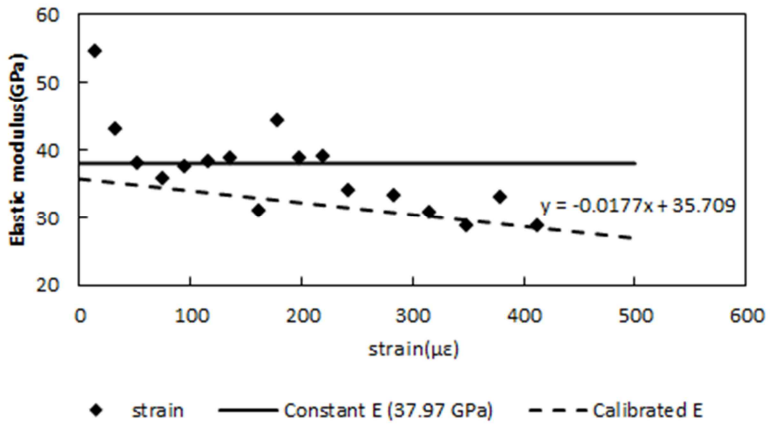

Figure 3.8 Calibrated elastic modulus of TP 3

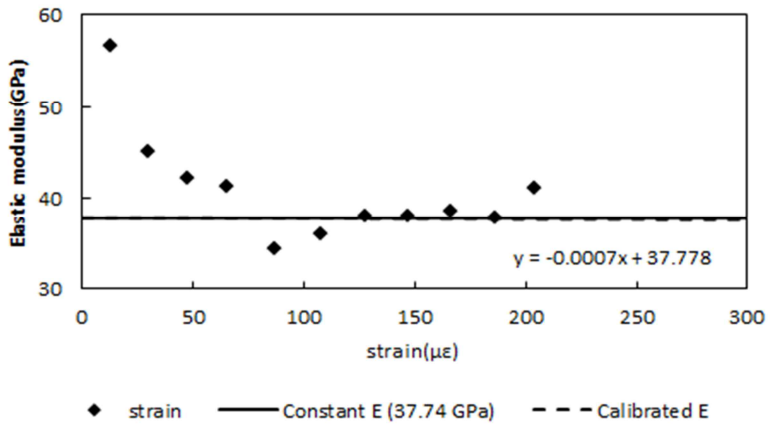

Figure 3.9 Calibrated elastic modulus of TP 4

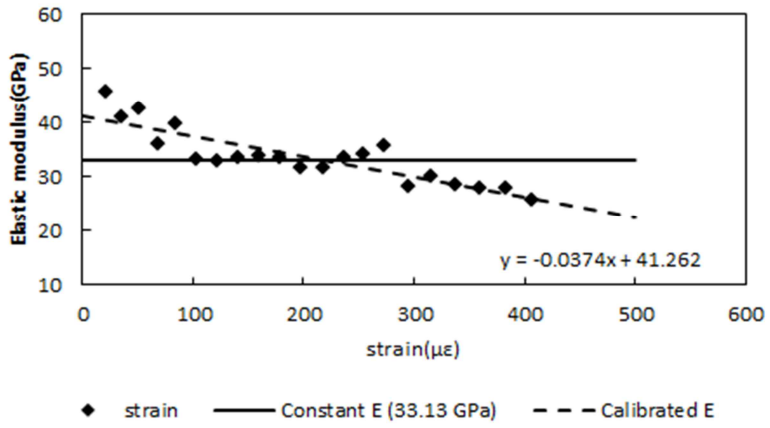

Figure 3.10 Calibrated elastic modulus of TP 5

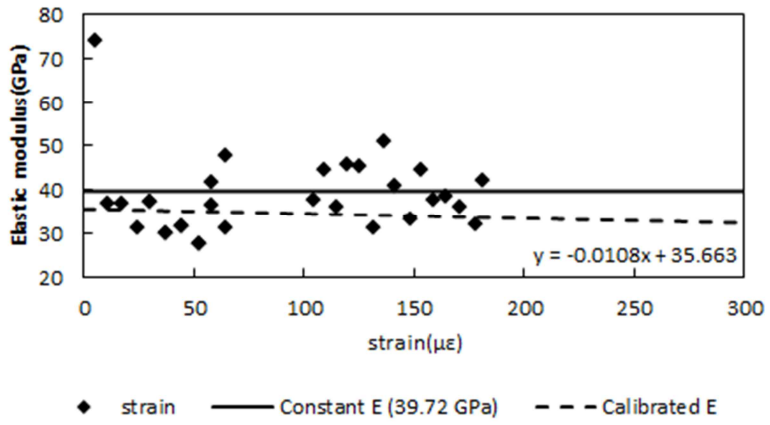

Figure 3.11 Calibrated elastic modulus of TP 6

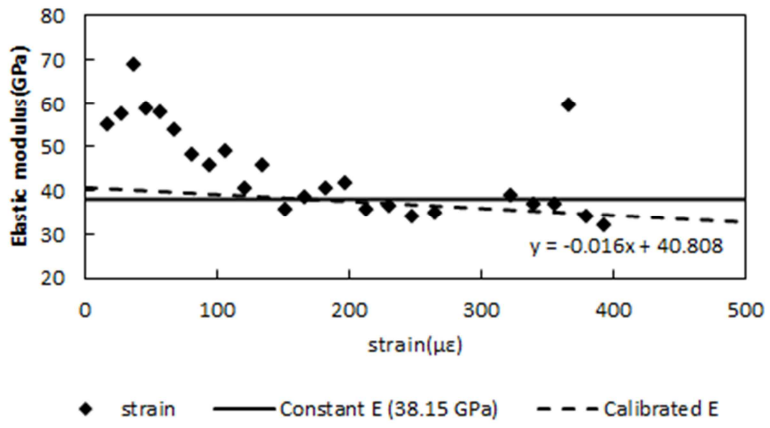

Figure 3.12 Calibrated elastic modulus of TP 7

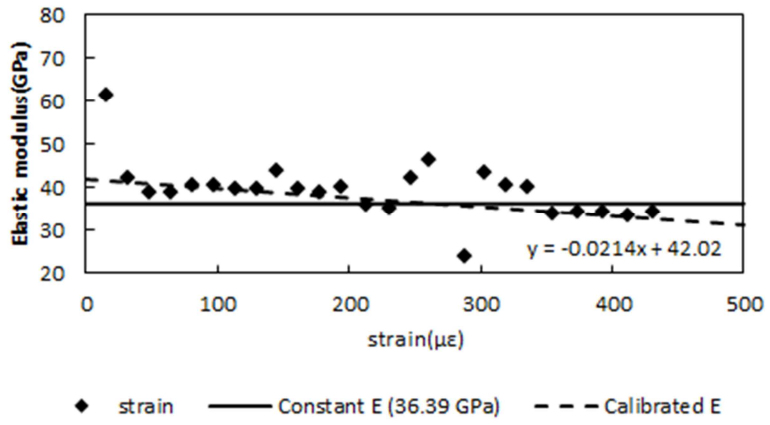

Figure 3.13 Calibrated elastic modulus of TP 8

After calibration of elastic modulus of test piles, calibrated elastic modulus of piles are applied to load transfer analysis. Load transfer analyses were conducted using measured strain data.

First of all, axial loads at each depth with strain gauge are calculated using below equation.

$$P = \varepsilon \times (E_{Felenius} \times A) \quad (3.1)$$

where P is the calculated axial loads at each depth with strain gauge, ε is measured strain, $E_{Felenius}$ is the calibrated elastic modulus, and A is the area of test piles.

The difference between the axial loads at any two gauge levels represents the shaft load carried by that specific portion of the pile. Dividing the load by area gives the average unit shaft resistance mobilized between the subjected gauges. The formula can be defined as:

$$f_i = \frac{P_i - P_{i+1}}{\pi D L_i} \quad (3.2)$$

where P_i is the calculated axial load at i^{th} strain gauge, P_{i+1} is the calculated axial load at $(i+1)^{th}$ strain gauge, and L_i is distance between each strain gauge.

Displacement w_i corresponding to unit shaft resistance (f_i) can be obtained from the subtraction of elastic compression as follow.

$$w_i = w_{i-1} - \frac{\overline{P_l} \times \overline{L_l}}{E_{felenius} \times A} = w_{i-1} - (\overline{\varepsilon_l} \times \overline{L_l}) \qquad (3.3)$$

where $\overline{P_l}$ is the average calculated axial loads at both end of the element, and $\overline{\varepsilon_l}$ is the average strain at i^{th} element, and $\overline{L_l}$ is the average segment length; in other words, $\overline{\varepsilon_l} = (3 \times \varepsilon_i + \varepsilon_{i+1})/4$, and $\overline{L_l} = (L_{i-1} + L_i)/2$.

According to the calculations for each load step using the above equations, f-w curves can be obtained at various depths.

For q-w curve, axial load at base was calculated by subtracting the entire shaft resistance which is the sum of shaft resistance from applied load, and unit base resistance were computed by dividing the axial load at base by base area. Displacement at base can be obtained by Equation (3.3).

Load transfer analysis results shows in Figure 3.14 to Figure 3.30. In case of test pile 1 (TP 1), load cell was installed in drilled shafts, therefore, f-w curves are drawn for upward displacement and downward displacement.

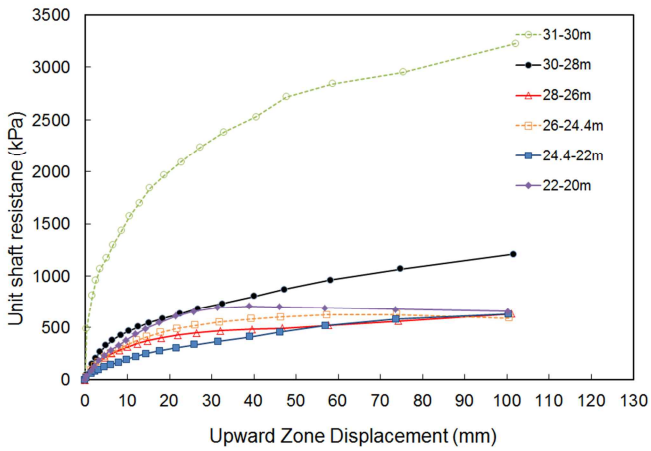

Figure 3.14 f-w curve (for upward displacement) for TP 1

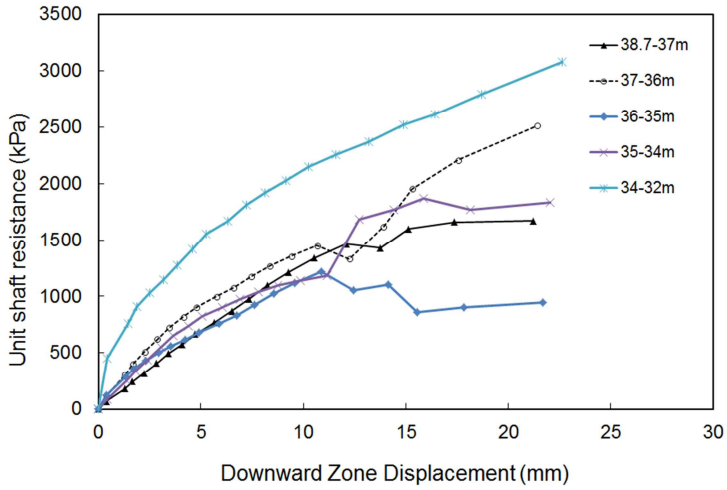

Figure 3.15 f-w curve (for downward displacement) for TP 1

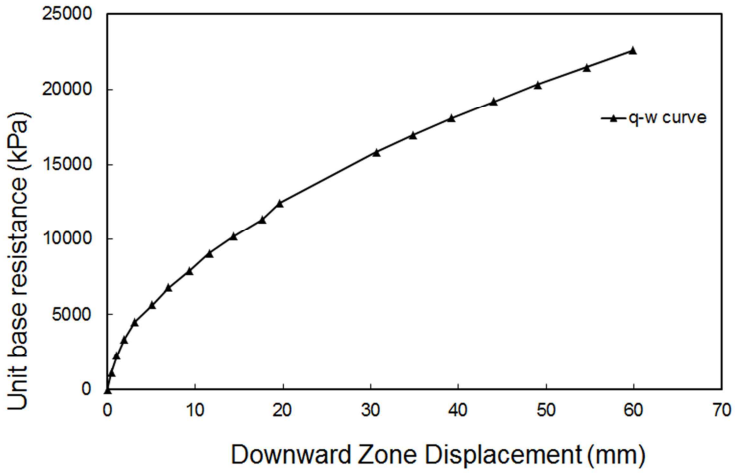

Figure 3.16 q-w curve for TP 1

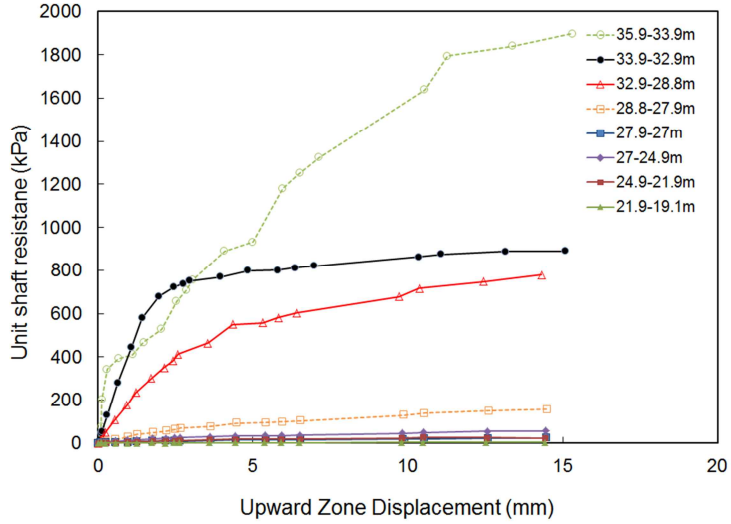

Figure 3.17 f-w curve for TP 2

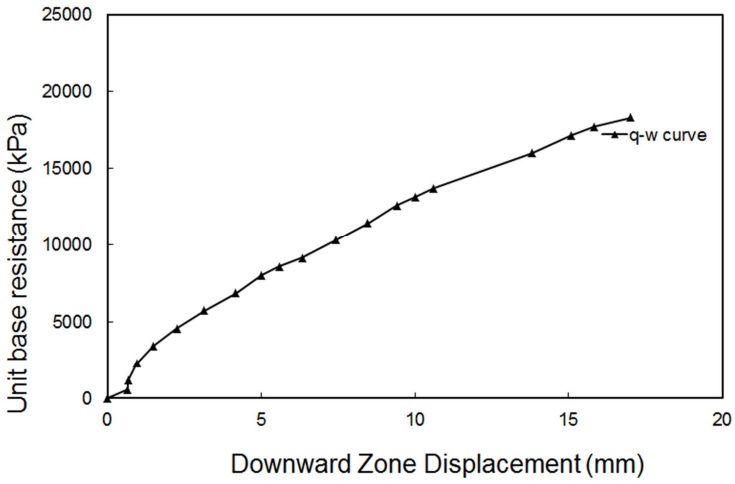

Figure 3.18 q-w curve for TP 2

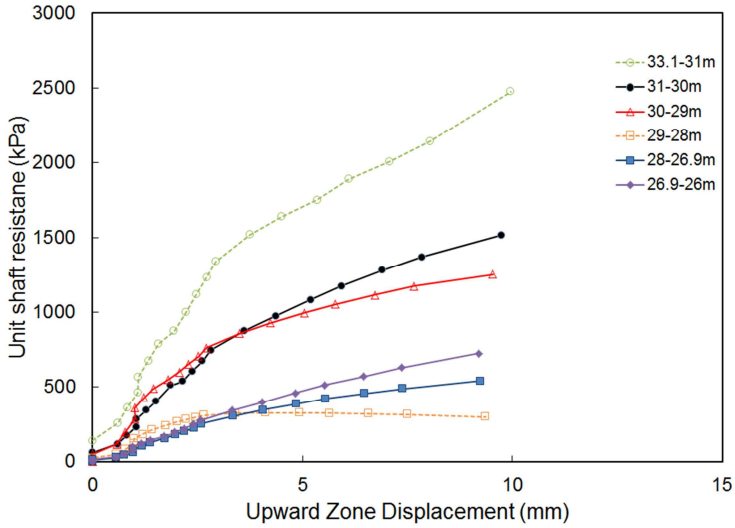

Figure 3.19 f-w curve for TP 3

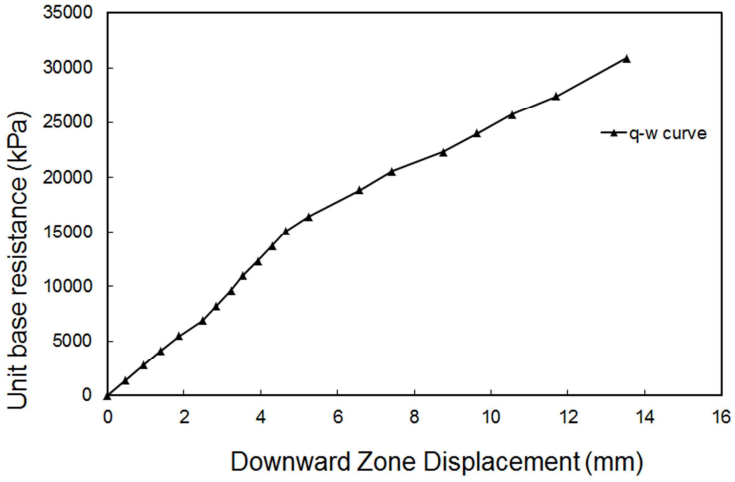

Figure 3.20 q-w curve for TP 3

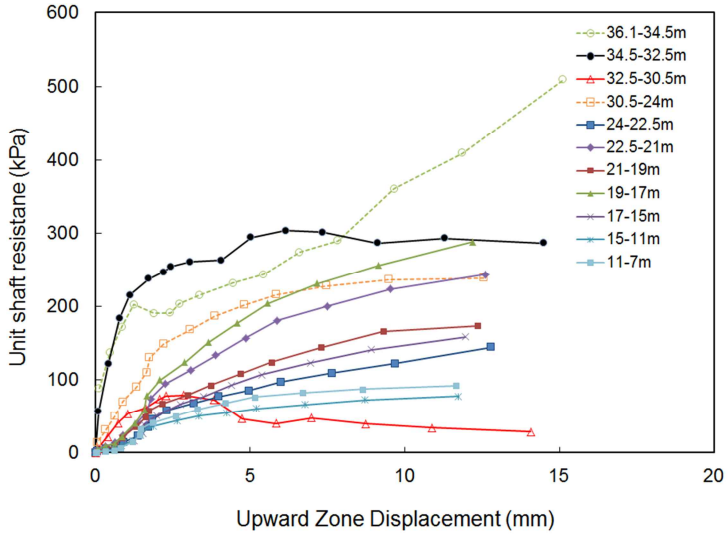

Figure 3.21 f-w curve for TP 4

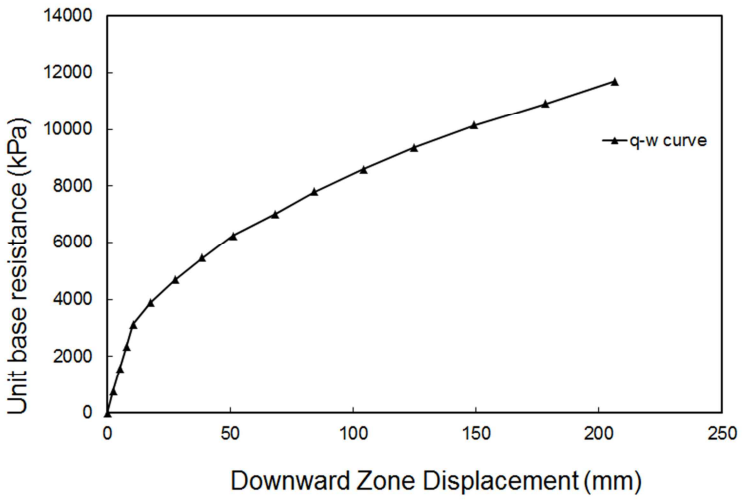

Figure 3.22 q-w curve for TP 4

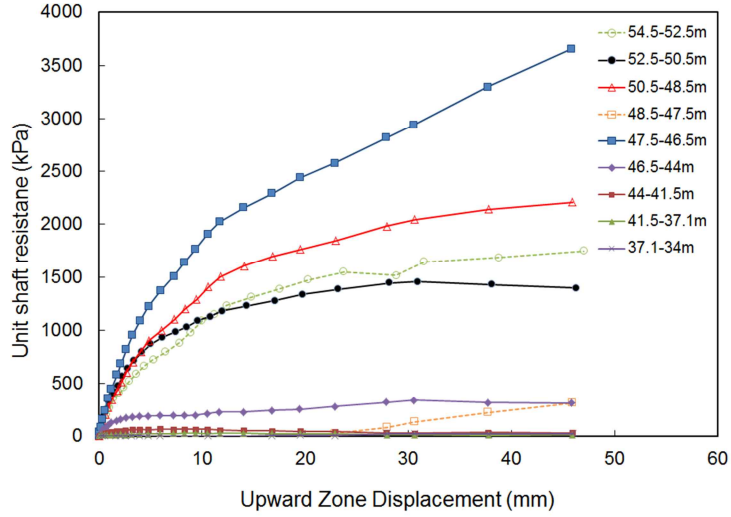

Figure 3.23 f-w curve for TP 5

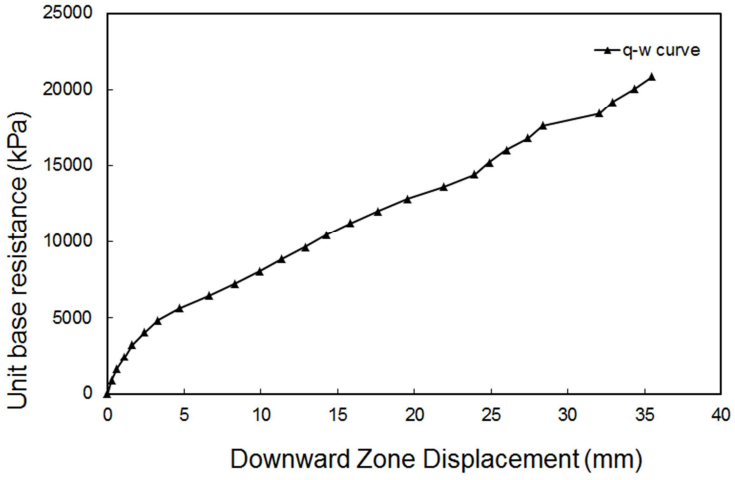

Figure 3.24 q-w curve for TP 5

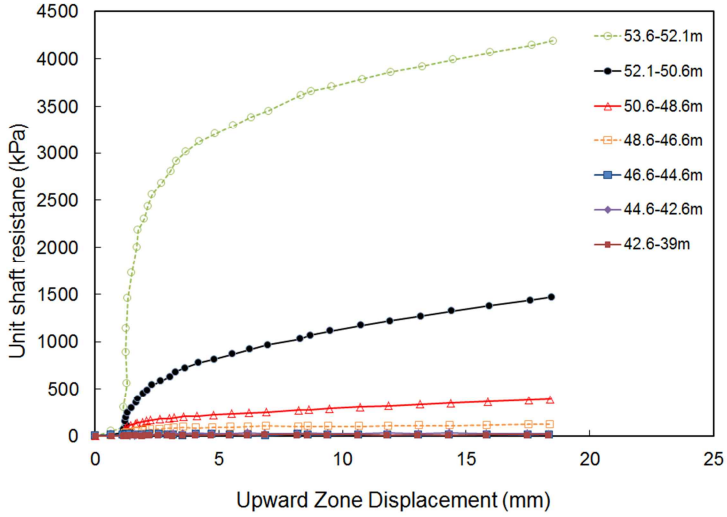

Figure 3.25 f-w curve for TP 6

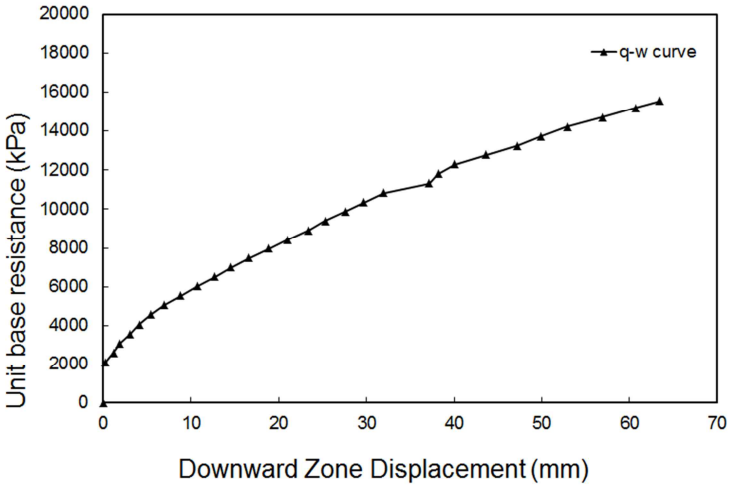

Figure 3.26 q-w curve for TP 6

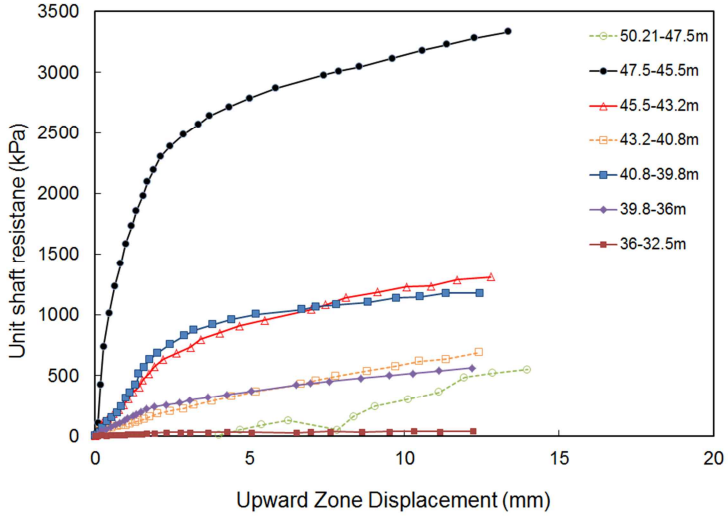

Figure 3.27 f-w curve for TP 7

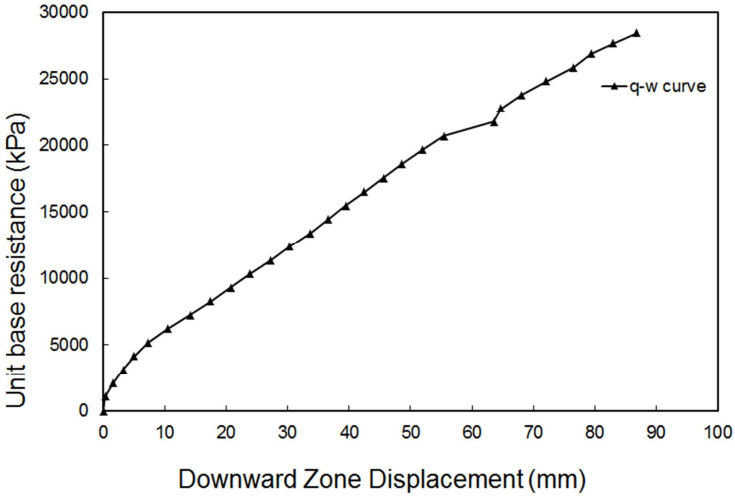

Figure 3.28 q-w curve for TP 7

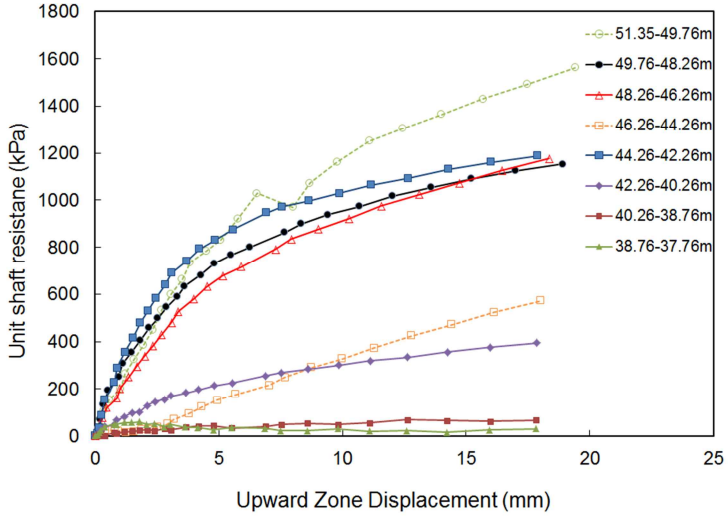

Figure 3.29 f-w curve for TP 8

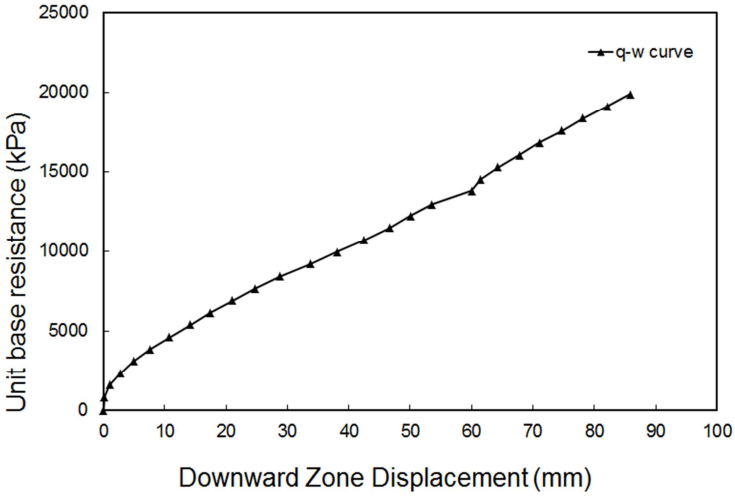

Figure 3.30 q-w curve for TP 8

3.2.2 Calibration for equivalent load-displacement curve

For the last decades, the bi-directional testing method has been advantageous over the conventional pile load testing method in many aspects. However, because the bi-directional test uses a loading mechanism entirely different from that of the conventional pile load testing method, many investigators and practicing engineers have been concerned that the bi-directional test would give inaccurate results, especially about the pile head settlement behavior. Kwon et al. (2006) compare the results of bi-directional load test with conventional top-down load tests. Bedrock of test sites were highly weathered rock and completely weathered rock and rock type was volcanic breccia. And test piles were executed on 1.5 m diameter cast-in-situ concrete piles at the same time and site. Strain gauges were placed on the test piles to compare load transfer behavior. As a result, the two tests gave similar load transfer curves at various depths of piles. Figure 3.31 and Figure 3.32 show the results of load transfer analysis at embedded rock and f-w curve and q-w curve. In Figure 3.31, f-w curves show the almost same behavior between top-down load test and bi-directional load test. In Figure 3.32, q-w curves show that base resistance from top-down load test is smaller than that of bi-directional load test. However, base resistance in same displacement from top-down load test is larger than that of bi-directional load test. It is due to concrete pouring method at base of piles. Pouring methods are selected as gravity grouting for top-down load tests and pressure grouting for bi-directional load test.

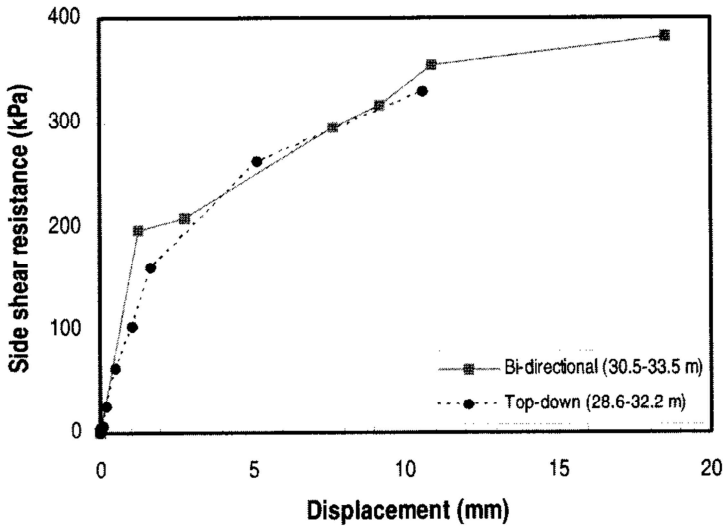

Figure 3.31 Comparison of f-w curves by top-down test and bi-directional test (Kwon et al., 2006)

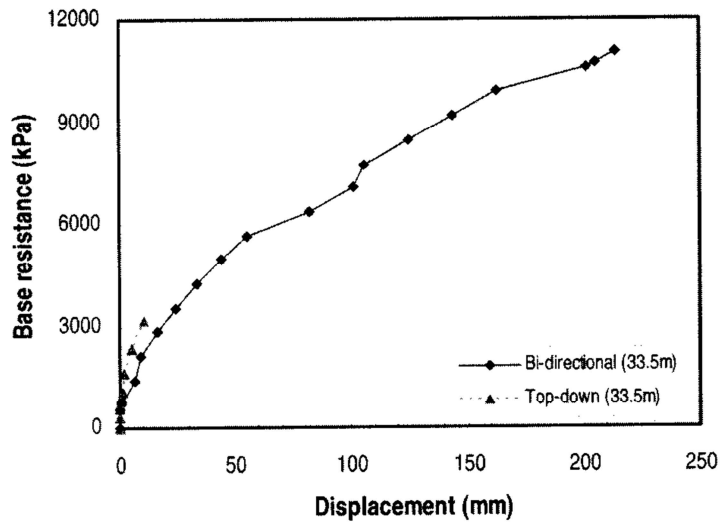

Figure 3.32 Comparison of q-w curves by top-down test and bi-directional test (Kwon et al., 2006)

From load transfer analysis results, equivalent load-displacement curves are drawn to determine load-displacement relationship of bi-directional load tests. Osterberg (1998) suggested the method for equivalent load-displacement curve using bi-directional load test result. This method assumed that pile is incompressible. Procedures for plotting equivalent load-displacement curve are summarized in below.

i. Select a point from load vs. upward displacement curve
ii. Find the point from load vs. downward displacement curve which have same displacement with i)
iii. Assumed that pile is incompressible, so displacements from pile head and base are same
iv. Sum of load from i) and ii) with same displacement means the load for equivalent load-displacement curve.
v. Iterate the i) to iv) for additional displacement and plot the equivalent load-displacement curves.

According to procedure, equivalent curve is plotted in Figure 3.33 and compared with top-down test curve. Under the design load of 12,000kN, displacement of top down test reached to 10mm, however the top-down equivalent curve constructed from the bi-directional load test results predicted the pile head displacement to be about one half of that predicted by the conventional top-down load test.

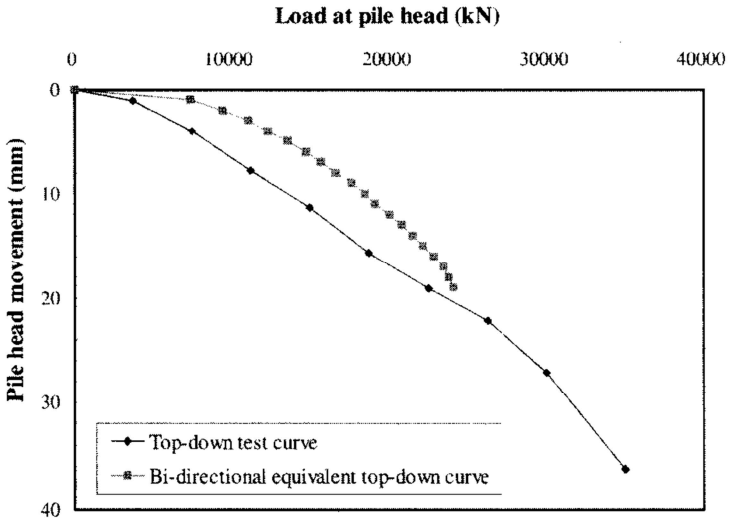

Figure 3.33 Comparison of top-down equivalent load-displacement curve (Kwon et al., 2006)

It is because that loading direction between conventional top down load test and bi-directional load test. In case of conventional load tests, loading direction is only top-down (or downward) direction, however, bi-directional load tests apply the load through load cell placed in bottom of drilled shaft, so loading directions are existed as upward and downward. Besides, in case of bi-directional load test, applied load transferred from rock layer of which elastic modulus is larger than soil layer, whereas in case of top-down load test, load transferred from soil layer with small elastic modulus which is much softer than rocks. Another reason for different displacement is elastic displacement. In general procedure for equivalent load-displacement curve (described at above part), it is assumed that pile is incompressible, so elastic compression of piles was neglected during the construction of the equivalent

load-displacement curve.

Therefore, Kwon et al. (2006) suggested the newly plotting method for the equivalent load-displacement curve considering elastic compression. First step is measuring the amount of pile compression in bi-directional loading. Pile compression was obtained by subtracting pile head movements from movement of the top of pressure cell.

After obtaining the pile compression under bi-directional test (Δw_s), the amount of the pile compression under the top-down loading condition was estimated by examining the axial load distribution. Figure 3.34 show the three different cases of load distribution along the pile axis for each load test methods. Because that ground elastic modulus becomes stiffer and stronger with depth, the load distribution of Figure 3.34 (a) would be the most common case. To quantify the difference of load distribution between top-down test and bi-directional test, the load ratio which affects pile compression was calculated by comparing the areas of □ABCDA and □ABCEA in Figure 3.35. For the particular case studied by Kwon et al., the load ratio (=□ABCEA / □ABCDA) was approximately 2 and this means that the pile head settlement should be $w + 2\Delta w_s$ to induce the downward movement of w at the pile toe when the pile is loaded from the top.

Next step is calculation of pile compression by end bearing load according to below equation.

$$\Delta w_p = \frac{Q_p L}{E_p A} \tag{3.4}$$

where, Qp is the end bearing load for the downward movement of the

pressure cell base of w, A and L are the cross-sectional area and the length of pile, respectively, and E_p is the Young's modulus of the pile. Taking as many random points as required, the top-down equivalent curve was constructed by connecting the points of the coordinate (Q_s+Q_p, w +2 $\Delta w_s + \Delta w_p$).

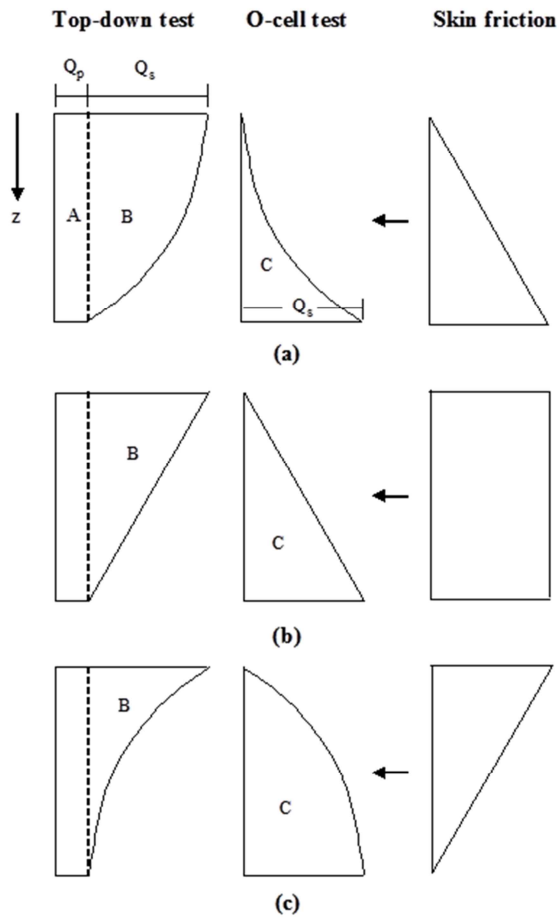

(a) skin friction increase linearly with depth(B=2C),
(b) skin friction remain constant with depth(B=C),
(c) skin friction decrease linearly with depth(B=0.5C).
Figure 3.34 Typical simple distributions of pile axial load & skin friction (Kwon et al., 2006)

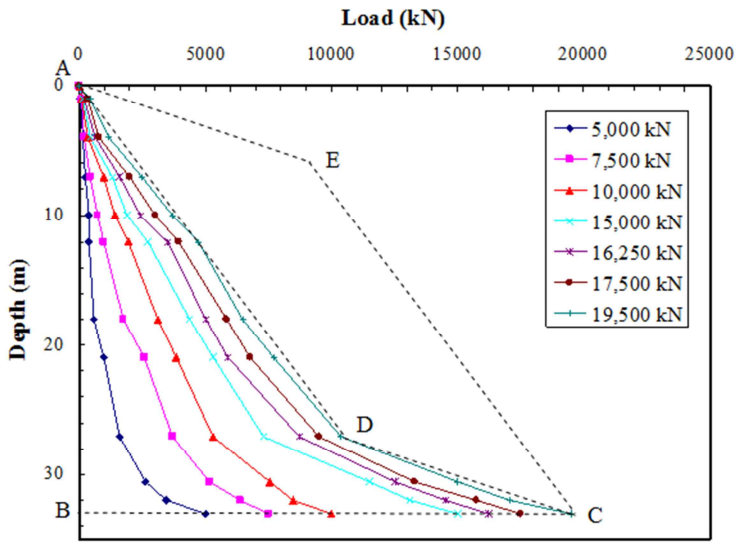

Figure 3.35 Estimation of top-down load distribution from that of bi-directional load test (Kwon et al., 2006)

For plotting of equivalent load-displacement curves in this study, axial load distributions of each test piles are constructed and the load ratio to quantify the difference of load distribution between top-down test and bi-directional test are calculated like Figure 3.35 according to Kwon et al. (2006) study. The estimated axial load distributions and load ratio are shown in Figure 3.36 to Figure 3.43. In Figure 3.36 to 3.43, x axis means the applied load for each loading steps by load cell, and y axis means the depth with strain gauge.

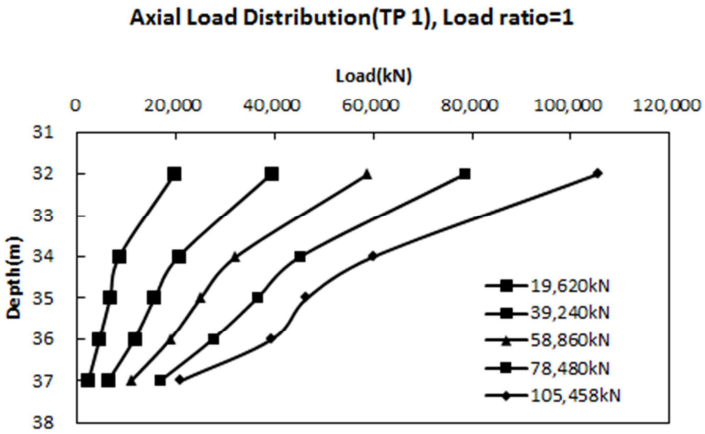

Figure 3.36 Axial load distribution of TP 1

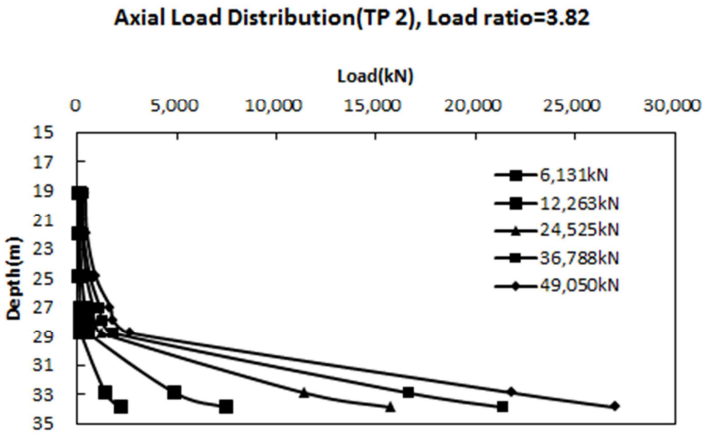

Figure 3.37 Axial load distribution of TP 2

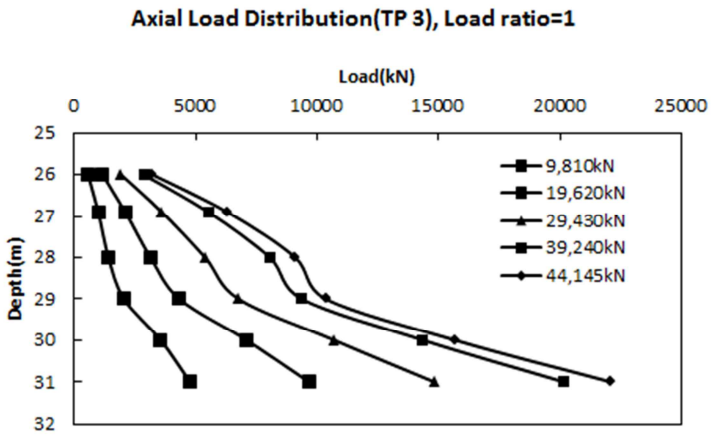

Figure 3.38 Axial load distribution of TP 3

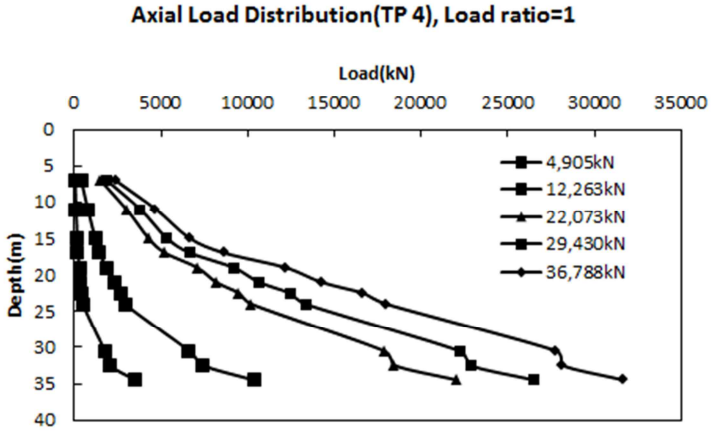

Figure 3.39 Axial load distribution of TP 4

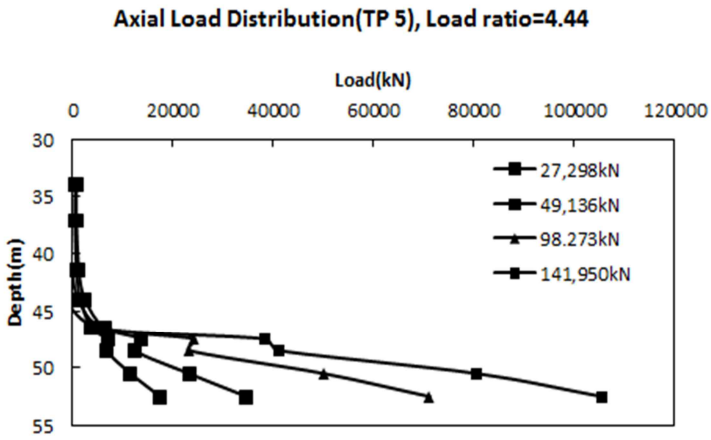

Figure 3.40 Axial load distribution of TP 5

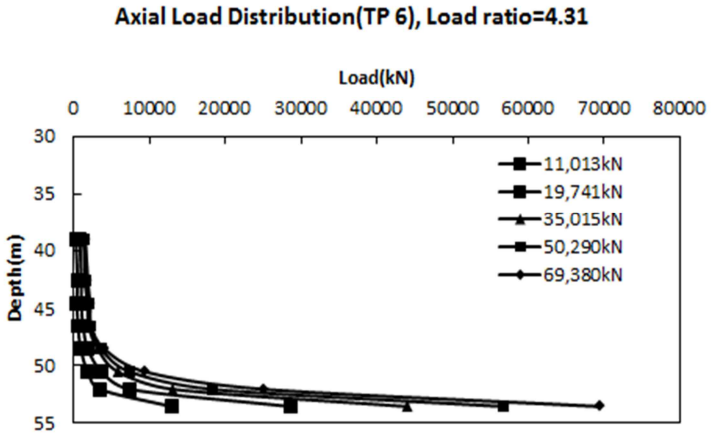

Figure 3.41 Axial load distribution of TP 6

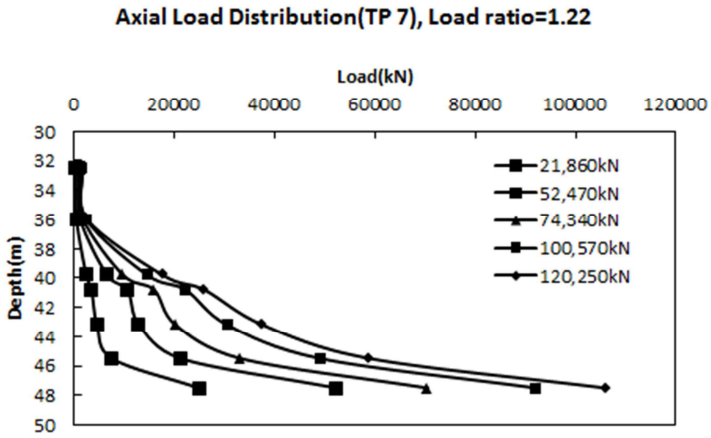

Figure 3.42 Axial load distribution of TP 7

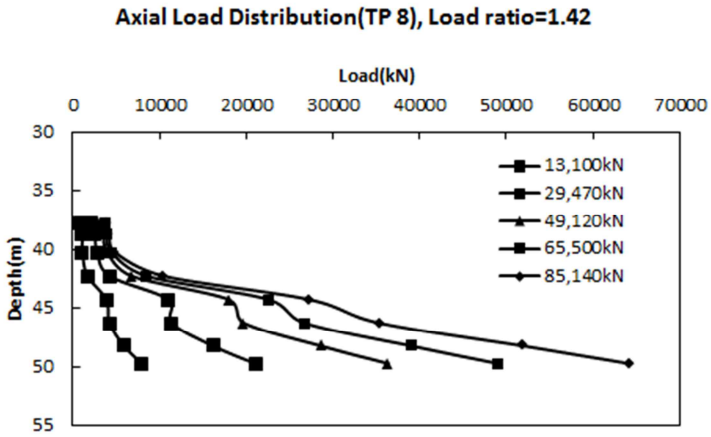

Figure 3.43 Axial load distribution of TP 8

Also, reductions of elastic modulus of test piles are included for calculation of pile compression by end bearing load as shown in Equation (3.1). The calibrated elastic modulus of each piles are shown in Figure 3.6 to Figure 3.13. With axial load distribution and reduction of elastic modulus, equivalent load-displacement curves for each test piles are constructed and compared with results of conventional methods. In this study, equivalent load-displacement curves by Kwon et al. (2006) with calibrated elastic modulus by Fellenius (1989) are selected to measure the resistance by test piles. The results of equivalent load displacement curves are shown in Figure 3.44 to Figure 3.51. As shown in Figures, the equivalent load-displacement curves by newly plotting method are placed between conventional curve and conventional curve with elastic modulus. It is because that applied load transferred from rock layer of which elastic modulus is larger than soil layer during bi-directional load test. Also, elastic moduli of test piles are reducing with increasing load. Consequently, elastic displacements are also increasing.

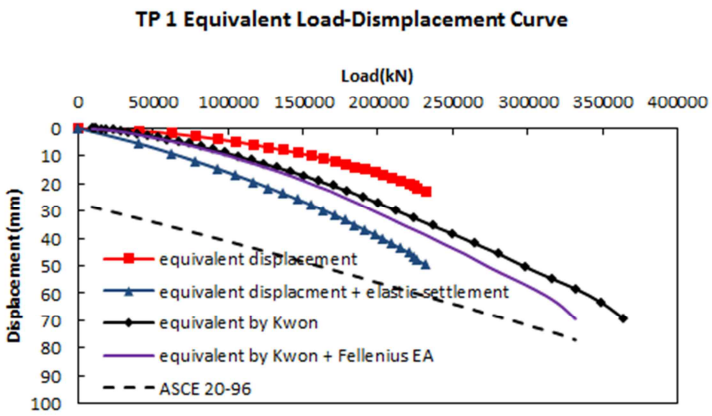

Figure 3.44 Equivalent load-displacement curve of TP 1

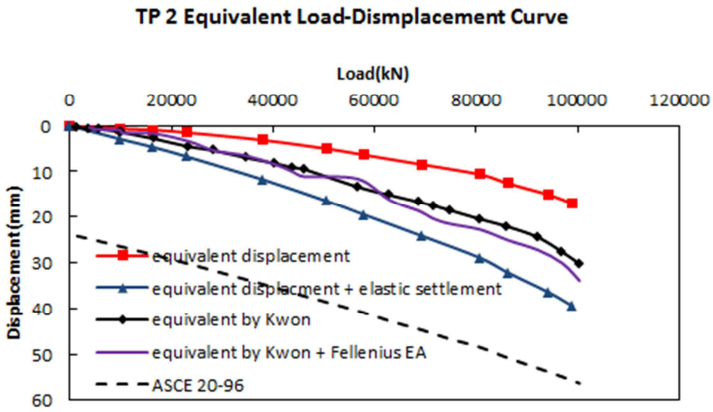

Figure 3.45 Equivalent load-displacement curve of TP 2

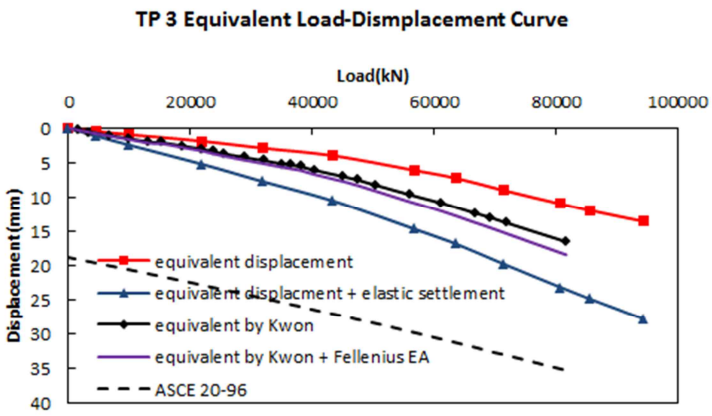

Figure 3.46 Equivalent load-displacement curve of TP 3

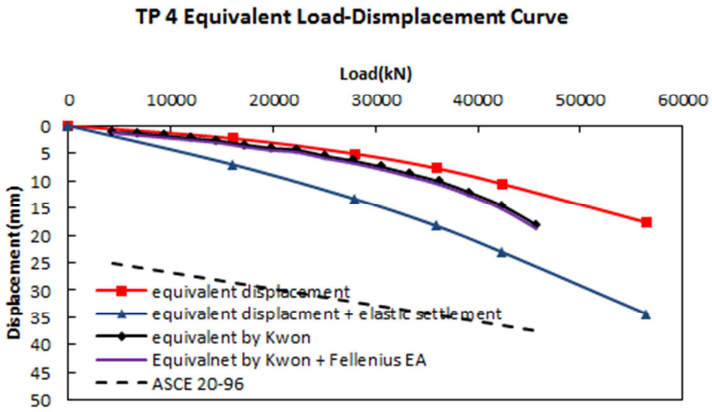

Figure 3.47 Equivalent load-displacement curve of TP 4

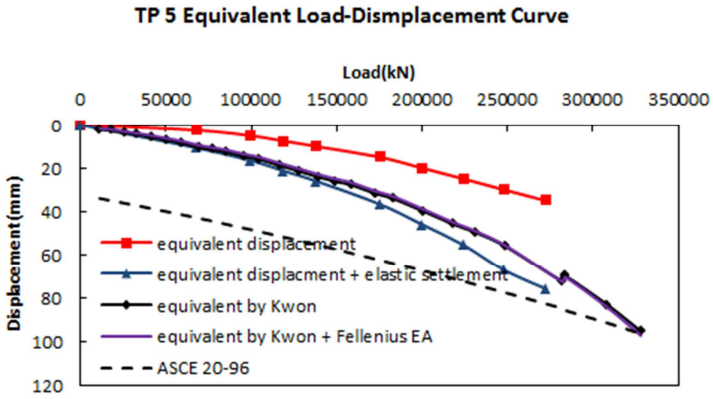

Figure 3.48 Equivalent load-displacement curve of TP 5

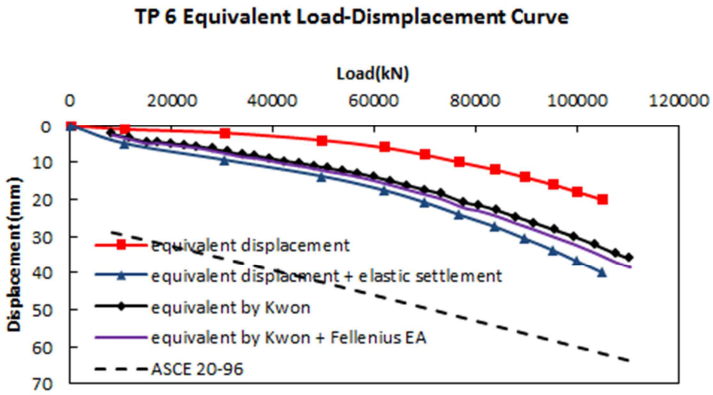

Figure 3.49 Equivalent load-displacement curve of TP 6

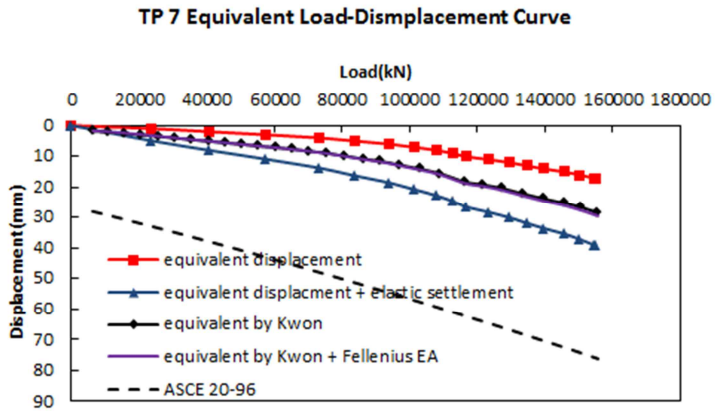

Figure 3.50 Equivalent load-displacement curve of TP 7

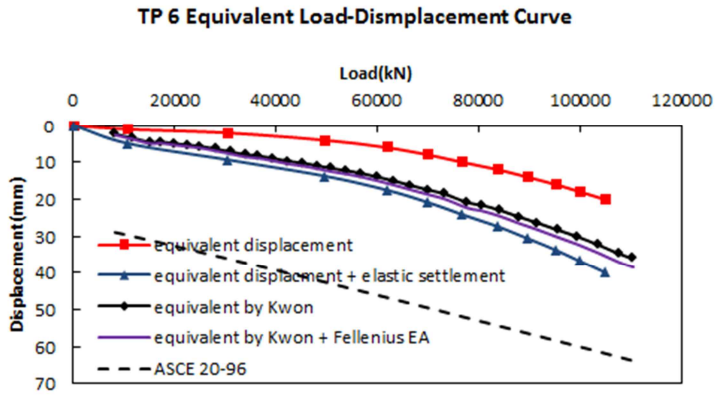

Figure 3.51 Equivalent load-displacement curve of TP 8

3.2.3 Determination of measured resistance from load test results

3.2.3.1 Measured shaft and base resistance

Load transfer analysis was performed to measure shaft and base resistances based on the pile load test results. Axial loads at each depth were calculated using the strain gage data, and the unit shaft resistance-displacement curves (f-w curve) for each depth and unit base resistance-displacement curves (q-w curve) at base of drilled shafts were then established using the calculated axial loads. There are some criteria for determining the ultimate shaft and base resistance from f-w curve and q-w curve. In this study, the ultimate shaft and base resistance is defined using O'Neill & Reese (1999) research. According to research by O'Neill & Reese (1999), ultimate shaft resistance is determined when the displacement of the pile is equal to 1% of the pile diameter. Thus, measured shaft resistance was determined when the displacement of the pile was equal to 1% of the pile diameter based on the f-w curve.

The shaft resistances were measured at 22 depths in the TP1~TP8 sites, of which the unconfined strength data were known. It is because that resistance characteristics are determined as the ratio of predicted resistance to measured resistance, so measured resistances without predicted resistances can't use for reliability analysis. Predicted resistances are calculated by bearing capacity equations using the unconfined strength, which was explained Chapter 3.3.

In the case of base resistance, most of the pile capacity increased linearly and ultimate base resistances were not defined at the end of loading. According to research by O'Neill & Reese (1999), ultimate base resistance is determined when the displacement of the pile is about to 5% of the pile diameter.

In this study, the displacement of test piles ranged about 0.73~14.26% of the pile diameter when loading was terminated, therefore, it is impossible to determine the measured shaft and base resistance using O'Neill & Reese criteria. In this cases, f-w curves and q-w curves were plotted and extrapolated by hyperbolic methods suggested by Jung (2010). Examples of determination of ultimate side and base resistance by extrapolated f-w curves and q-w curve are shown in Figure 3.52 and Figure 3.53. Also, determined shaft and base resistances for each test piles are summarized in Table 3.2 and Table 3.3.

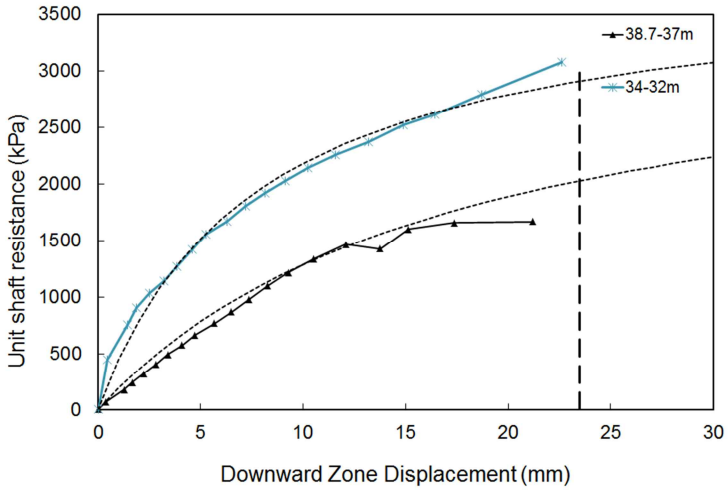

Figure 3.52 Example of determination of ultimate shaft resistance at TP 1

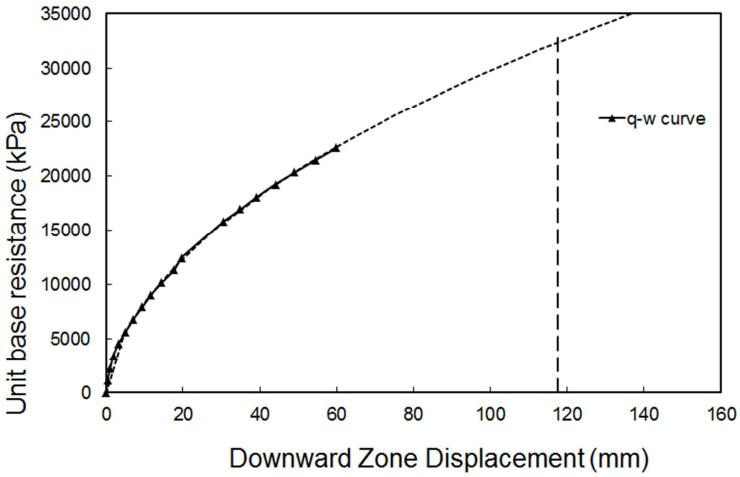

Figure 3.53 Example of determination of ultimate base resistance at TP 1

Table 3.2 Measured shaft resistance of test piles for each depth

	Depth(m)	Weathering degree	Measured shaft resistance(kPa)
TP1	32.0-34.0	SR	2912.45
	35.0-36.0	SR	1218.01
	36.0-37.0	SR	2446.51
	37.0-38.7	SR	1901.55
TP2	28.8-32.9	WR+SR	807.03
	32.9-33.9	SR	889.08
	33.9-35.3	SR	2058.23
TP3	26.9-28.0	SR	680.06
	28.0-29.0	SR	369.93
	29.0-30.0	SR	1402.69
	30.0-31.0	SR	1791.84
	31.0-33.1	SR	2687.67
TP4	24.0-30.5	WR	238.87
TP5	44.0-45.85	WR	324.04
	46.5-48.5	SR	2847.99
	48.5-50.5	SR	1996.79
	50.5-52.5	SR	1442.49
	52.5-54.5	SR	1515.30
TP7	45.5-50.2	SR	3348.91
TP8	46.26-48.26	WR	1215.68
	48.26-49.76	SR	1166.79
	49.76-51.35	SR	1604.19

Table 3.3 Measured base resistance of test piles

	Depth(m)	Weathering degree	Measured base resistance(kPa)
TP 1	38.96	SR	32331.29
TP 2	36.21	SR	40425.40
TP 3	33.41	HR	46678.54
TP 5	55.42	HR	55726.04
TP 7	51.2	SR	21168.36
TP 8	52.26	SR	35011.27
TP 9	33.5	WR	6417.82
TP 10	13.5	WR(HW)	10133.72
TP 11	13.5	WR(CW)	14752.66
TP 12	13.5	WR(MW)	32940.25
TP 13	13.5	WR(MW)	13238.29

3.2.3.2 Measured total resistance

There are various procedures for determining the ultimate total resistance from load-displacement curve of the pile load test. Among them, ASCE 20-96 method (ASCE, 1997) is selected to determine the ultimate total resistance in this study. It is because that this method was investigated for their universal validity by many previous researchers, and verified the application for rock in Korea. From researches by Jung (2010) and Park (2011), it is verified that ASCE 20-96 (1997) method gives the most conservative values with small standard deviation for determining ultimate total resistance. So, ultimate total resistance is determined using ASCE 20-96 method (1997). In ASCE 20-96 method (1997), ultimate total resistance is defined as the load when the displacement of the piles is equal to elastic displacement + 3.81 + D/100 mm. For determination of ultimate total resistance, equivalent load-displacement curves by procedure described in Chapter 3.2.2 are used, and if load test was terminated when applied load was not reached to ultimate resistance, equivalent load-displacement curve is extrapolated by hyperbolic method (Jung, 2010) like f-w curves and q-w curves. Examples of determination of ultimate total resistance by extrapolated equivalent load-displacement curve are shown in Figure 3.54 and determined total resistances for each test piles are summarized in Table 3.4.

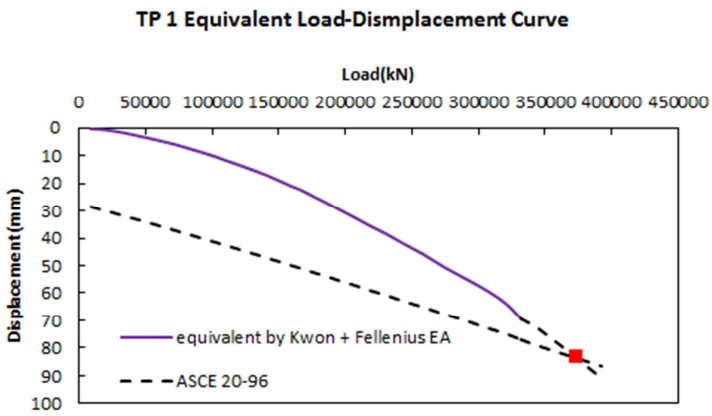

Figure 3.54 Example of determination of ultimate total resistance at TP 1

Table 3.4 Measured total resistance of test piles

	Depth(m)	Weathering degree1)	Measured total resistance(kN)
TP 1	38.96	WR + SR	373,863
TP 2	36.21	WR + SR	144,847
TP 3	33.41	WR + SR	151,503
TP 4	36.38	WR + SR	71,993
TP 5	55.42	WR + SR	335,885
TP 6	56.60	WR	190,161
TP 7	51.20	WR + SR	356,005
TP 8	52.26	WR + SR	200,610

3.3 Predicted Resistance by Bearing Capacity Equations

Predicted resistances are necessary to calibrate the resistance factors, and determination of representative predicted resistance is important. With measured resistances from load test data, predicted resistances are used for evaluating of pile resistance uncertainty. While measured resistances are determined from analyzing of load test data, predicted resistances are calculated by bearing capacity equation. There are many bearing capacity equations available to estimate resistance using rock mass properties, and some of them are empirical equations base on load test results.

In this study, predicted resistances were calculated by bearing capacity equation using unconfined compressive strength of rock core. Because that test piles are embedded in rock and unconfined compressive strengths of rock cores are easily obtained from field tests and laboratory test. Also, selected bearing capacity equations are widely used in actual work and specifications. Selected bearing capacity equations, required parameters, and remarks for predicted shaft, base, and total resistances are summarized in Table 3.5, Table 3.6 and Table 3.7. Furthermore, bearing capacity equations adopted by AASHTO (2007, 2010) are selected for comparison of results after determination of resistance factors.

Table 3.5 Bearing capacity equations for predicted shaft resistance

Resistance component	Design method	Bearing capacity equation	Parameter	Note
Shaft Resistance	Carter & Kulhawy (1988)	$f_s = 6.47\sqrt{q_u}(\text{kPa})$	q_u: Unconfined compressive strength of rock core (kPa)	Bearing capacity equations used in AASHTO (2010)
	Horvath & Kenney (1979)	$f_s = 6.88\sqrt{q_u}(\text{kPa})$	q_u: Unconfined compressive strength of rock core (kPa)	
	FHWA (1999)	$f_s = 0.65 \times p_a[q_u/p_a]^{0.5}(\text{kPa})$	p_a: atmospheric pressure =101kPa q_u: Unconfined compressive strength of rock core (kPa)	
	Rowe & Armitage (1987)	$f_s = 14.89\sqrt{q_u}(\text{kPa})$	q_u: Unconfined compressive strength of rock core (kPa)	

Table 3.6 Bearing capacity equations for predicted base resistance

Resistance component	Design method	Bearing capacity equation	Parameter	Note
Base Resistance	Carter & Kulhawy (1988)	$q_b = [s^{0.5} + (m \cdot s^{0.5} + s)^{0.5}]q_u(\text{MPa})$	m,s: mass properties q_u: Unconfined compressive strength of rock core (MPa)	Bearing capacity equations used in AASHTO (2010)
	FHWA(1999)	$q_b = 3K_{sp}\theta q_u(\text{MPa})$	K_{sp} : Emperical factor θ: Depth factor q_u: Unconfined compressive strength of rock core (MPa)	
	Zhang & Einstein (1998)	$q_b = 4.83q_u{}^{0.51}(\text{MPa})$	q_u: Unconfined compressive strength of rock core (MPa)	

Table 3.7 Bearing capacity equations for predicted total resistance

Resistance component	Design method	Bearing capacity equation	Parameter	Note
Total Resistance	Carter & Kulhawy (1988)	$f_s = 6.47\sqrt{q_u}(\text{kPa})$	q_u: Unconfined compressive strength of rock core (kPa)	Shaft resistance
		$q_b = [s^{0.5} + (m \cdot s^{0.5} + s)^{0.5}]q_u(\text{MPa})$	m,s: mass properties q_u: Unconfined compressive strength of rock core (MPa)	Base resistance
	FHWA (1999)	$f_s = 0.65 \times p_a[q_u/p_a]^{0.5}(\text{kPa})$	p_a: atmospheric pressure =101kPa q_u: Unconfined compressive strength of rock core (kPa)	Shaft resistance
		$q_b = 3K_{sp}\theta q_u(\text{MPa})$	K_{sp} : Emperical factor θ: Depth factor q_u: Unconfined compressive strength of rock core (MPa)	Base resistance

3.3.1 Shaft resistance

■ **Carter & Kulhawy (1988) and Rowe & Armitage (1987)**

Carter and Kulhawy (1988) suggested the empirical bearing capacity equation for shaft resistance based on the work of Rowe and Armitage (1984, 1987). Load tests are 25 cases of drilled shaft socketed into soft rock and main rock types are almost sedimentary rock like shale, sandstone, chalk, and mudstone. Relationships between shaft resistances with unconfined compressive strength of rock are shown in Figure 3.55. In each bearing capacity equations, unconfined compressive strengths are the value of intact rock. From the Figure 3.55, Carter and Kulhawy equation (1988) are based on lower value and Rowe and Armitage equation (1987) are based on mean value of relationship between shaft resistance and unconfined compressive strength of rock core.

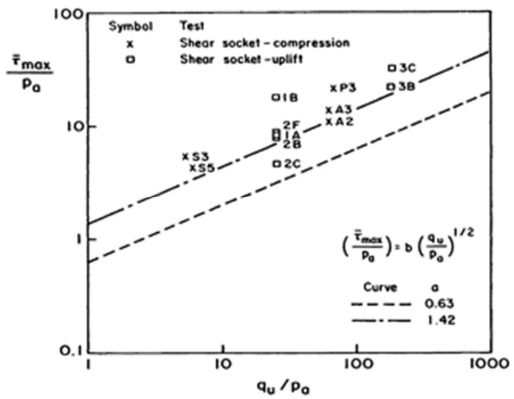

Figure 3.55 Relationships between peak side shear and uniaxial compressive strength of rock (Carter and Kulhawy, 1988)

Considering atmospheric pressure (101.3kPa) and unit conversion from MPa to kPa, bearing capacity equations by Carter and Kulhawy (1988) and Rowe and Armitage (1987) are defined as below.

Carter & Kulawy (1988): $f_s = 6.47\sqrt{q_u}(\text{kPa})$ (3.5)

Rowe & Armitage (1987): $f_s = 14.89\sqrt{q_u}(\text{kPa})$ (3.6)

■ **Horvath & Kenney (1979)**

Horvath and Kenny (1979) suggested shaft resistance for not artificially grooving smooth wall based on the results of pile load test conducted at Southern Ontario shale. If the piles are embedded in rock layer, the bore hole interface classified as smooth or rough. Also, empirical equations are suggested considering diameter of piles and unconfined compressive strength of rock core. Test pile diameter for this study range from 1m to 3m. These values are grouped as large diameter drilled shafts, larger than 16 in (410 mm) of Horvath & Kenney criteria. Considering unit conversion from MPa to kPa, bearing capacity equations by Horvath and Kenney (1979) are defined as following equation.

Horvath & Kenney (1979): $f_s = 6.88\sqrt{q_u}(\text{kPa})$ (3.7)

■ **FHWA (1999)**

Piers that excavated and constructed using conventional methods have a relatively smooth concrete-rock interface. An approximate relationship has been developed as follows.

FHWA (1999): $$f_s = 0.65 \times p_a[q_u/p_a]^{0.5}(\text{kPa}) \quad (3.8)$$

■ **Predicted shaft resistances**

Table 3.8 present a summary of the predicted shaft resistance calculated using each bearing capacity equations. In the same table, bias factors are also summarized. Bias factor is defined as the ratio of the measured to predicted resistance, and used for reliability analysis.

Table 3.8 Predicted resistances and bias factor for shaft resistance

	Depth(m)	Measured shaft resistance (kPa)	Carter & Kulhawy (1988)		Horvath & Kenney (1979)		FHWA (1999)		Rowe & Armitage (1987)	
			Predicted resistance (kPa)	Bias factor	Predicted resistance (kPa)	Bias factor	Predicted resistance (kPa)	Bias factor	Predicted resistance (kPa)	Bias factor
TP1	32.0-34.0	2912.45	471.02	6.18	500.87	5.81	475.57	6.12	1084.01	2.69
	35.0-36.0	1218.01	360.23	1.53	383.06	1.44	363.71	1.51	829.04	0.66
	36.0-37.0	2446.51	797.68	3.18	848.22	2.99	805.37	3.15	1835.76	1.38
	37.0-38.7	1901.55	768.27	2.09	816.95	1.96	775.68	2.07	1768.09	0.91
TP2	28.8-32.9	807.03	894.17	0.90	950.83	0.85	902.80	0.89	2057.84	0.39
	32.9-33.9	889.08	769.63	1.16	818.40	1.09	777.06	1.14	1771.22	0.50
	33.9-35.3	2058.23	1031.15	2.00	1096.49	1.88	1041.10	1.98	2373.08	0.87
TP3	26.9-28.0	680.06	571.41	1.19	607.63	1.12	576.93	1.18	1315.05	0.52
	28.0-29.0	369.93	650.23	0.57	691.43	0.54	656.50	0.56	1496.43	0.25
	29.0-30.0	1402.69	823.50	1.70	875.68	1.60	831.44	1.69	1895.19	0.74
	30.0-31.0	1791.84	809.40	2.21	860.69	2.08	817.21	2.19	1862.74	0.96

Table 3.8 Predicted resistances and bias factor for shaft resistance (Continued)

	Depth(m)	Measured shaft resistance (kPa)	Carter & Kulhawy (1988)		Horvath & Kenney (1979)		FHWA (1999)		Rowe & Armitage (1987)	
			Predicted resistance (kPa)	Bias factor	Predicted resistance (kPa)	Bias factor	Predicted resistance (kPa)	Bias factor	Predicted resistance (kPa)	Bias factor
TP3	31.0-33.1	2687.67	669.26	4.02	711.67	3.78	675.72	3.98	1540.23	1.74
TP4	24.0-30.5	238.87	274.50	0.87	291.89	0.82	277.15	0.86	631.73	0.38
TP5	44.0-45.85	324.04	2177.81	0.15	2315.81	0.14	2198.82	0.15	5011.98	0.06
	46.5-48.5	2847.99	2584.52	1.10	2748.30	1.04	2609.45	1.09	5947.99	0.48
	48.5-50.5	1996.79	2849.74	0.70	3030.33	0.66	2877.23	0.69	6558.36	0.30
	50.5-52.5	1442.49	2667.65	0.54	2836.70	0.51	2693.39	0.54	6139.30	0.23
	52.5-54.5	1515.30	1261.24	1.20	1341.16	1.13	1273.40	1.19	2902.60	0.52
TP7	45.5-50.2	3348.91	1361.47	2.46	1447.75	2.31	1374.60	2.44	3133.27	1.07
TP8	46.26-48.26	1215.68	279.04	4.36	296.72	4.10	281.73	4.32	642.17	1.89
	48.26-49.76	1166.79	384.41	3.04	408.77	2.85	388.12	3.01	884.67	1.32
	49.76-51.35	1604.19	552.80	2.90	587.83	2.73	558.13	2.87	1272.20	1.26

3.3.2 Base resistance

■ **Carter & Kulhawy (1988)**

Carter and Kulhawy (1988) suggested a lower bound solution for bearing resistance for a drilled shaft bearing on randomly jointed rock or socketed in a fractured rock mass. In this method, the rock has mass properties s, and m, which are roughly equivalent to c' (cohesion), and ϕ' (internal friction angle) for a soil, respectively. This method is appropriate for rock with joints that are not necessarily oriented preferentially and the joints may be open, closed, or filled with weathered material.

To estimate the mass properties s and m, the failure criterion of Hoek et al (2002) are used. Mass property m is a reduced value of the material constant and given by Equation (3.9), s is a constant for the rock mass given by the Equation (3.10). In Equation (3.11), m_i is recommended for gneiss, which is the representative rock type in Korea. Using the mass properties, base resistance is calculated by Equation (3.11)

$$\mathrm{m_b} = m_i \exp\left(\frac{GSI-100}{28}\right) \tag{3.9}$$

$$s = exp\left(\frac{GSI-100}{9}\right) \tag{3.10}$$

$$q_b = [s^{0.5} + (m \cdot s^{0.5} + s)^{0.5})]q_u \tag{3.11}$$

■ **FHWA (1999)**

FHWA recommends the use of Equation (3.12) for base resistance where the rock is sedimentary jointed and where the joints are primarily horizontal. This method involves both theoretical and empirical components. It is the method for estimating base resistance of drilled shafts in rock for which resistance factors are recommended in AASHTO.

$$q_b = 3K_{sp}\theta q_u(\text{MPa}) \tag{3.12}$$

Where, K_{sp} is bearing capacity factor based on vertical joint spacing and quality, and θ is depth factor. These factors are calculated by following Equations (3.13) and Equation (3.14).

$$K_{sp} = \frac{3+\frac{c}{B_s}}{10\sqrt{\left(1+\frac{300\ \delta}{c}\right)}} \tag{3.13}$$

$$\theta = 1 + 0.4\frac{L_s}{B_s} \tag{3.14}$$

Where, c is vertical spacing between joints, δ is thickness, or "aperture" of joints (open joints or joints filled with debris), B_s is diameter of the base of the drilled shaft, and L_s is the depth of the drilled shaft socket measured from the top of the rock surface (not from the ground surface).

According to CFEM (2006), the bearing-pressure coefficient,K_{sp} takes into account the size effect and the presence of discontinuities and includes a nominal safety factor of 3 against the lower-bound bearing capacity of the rock foundations.

- **Zhang & Einstein (1998)**

Zhang and Einstein (1998) developed empirical relationship between the unconfined compressive strength of rock core and the end bearing resistance of drilled shafts in rock using 39 load test and plotted in Figure 3.56. Bearing capacity equations by Zhang and Einstein (1998) is defined as Equation (3.15).

$$q_b = 4.83 {q_u}^{0.51} (\text{MPa}) \tag{3.15}$$

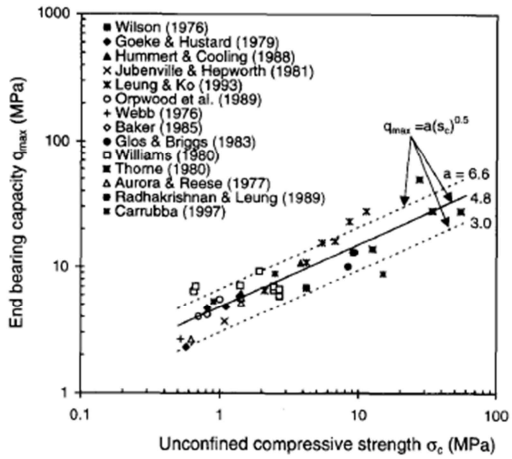

Figure 3.56 Design curves for q_{max} versus σ_c (Zhang and Einstein, 1998)

■ **Predicted base resistances**

Table 3.9 present a summary of the predicted base resistance calculated using each bearing capacity equations. In the same table, bias factors are also summarized. Bias factor is defined as the ratio of the measured to predicted resistance, and used for reliability analysis.

Table 3.9 Predicted resistances and bias factor for base resistance

	Depth(m)	Measured base resistance(MPa)	Carter & Kulhawy (1988)		FHWA (1999)		Zhang & Einstein(1999)	
			Predicted resistance (MPa)	Bias factor	Predicted resistance (MPa)	Bias factor	Predicted resistance (MPa)	Bias factor
TP 1	38.96	32.33	11.76	2.75	12.71	2.54	21.91	1.48
TP 2	36.21	40.43	10.64	3.80	18.92	2.14	26.42	1.53
TP 3	33.41	46.68	61.92	0.75	93.65	0.50	31.70	1.47
TP 5	55.42	55.73	105.72	0.53	151.32	0.37	49.83	1.12
TP 7	51.2	35.01	14.15	2.48	34.17	1.02	34.42	1.02
TP 8	52.26	23.94	26.30	0.91	19.94	1.20	31.12	0.77
TP 10	13.5	10.13	9.49	1.07	20.52	0.49	30.88	0.33
TP 11	13.5	14.75	9.49	1.55	21.43	0.69	30.88	0.48
TP 12	13.5	32.94	26.50	1.24	20.52	1.61	30.88	1.07
TP 13	13.5	13.24	33.49	0.40	20.52	0.65	30.88	0.43

3.3.3 Total resistance

In this study, predicted total resistances for each test piles are calculated as the sum of shaft and base resistances. This calculation method assumes that the shaft and base resistances can be determined separately and these two values do not affect each other. However, it is necessary to consider this assumption. According to AASHTO (2010), designs which consider combined effects of side friction and end-bearing of a drilled shaft in rock require that side friction resistance and end bearing resistance be evaluated at a common value of axial displacement, since maximum values of side friction and end-bearing are not generally mobilized at the same displacement.

Where combined side friction and end-bearing in rock is considered, the designer needs to evaluate whether a significant reduction in side resistance will occur after the peak side resistance is mobilized. As indicated in Figure 3.57, when the rock is brittle in shear, much shaft resistance will be lost as vertical movement increases to the value required to develop the full value of base resistance. If the rock is ductile in shear, i.e., deflection softening does not occur, then the side resistance and end-bearing resistance can be added together directly. If the rock is brittle, however, adding them directly may be unconservative.

To consider the reduction in side resistance for this study, f-w curves of this study from Figure 3.14 to 3. 30 are reviewed. As a result, almost f-w curves for shaft resistances shows ductile behavior, and there are not deflection softening. Therefore, predicted total resistances for each test piles

are calculated as the sum of shaft and base resistances in this study.

For predicted total resistance, bearing capacity equations suggested by Carter & Kulhawy (1988) and FHWA (1999) are selected and summarized in Table 3.7. The results of predicted base resistance calculation and bias factors for total resistance are summarized in Table 3.10.

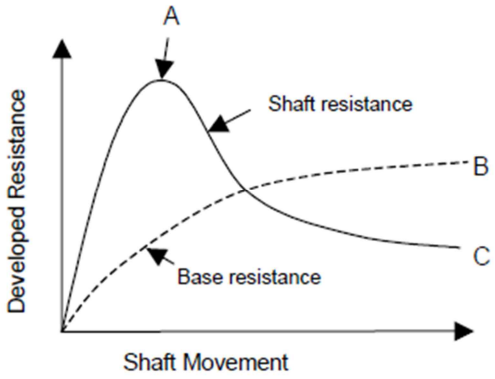

Figure 3.57 Design curves for q_{max} versus σ_c (Zhang and Einstein, 1998)

Table 3.10 Predicted resistances and bias factor for total resistance

	Depth(m)	Measured total resistance (MN)	Carter & Kulhawy (1988)		FHWA (1999)	
			Predicted resistance (MN)	Bias factor	Predicted resistance (MN)	Bias factor
TP 1	38.96	373.86	83.60	4.47	88.07	4.25
TP 2	36.21	144.85	64.49	2.25	87.09	1.66
TP 3	33.41	151.50	107.23	1.41	152.83	0.99
TP 5	55.42	335.88	854.78	0.39	1147.41	0.29
TP 7	51.2	356.00	101.48	3.51	181.52	1.96
TP 8	52.26	200.61	118.79	1.69	93.65	2.14

3.4 Summary

The purpose of this chapter was evaluation the resistance of test piles. To determine the measured and predicted resistance, collecting the load test data, calibration for measured resistance, and review of bearing capacity equations were performed. The summary of this chapter were presented in below.

1. For this study, load tests data were reviewed. First of all, target pile foundation type of this thesis was selected as drilled shafts. Secondly, bi-directional load test for drilled shafts was mainly selected for this study. Also, load test data with strain gauge in test piles were collected for accurate measurements of shaft and base resistance. Synthesizing the overall considerations, 13 sets of load test results of drilled shafts were collected for this study.

2. When the measured resistances were determined from pile-load tests, some calibrations were performed to determine the more accurate and realistic resistances. In load transfer analysis steps for shaft and base resistances, reduction of elastic modulus of drilled shafts was considered using the method suggested by Fellenius (1989). Also in step of equivalent load-displacement curve for total resistances, the modified method for equivalent load-displacement curve suggested by Kwon (2006) was adopted. Based on calibrated results, f-w curves, q-w curves, and equivalent load-displacement curves for each test piles were obtained.

From these results with extrapolation method suggested by Jung (2010), measured shaft, base, and total resistances were determined.

3. Predicted resistances were calculated by bearing capacity equation using unconfined compressive strength of rock core: shaft resistance (Carter and Kulhawy, 1988; Horvath and Kenney, 1979; FHWA, 1999; Rowe and Armitage, 1987); base resistance (Carter and Kulhawy, 1988; FHWA, 1999; Zhang and Einstein, 1987); and total resistance (Carter and Kulhawy, 1988; FHWA, 1999).

4. Determination of Resistance Factor

4.1 Introduction

Load Resistance Factor Design (LRFD) method uses partial factor of safety on both load and resistance, and enables identification and separation of different uncertainties in loading and resistance. The use of separate of load and resistance factors is logical because load and resistance have largely separate and unrelated sources of uncertainty. Among these terms, the factored resistance combines all uncertainty associated with the calculation of resistance into one term, a resistance factor. The value of a resistance factor reflects the probability that the actual resistance may be smaller than the calculated nominal resistance using characteristic values of soil strength as a result of the uncertainties associated with the strength parameters, geometry, the theoretical model or analysis used to calculate resistance, and the consequence of failure. The LRFD criterion can be expressed as following Equation (4.1).

$$\varphi R_n \geq \sum \gamma_i Q_i \tag{4.1}$$

where, φ is the resistance factor, R is the nominal resistance, $\gamma_i$is the load factor, and Q_i is the load.

The procedure for calibration of resistance factors for this thesis is summarized in below.

i. Collect available load test data
ii. Evaluate the measured capacity of all cases from pile load test
iii. Evaluate the predicted capacity of drilled shaft for all static analysis methods
iv. Calculate the ratio of the measured capacity to predicted capacity (bias factor)
v. Develop statistical parameters for the load and resistance
vi. Research and establish recommended probability of failure or target reliability index
vii. Calculate and recommended the resistance factors

Steps for i) to iv) are explained in previous Chapter 3, and the rest steps for determination of resistance factor are presented in this Chapter 4.

4.2 Determination of Statistical Parameters

4.2.1 Load statistics

To perform the reliability analysis for determination of resistance factors, load information in terms of statistics of load bias factors and resistance information in terms of statistics of resistance bias factors. Contrary to

resistance statistics, load statistics are known that regional variations are negligible. So, it is assumed that the load statistics in Korea are not significantly different from those in the US, therefore, this thesis is used the load statistical characteristics and load factors from the current AASHTO LRFD Specifications (2010) to make the consistent design between drilled shaft and superstructure design.

In this thesis, the load combination of dead load and live load for the Strength I case (AASHTO, 2010) is selected, because this combination is considered the most conservative for the calibration of the resistance factors of axially loaded pie and usually used the governing design load case for bridge design. Load combination of Strength I case is shown in Equation (4.2).

$$Q = QD + QL \tag{4.2}$$

where, QD is dead load of structural components and nonstructural attachments, and QL is vehicular live loads.

The load factors used in this thesis are 1.25 for dead load and 1.75 for live load. Also, the load statistics are presented in terms of mean and coefficient of variation (COV) of the bias factors. Nowak (1999) presented the results of statistical analysis of dead and live loads in calibration of LRFD bridge design code, and these values were adopted by AASHTO (2010). The load factors and load statistical parameters are summarized in Table 4.1. The distribution of the bias factors of dead and live loads is assumed to be log-

normal distribution.

Table 4.1 Statistical characteristics of load (Nowak, 1999; AASHTO, 2010)

Load Factor of Dead Load (γ_D=1.25)		Load Factor of Live Load (γ_L=1.75)	
Bias factor(λ_D)	Coefficient of Variation (COV_D)	Bias factor(λ_L)	Coefficient of Variation (COV_L)
1.05	0.10	1.15	0.20

The ratio of dead load to live load is a function of bridge span length expressed by below Equation (4.3).

$$QD/QL = (1 + IM)(0.0132L) \quad (4.3)$$

Where, IM means the dynamic load impact factor (=0.33 for LRFD load), and L is the bridge span length (=feet, most common span length of Korea is 98 feet, KICT; 2008).Thus, load ratio of 1.72 was chosen for reliability analysis for this study.

4.2.2 Resistance statistics

Statistical characteristics of resistance are represented in terms of the bias factor, which is evaluated using the predicted resistance and measured

resistances and defined as the ratio of the measured to predicted resistance. The bias factor is used as an index of the uncertainty of ground, design and bearing capacity equations, and resistance. The bias factor was calculated for all data set but the statistical characteristics of bias factor were influenced by both the size of data set and the variation. According to Paikowsky (2004), it is necessary to check the number of case histories needed to be eliminated when limiting the set being investigated to those within the two standard deviation band. Extremely outlining data points may not representative of the resistance due to large error, therefore, the bias factor values outside the boundary defined by the mean plus two times the standard deviation were omitted. Determined resistance statistical characteristics for this thesis are summarized in Table 4.2, Table 4.3, and Table 4.4 for each resistance category and bearing capacity equations. Also, as stated in previous part, the distributions of the bias factors for resistances are assumed to be log-normal distribution like load distribution.

Table 4.2 Statistical characteristics of shaft resistance

Design method	Pile No.	Bias factor (λ_R)	Standard deviation	Coefficient of Variation (COV_R)
Carter & Kulhawy (1988)	21	1.80	1.17	0.65
Horvath & Kenney (1979)	21	1.70	1.10	0.65
FHWA (1999)	21	1.79	1.16	0.65
Rowe & Armitage (1987)	21	0.78	0.51	0.65

Table 4.3 Statistical characteristics of base resistance

Design method	Pile No.	Bias factor (λ_R)	Standard deviation	Coefficient of Variation (COV_R)
Carter & Kulhawy (1988)	9	1.30	0.83	0.64
FHWA (1999)	10	1.12	0.75	0.67
Zhang & Einstein (1998)	10	0.97	0.45	0.47

Table 4.4 Statistical characteristics of total resistance

Design method	Pile No.	Bias factor (λ_R)	Standard deviation	Coefficient of Variation (COV_R)
Carter & Kulhawy (1988)	6	2.29	1.48	0.65
FHWA (1999)	6	1.88	1.34	0.71

4.3 Determination of Target Reliability Index

4.3.1 Reliability analysis method

4.3.1.1 MVFOSM (Mean Value First-Order Second-Moment) method

The MVFOSM is Mean Value First-Order Second-Moment analysis. The MVFOSM is based on a first-order Taylor series approximation of the limit state function linearized at the mean values of the random variables (e.g. load and resistance), and it uses only second-moment statistics (means and COVs) of the random variables. From the LRFD basic equation, both load (Q) and resistance (R) follow a lognormal distribution, and the limit state function is defined as below equation.

$$g(R,Q) = \ln(R) - \ln(Q) = \ln(R/Q) \tag{4.4}$$

If the variables R and S are statistically independent with lognormal distribution, the mean value of $g(R,Q)$ can be expressed as:

$$\overline{g} = \overline{\ln(R)} - \overline{\ln(Q)} \tag{4.5}$$

where, $$\overline{\ln(R)} = \ln(\overline{R}) - \frac{1}{2}\ln(1 + COV_R^2) \quad (4.6)$$

$$\overline{\ln(Q)} = \ln(\overline{Q}) - \frac{1}{2}\ln(1 + COV_Q^2) \quad (4.7)$$

Substitute the Equation (4.6) and (4.7) into Equation (4.5),

$$\overline{g} = \ln\left(\frac{\overline{R}}{\sqrt{1+COV_R^2}}\right) - \ln\left(\frac{\overline{Q}}{\sqrt{1+COV_Q^2}}\right) = \ln\left[\frac{\overline{R}}{\overline{Q}}\sqrt{\frac{1+COV_Q^2}{1+COV_R^2}}\right] \quad (4.8)$$

And the standard deviation is defined as:

$$\zeta_g = \sqrt{\sigma^2_{\overline{\ln(R)}} + \sigma^2_{\overline{\ln(Q)}}} \quad (4.9)$$

Where, $$\sigma^2_{\overline{\ln(R)}} = \ln(1 + COV_R^2) \quad (4.10)$$

$$\sigma^2_{\overline{\ln(Q)}} = \ln(1 + COV_Q^2) \quad (4.11)$$

$\overline{R}$, $\overline{Q}$: mean values of resistance and load, respectively

COV_R, COV_Q : Coefficient of Variation of resistance and load, respectively

Substitute the Equation (4.10) and (4.11) into Equation (4.9),

$$\zeta_g = \sqrt{\ln(1+COV_R^2) + \ln(1+COV_Q^2)} = \sqrt{\ln(1+COV_R^2)(1+COV_Q^2)} \quad (4.12)$$

From the definition, the reliability index (β) is the ratio of $\overline{g}$ to ζ_g :

$$\beta = \frac{\overline{g}}{\zeta_g} = \frac{\ln\left[\frac{\overline{R}}{\overline{Q}}\sqrt{\frac{1+COV_Q^2}{1+COV_R^2}}\right]}{\sqrt{\ln(1+COV_R^2)(1+COV_Q^2)}} \quad (4.13)$$

The mean values of the load and resistance are:

$$\overline{Q} = \lambda_Q Q_n \quad (4.14)$$

$$\overline{R} = \lambda_R R_n \quad (4.15)$$

Therefore, Equation (4.13) can be expressed as follows:

$$\beta = \frac{\overline{g}}{\zeta_g} = \frac{\ln\left[(\lambda_R R_n / \lambda_Q Q_n)\sqrt{(1+COV_Q^2)/(1+COV_R^2)}\right]}{\sqrt{\ln(1+COV_R^2)(1+COV_Q^2)}} \quad (4.16)$$

R_n and Q_n can be expressed in terms of factor of safety (FS) like this ;

$R_n = FS \times Q_n$. In the Strength I load combination, load considers dead load (QD) and live load (QL). So, $R_n = FS \times (QD + QL)$, $\overline{Q} = \lambda_Q Q_n = \lambda_{QD} QD + \lambda_{QL} QL$. And, QD and QL are assumed in the statistically independent, so $COV_Q^2 = COV_{QD}^2 + COV_{QL}^2$.

Therefore, as using above relationship, Equation (4.16) can be rewritten as:

$$\beta = \frac{\ln\left[\left(\frac{\lambda_R FS(Q_D/Q_L+1)}{\lambda_{QD}Q_D/Q_L+\lambda_{QL}}\right)\sqrt{(1+COV_{QD}^2+COV_{QL}^2)/(1+COV_R^2)}\right]}{\sqrt{\ln(1+COV_R^2)(1+COV_{QD}^2+COV_{QL}^2)}} \quad (4.17)$$

From Equation (4.17), the reliability index, β, is seen as a function of the load statistics (COV_{QD}, COV_{QL}, λ_{QD}, λ_{QL}), factor of safety, the ration of dead load to live load, and the resistance statistics (λ_R, COV_R).

The ratio of dead load to live load is a function of bridge span length (Kim, 2002). Hansell and Viest (1971) suggested that the load ratio could be expressed by the empirical equation as:

$$QD/QL = (1+IM)(0.0132L) \quad (4.18)$$

Where, IM: the dynamic load impact factor (=0.33 for LRFD load), L: bridge span length (=feet, most common span length of Korea is 98 feet, KICT;2008)

This method was used for reliability analysis and the resistance factor calibration in this thesis. It is noted that the limit state function of the MVFOSM method is linearized at the mean values of random variables. When limit state function is non-linear, significant error may be introduced by neglecting higher order terms. And the reliability index fails to be constant under different but mechanically equivalent formulations of the same limit state function. To overcome these problems, Advanced First-Order Second Moment (AFOSM) method is also used in this thesis.

4.3.1.2 AFOSM (Advanced First-Order Second-Moment) method

The AFOSM method is considered to be one of the most accurate methods for reliability analysis. If the limit state function for both load and resistance is linear and all the variables are statistically independent with normal distribution, the reliability index calculated by two methods will be the same. But this situation does not occur in engineering problems. So, the AFOSM method suggested by Hasofer and Lind (1974) are used when they are normal. In this study, explanation of procedures follows those described by Haldar and Mahadevan (2000). The basic concept was developed by Hasofer and Lind (1974). In the Hasofer and Lind method, the original limit state, $g(X') = 0$, is transformed into the reduced limit state, $g(X') = 0$ using below equation.

$$X_i^{'} = \frac{X_i - \mu_{X_i}}{\sigma_{X_i}} \quad (i=1, 2, 3,\ldots..n) \tag{4.19}$$

Where, $X_i^{'}$: a random variable with zero mean and unit standard deviation

The reliability index is defined as the minimum distance from the origin of the reduced coordinate system to the limit state surface. It can be expressed as:

$$\beta_{HL} = \sqrt{(X^{'*})^t (X^{'*})} \tag{4.20}$$

Where, X^* : the vector in the original coordinate system

$X^{'*}$: the vector in the reduced coordinate system

And the minimum distance point on the limit state surface is called the design point or checking point. Hence, the reduced variables are defined as:

$$R^{'} = \frac{R - \mu_R}{\sigma_R} \tag{4.21}$$

$$Q^{'} = \frac{Q - \mu_Q}{\sigma_Q} \tag{4.22}$$

Where, μ_R , μ_Q : the means of resistance and load, respectively

σ_R , σ_Q : standard deviation of resistance and load, respectively

Substituting Equation (4.21) and (4.22) into limit state function becomes as:

$$g(R,Q) = \sigma_R R' - \sigma_Q Q' + \mu_R - \mu_Q \tag{4.23}$$

The coordinates of the intercepts of Equation (4.23) on the R' and Q' axes can be shown to be $[-(\mu_R - \mu_Q)/\sigma_R, 0]$ and $[0, (\mu_R - \mu_Q)/\sigma_S]$, respectively. Using simple trigonometry, it can calculate the distance of the limit state surface from the origin as:

$$\beta_{HL} = \frac{\mu_R - \mu_Q}{\sqrt{\sigma_R^2 + \sigma_Q^2}} \tag{4.24}$$

But as stated previous, the deficiency in the Hasofer and Lind method is the applicable only for normal variables. If all the variables are not normally distributed, it is necessary to transform the non-normal variables into equivalent normal variables. So, this study used the iteration algorithm known as the Rackwitz-Fiessler (1976) method. Iteration procedures summarized below.

i. Define the limit state function (g)

$$g = \ln\left(\frac{FS * \lambda_R * (Q_D / Q_L + 1)}{\lambda_{QD} * Q_D / Q_L + \lambda_{QL}}\right) \tag{4.25}$$

ii. Assume an initial value of the reliability index(β). Generally, an initial β value of 3.0 is reasonable.

iii. Assume the initial values of design point (x_i^*). The initial design point can be assumed to be the mean values of the random variables.

iv. Compute the mean and standard deviation at the design point of the equivalent normal distribution for non-normal variables (the distribution type of this study is lognormal).

Lognormal standard deviation: $\xi = \sqrt{\ln(1 + COV^2)}$

Mean: $\lambda = \ln(\mu) - 0.5\xi^2$

Equivalent normal standard deviation: $\sigma_x^N = \xi * dp$

Mean: $\mu_x^N = dp * (1 - \ln(dp) + \lambda)$

v. Compute partial derivatives $\left(\frac{\partial g}{\partial X_i}\right)^*$ evaluated at the design point x_i^*

vi. Compute the direction cosines α_i at the design point as:

$$\alpha = \frac{\left(\frac{\partial g}{\partial X_i}\right)^* \sigma_{X_i}^N}{\sqrt{\sum_{i=1}^{n}\left(\frac{\partial g}{\partial X_i}\sigma_{X_i}^N\right)^{2^*}}}$$

vii. Compute the new values for checking point x_i^* as :

$$x_i^* = \mu_{X_i}^N - \alpha_i \beta \sigma_{X_i}^N$$

Repeat from step iv) to step vii) until the direction cosines converge to a specified tolerance level of 0.0005

viii. When α converges, the new design points can be expressed in terms of β. This new design must be satisfied at the limit state function.

ix. Substitute the random variables into the limit state function with these new design points and solve for β from Equation (4.25) in step i).

x. Repeat step iii) through step ix) until β converges to a tolerance value of 0.0001

4.3.2 Calculation of reliability index of the current design practice

To consider a transition period from Allowable Stress Design (ASD) to Load Resistance Factor Design (LRFD), reliability analysis was performed and reliability index of the current design practice, ASD, were estimated. The Korean design standard for foundation structures requires a safety factor of 3.0 for pile bearing capacity design, and the range of factor of safety ranged from 2.0 to 3.0 which were generally practiced in construction. Therefore, reliability analysis was performed for factor of safety from 2.0 to 5.0 using MVFOSM and AFOSM methods. The results of reliability analysis are summarized in Table 4.5 for shaft resistance, Table 4.6 for base resistance, and Table 4.7 for total resistance.

Table 4.5 Reliability analysis results for shaft resistance

Bearing capacity Equation	FOS	Reliability Index			
		2.0	3.0	4.0	5.0
Carter & Kulhawy (1988)	AFOSM	1.73	2.40	2.88	3.25
	MVFOSM	1.66	2.30	2.76	3.11
Horvath & Kenney (1979)	AFOSM	1.62	2.30	2.78	3.15
	MVFOSM	1.56	1.92	2.66	3.01
FHWA (1999)	AFOSM	1.71	2.39	2.87	3.24
	MVFOSM	1.65	2.23	2.74	3.10
Rowe & Armitage (1987)	AFOSM	0.34	1.01	1.49	1.86
	MVFOSM	0.34	0.98	1.44	1.79

Table 4.6 Reliability analysis results for base resistance

Bearing capacity Equation	FOS	Reliability Index			
		2.0	3.0	4.0	5.0
Carter & Kulhawy (1988)	AFOSM	1.20	1.89	2.37	2.75
	MVFOSM	1.16	1.81	2.27	2.63
FHWA (1999)	AFOSM	0.89	1.41	2.02	2.38
	MVFOSM	0.87	1.50	1.94	2.29
Zhang & Einstein (1998)	AFOSM	1.08	1.97	2.60	3.08
	MVFOSM	1.02	1.83	2.41	2.86

Table 4.7 Reliability analysis results for total resistance

Bearing capacity Equation	FOS	Reliability Index			
		2.0	3.0	4.0	5.0
Carter & Kulhawy (1988)	AFOSM	2.12	2.80	3.26	3.65
	MVFOSM	2.04	2.68	3.13	3.49
FHWA (1999)	AFOSM	1.61	2.24	2.68	3.03
	MVFOSM	1.56	2.16	2.59	2.91

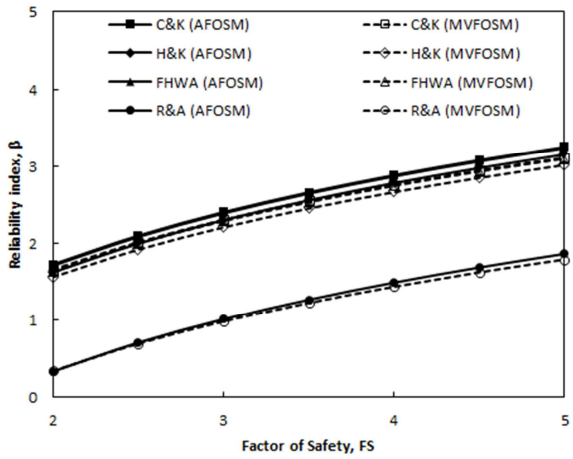

Figure 4.1 Comparison of reliability indices for shaft resistance by AFOSM and MVFOSM

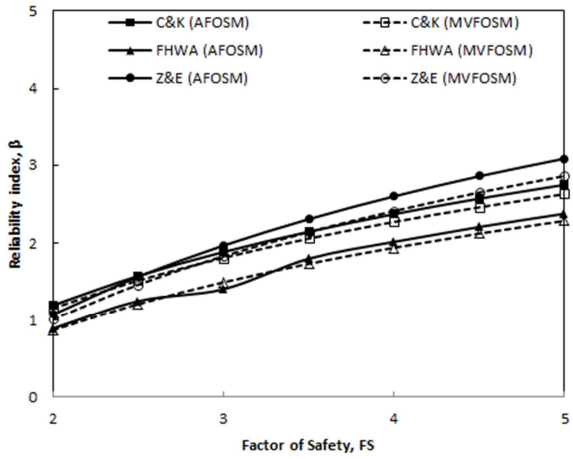

Figure 4.2 Comparison of reliability indices for base resistance by AFOSM and MVFOSM

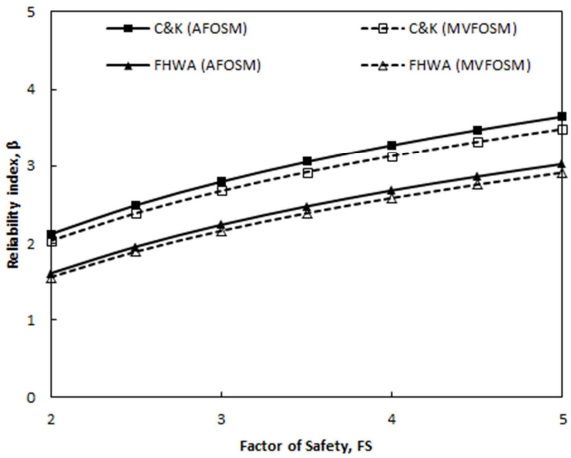

Figure 4.3 Comparison of reliability indices for total resistance by AFOSM and MVFOSM

The calculated reliability indices vary along with bearing capacity equations. This means that the different bearing capacity equations provide different levels of reliability, even though they have same factor of safety. The reliability indices from Carter and Kulhawy (1988) for shaft resistance, Zhang and Einstein (1998) for base resistance, and Carter and Kulhawy (1988) for total resistance are largest values. This results mean that these bearing capacity equations are conservative than other equations for each resistance at same factor of safety, and calibrated resistance factors using these equations may be larger than other equations. Also, AFOSM method resulted in a higher reliability index than MVFOSM method on the average. These results support that AFOSM method is more reliable than MVFOSM method. The reliability indices from AFOSM method with the factor of safety range of 2.0-5.0 are

summarized in Table 4.8

Table 4.8 Reliability analysis results (AFOSM, FS: 2.0-5.0)

Resistance	Bearing Capacity Equations	Reliability index (AFOSM, FS: 2.0-5.0)
Shaft Resistance	Carter & Kulhawy (1988)	1.73-3.25
	Horvath & Kenney (1979)	1.62-3.15
	FHWA (1999)	1.71-3.24
	Rowe & Armitage (1987)	0.34-1.86
Base Resistance	Carter & Kulhawy (1988)	1.20-2.75
	FHWA (1999)	0.89-2.38
	Zhang & Einstein (1998)	1.08-3.08
Total Resistance	Carter & Kulhawy (1988)	2.12-3.65
	FHWA (1999)	1.61-3.03

4.3.3 Determination of target reliability index

The target reliability index will be determined based on the results of reliability analysis of the current Allowable Stress Design method and previous research.

In previous researches, Meyerhof (1970) suggested the probability of failure of foundation as 10^{-3}~10^{-4} corresponding to reliability index of 3.0~3.6, and Wu et al. (1989) suggested the probability of failure of offshore piles as corresponding to reliability index of 2.0~3.0. Also, Barker et al. (1991) selected a target reliability index of 1.5 to 2.8 for driven pile, and Mcvay et al. (2003) suggested a target reliability index of 3.5 for statnamic load test. In

NCHRP Report 507 (2004), target reliability index of 2.33 for highly redundant system, such as pile groups, and 3.0 for nonredundant piles are selected. Recently, AASHTO LRFD (2010) selected the target reliability index of 3.0 for typical drilled shaft. Moreover, KICT (2008) suggested the target reliability index as 2.0~2.5 for driven pile and 3.0~3.5 for drilled shaft. It can be seen that the reliability indices implicit in existing global factor of safety designs lie in the approximate range of 2.6 to 3.7.

Other important data to consider include the failure rates estimated from actual case histories. However, these failure rates cannot be used directly for assessing the target reliability index, because the theoretical probability of failure obtained from reliability theory usually is one order of magnitude smaller than the actual failure rate. An example of empirical rates of failure for civil engineering facilities and the related costs of failure is given in Figure 4.4. For foundations, the empirical rate of failure lies between 0.1 and 1%. This failure rate implies a theoretical probability of failure in the neighborhood of 0.01 to 0.1%. In terms of the reliability index, the currently accepted risk level, therefore, is between 3.1 and 3.7.

Therefore, to consider a transition period from ASD to LRFD, the target reliability indices were determined based on reliability analysis results and previous research. Considering that Korean design standard for foundation structure requires a safety factor of ASD, reliability analysis results shown in Table 4.8 are used. And the target reliability indices ranged from 2.5 to 3.7 in previous researches. Thus, the target reliability index of 2.5, 3.0 and 3.5 were selected for the calibration of resistance factors in this thesis. These values correspond to probability of failure between 0.6%, 0.1% and 0.02%

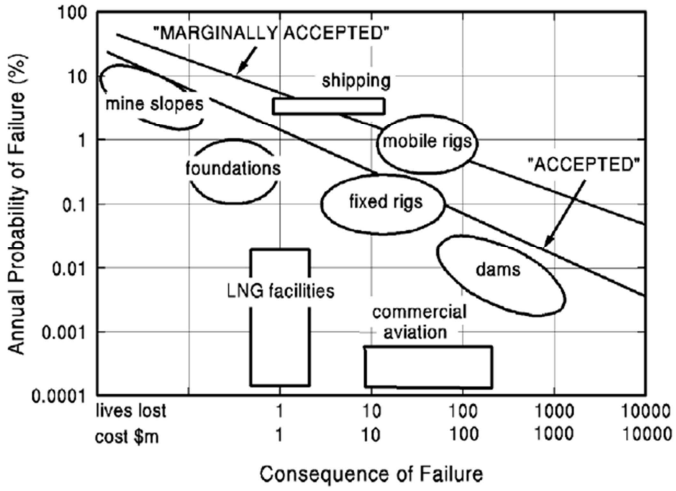

Figure 4.4 Empirical rates of failure for civil engineering facilities (Baeher, 1987; Kulhawy, 1996)

Table 4.9 Relationship between reliability index and probability of failure (Kulhawy, 1996)

Reliability index	Probability of failure
1.0	0.159
1.5	0.0668
2.0	0.0228
2.5	0.00621
3.0	0.00135
3.5	0.000233
4.0	0.0000316

4.4 Determination of Resistance Factors

4.4.1 Resistance factor calibration method using AFOSM method

AFOSM method resulted in a higher reliability index than MVFOSM method on the average. These results support the general belief that AFOSM method is more reliable and accurate than MVFOSM method.

So, only AFOSM method is utilized for calibration of resistance factors in this study.

The limit state function for the calibration of resistance factor is defined as:

$$g = \ln \overline{R} - \ln(\sum Q_i) = \ln \frac{\overline{R}}{\sum Q_i} \tag{4.26}$$

Considering that the dead load and the live load, and Equation (4.26) can be expressed as following equation.

$$g = \ln \left[\frac{\lambda_R R_n}{\lambda_{QD} Q_D + \lambda_{QL} Q_L} \right] \tag{4.27}$$

And the basic LRFD equation is:

$$\phi R_n = \lambda_{QD} Q_D + \lambda_{QL} Q_L \tag{4.28}$$

Substituting Equation (4.28) into Equation (4.27) and dividing the numerator and the denominator by Q_L , the limit state function can be expressed as following equation.

$$g = \ln\left[\frac{\lambda_R(\gamma_{QD} Q_D / Q_L + \gamma_{QL})}{\phi(\lambda_{QD} Q_D / Q_L + \lambda_{QL})}\right] \tag{4.29}$$

Equation (4.29) is very similar to limit state function for reliability analysis. Like the algorithm used reliability analysis, iteration procedures are performed.

4.4.2 Determination of resistance factors

In this study, calibration was performed only for the resistance factors because load factors suggested by AASHTO (2010) were used for reliability analysis. As mentioned in previous Chapter 4.2, load statistics are known that

regional variations are negligible. So, it is assumed that the load statistics in Korea are not significantly different from those in the US, therefore, this thesis is used the load statistical characteristics and load factors from the current AASHTO LRFD Specifications (2010) to make the consistent design between drilled shaft and superstructure design.

Resistance factor calibration methods were used both MVFOSM and AFOSM with determined target reliability index 2.5, 3.0, and 3.5

4.4.2.1 Shaft resistance

Calibration results are shown as relationship between reliability index and resistance factor. Figure 4.5 shows the results of calibration results for shaft resistance. Resistance factors decreases with the increase of the reliability index. Also, resistance factors by Carter and Kulhawy (1988), Horvath and Kenney (1979), and FHWA (1999) are similarly obtained, however, resistance factors by Rowe and Armitage (1987) are smaller than that by other bearing capacity equations. This means that Rowe and Armitage (1987) bearing capacity equation is unconservative method to predict the resistance compared with other bearing capacity equations.

The resistance factors for shaft resistance with determined target reliability index of 2.5, 3.0, and 3.5 are shown in Table 4.10. Note in table shows the resistance factor suggested by AASHTO with target reliability index of 3.0 (β_T=3.0). For target reliability index of 3.0(AASHTO

recommended value), shaft resistance factors for each bearing capacity equations are in range of 0.13 to 0.32. These values are about 30~60% in comparison with AASHTO suggested resistance factors. It is due to discrepancy of target rock for bearing capacity equations.

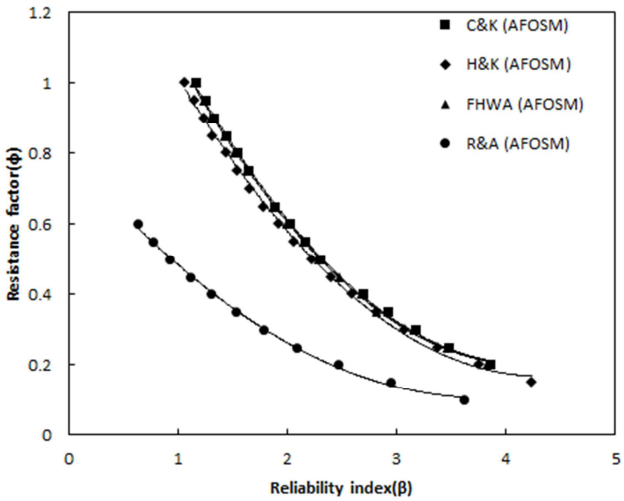

Figure 4.5 Relationship between reliability index and resistance factor for shaft resistance

Table 4.10 Reliability analysis results for shaft resistance

Bearing capacity Equation	Analysis method	Resistance factor			Note
		β_T=2.5	β_T=3.0	β_T=3.5	AASHTO (2010)
Carter & Kulhawy (1988)	AFOSM	0.45	0.32	0.24	0.5
Horvath & Kenney (1979)	AFOSM	0.42	0.30	0.22	0.55
FHWA (1999)	AFOSM	0.44	0.32	0.24	0.55
Rowe & Armitage (1987)	AFOSM	0.19	0.13	0.11	-

4.4.2.2 Base resistance

Figure 4.6 shows the results of calibration results for base resistance. Resistance factors decreases with the increase of the reliability index.

In reliability index range of lower than 2.0, resistance factors by Carter and Kulhawy (1988) are larger than that by Zhang and Einstein (1998), on the other hand, resistance factors by Zhang and Einstein (1998) are larger than that by Carter and Kulhawy (1988) with the increase of the reliability index. Considering that the general range of target reliability index is bigger than 2.0, it can be concluded that Zhang and Einstein (1998) method has more conservative predicted base resistance compared to Carter and Kulhawy (1988) method. Also, resistance factors by FHWA (1999) are smallest results. This means that FHWA (1999) bearing capacity equation is unconservative method to predict the base resistance compared with other bearing capacity equations.

The resistance factors for base resistance with determined target reliability index of 2.5, 3.0, and 3.5 are shown in Table 4.11. Note in table shows the resistance factor suggested by AASHTO with target reliability index of 3.0 (β_T=3.0). For target reliability index of 3.0(AASHTO recommended value), base resistance factors for each bearing capacity equations are in range of 0.19 to 0.29. These values are about 40~60% in comparison with AASHTO suggested resistance factors. It is due to discrepancy of target rock for bearing capacity equations.

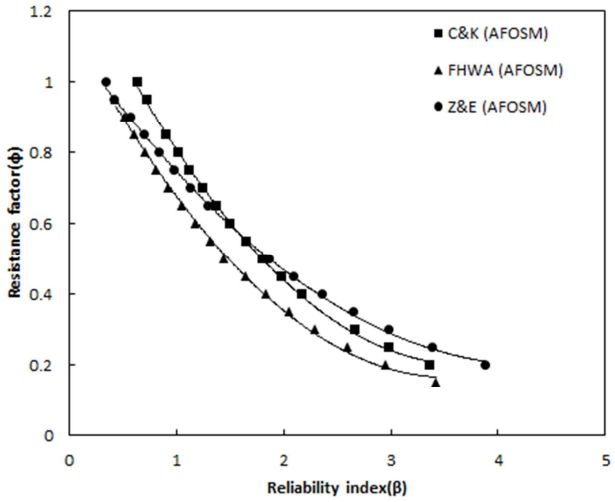

Figure 4.6 Relationship between reliability index and resistance factor for base resistance

Table 4.11 Reliability analysis results for base resistance

Bearing capacity Equation	Analysis method	Resistance factor			Note
		β_T=2.5	β_T=3.0	β_T=3.5	AASHTO (2010)
Carter & Kulhawy (1988)	AFOSM	0.32	0.24	0.21	0.5
FHWA (1999)	AFOSM	0.25	0.19	0.17	0.5
Zhang & Einstein (1998)	AFOSM	0.37	0.29	0.24	-

4.4.2.3 Total resistance

Figure 4.7 shows the results of calibration results for total resistance. Resistance factors decreases with the increase of the reliability index.

Resistance factors by Carter and Kulhawy (1988) are larger than FHWA (1999. This means that Carter and Kulhawy (1988) bearing capacity equation is conservative method to predict the resistance compared to FHWA (1999) equation.

The resistance factors for total resistance with determined target reliability index of 2.5, 3.0, and 3.5 are shown in Table 4.12.

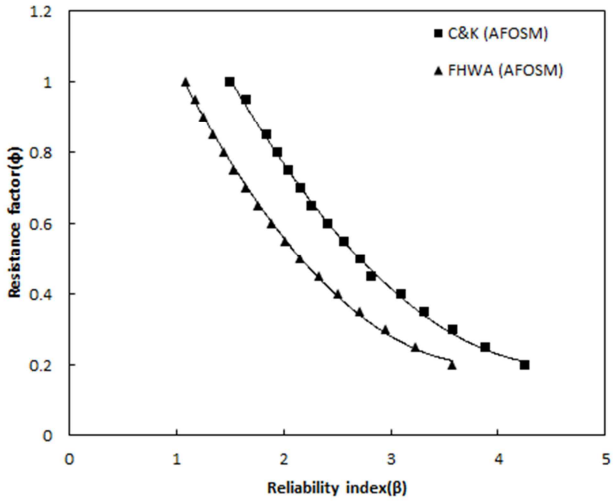

Figure 4.7 Relationship between reliability index and resistance factor for total resistance

Table 4.12 Reliability analysis results for total resistance

Bearing capacity Equation	Analysis method	Resistance factor			Note
		β_T=2.5	β_T=3.0	β_T=3.5	AASHTO (2010)
Carter & Kulhawy (1988)	AFOSM	0.57	0.42	0.30	-
FHWA (1999)	AFOSM	0.40	0.28	0.22	

4.5 Summary

The purpose of this chapter was to determine the target reliability index and calibrate the resistance factor for the shaft, base, and total resistance for drilled shafts using reliability analysis. The summary of this chapter were presented in below.

1. To perform the reliability analysis, load and resistance statistical characteristics are necessary. Contrary to resistance statistics, load statistics are known that regional variations are negligible. Therefore, this thesis used the load statistical characteristics from the current AASHTO LRFD Specifications (2010). Resistance statistics were evaluated using the ratio of the measured to predicted resistance. According to Paikowsky (2004), extremely outlining data points which were outside the boundary defined by the mean plus two times the standard deviation were omitted.

2. To consider a transition period from Allowable Stress Design (ASD) to Load Resistance Factor Design (LRFD), reliability analysis was performed and reliability index of ASD, were estimated. When factor of safety is 3, reliability analysis results for each resistances and bearing capacity equations with AFOSM are summarized as 1.01~2.40 for shaft resistance, 1.41~1.97 for base resistance, and 2.24~2.80 for total resistance. Further, the reliability indices implicit in existing global factor of safety designs lie in the approximate range of 2.6 to 3.7. Thus, the

target reliability index of 2.5, 3.0 and 3.5 were selected for the determination of resistance factors in this thesis.

3. In this thesis, AFOSM method is used for determination of resistance factors. For target reliability index of 3.0(AASHTO recommended value), resistance factors for each bearing capacity equations were determined as following. In comparison with AASHTO (2010) suggested resistance factors, determined resistance factors were about 30~60% for shaft resistance, and 40~60% for base resistance. These differences of resistance factor between AASHTO with this study were induced because of discrepancy of target rock for bearing capacity equations.

Resistance	Bearing capacity Equation	Resistance factor			Note
		β_T=2.5	β_T=3.0	β_T=3.5	AASHTO (2010)
Shaft resistance	Carter & Kulhawy (1988)	0.45	0.32	0.24	0.5
	Horvath & Kenney (1979)	0.42	0.30	0.22	0.55
	FHWA (1999)	0.44	0.32	0.24	0.55
	Rowe & Armitage (1987)	0.19	0.13	0.11	-
Base resistance	Carter & Kulhawy (1988)	0.32	0.24	0.21	0.5
	FHWA (1999)	0.25	0.19	0.17	0.5
	Zhang & Einstein (1998)	0.37	0.29	0.24	-
Total resistance	Carter & Kulhawy (1988)	0.57	0.42	0.30	-
	FHWA (1999)	0.40	0.28	0.22	-

5. Calibration of Resistance Factor considering Lower-Bound Resistance

5.1 Introduction

As mentioned in Chapter 2.2, a lower bound on the capacity has rarely been accounted for in performing reliability analyses and developing reliability-based design codes. In many design code including the AASHTO LRFD (2010), resistances of piles are generally modeled using a lognormal distribution, with a lower tail of resistance extends to zero. However, there is generally a physical limit to the smallest possible capacity for a deep foundation, because that even highly disturbed soil generally has finite shear strength, and there is a physical limit to the smallest possible capacity which is greater than zero for a pile foundation. So, there is a general belief that calculated probabilities of failure from conventional reliability analysis are not realistic due to conservative bias used to predicted resistance and tails of probability distribution. Therefore, Najjar (2005) analyzed the load test results of driven pile into sand and clay and explored the effect of lower-bound resistance on reliability and resistance factors. Consequently, he verified that lower-bound of resistance have a significant effect on the reliability, and suggested the method to incorporate lower-bound resistance into LRFD.

This chapter addresses the estimation of lower-bound resistance for drilled shaft in this study and calibration of resistance factor, which were

determined in previous Chapter 4, using lower-bound resistance information.

5.2 Estimation of Lower-Bound Resistance

5.2.1 Hoek-Brown failure criteria

In study by Najjar (2005), lower-bound were determined using API method and replacing the input parameter. For calculation of lower-bound resistance in clay, remolded shear strength was used instead of undrained shear strength, and calculation of lower-bound resistance in sand, the lateral coefficient of earth pressure was replaced with the at-rest value and the soil-pile friction angle and end-bearing capacity factors were replaced with the values for one-category less in density. These methods were based on the principals of critical state soils mechanics. Critical state of sand and clay could be simulated by downgrading of these input parameters, and the results by these methods were treated physical lower-bound resistance for each pile.

In this thesis, Hoek-Brown failure criteria (1988, 2002) were adopted for determination of lower-bound resistance. Predicted resistances were calculated by bearing capacity equations using unconfined compressive strength of rock core. However, unconfined compressive strengths of rock core are the value of intact rock. Considering that there are many discontinuities and weathering in bedrock in Korea, it is not appropriate to

describe realistic bedrock condition and simulate the critical state of bedrock. Therefore, Hoek-Brown failure criteria (1988, 2002) were adopted to calculate the unconfined compressive strength of rock mass. Hoek et al. (2002) proposed the concept of a global rock mass strength for weathered and decomposed rock mass as following Equation (5.1).

$$q_{u,m\ ass} = q_{u,core} \times \frac{(m_b+4s-a(m_b-8s))\left(\frac{m_b}{4}+s\right)^{a-1}}{2(1+a)(2+a)} \tag{5.1}$$

Here, m_b is a reduced value of the material constant m_i (28 is recommended for gneiss which is the main rock type in Korea.), s and a are constants for the rock mass. These material constants are given by following equations.

$$m_b = m_i \exp\left(\frac{GSI-100}{28}\right) \tag{5.2}$$

$$s = \exp\left(\frac{GSI-100}{9}\right) \tag{5.3}$$

$$a = \frac{1}{2} + \frac{1}{6}\left(e^{-GSI/15} - e^{-20/3}\right) \tag{5.4}$$

Determined unconfined compressive strengths of rock mass were applied into bearing capacity equations to calculate the lower-bound resistance.

5.2.1.1 Lower-bound of shaft resistance

- **Carter & Kulhawy (1988) & Rowe & Armitage (1987)**

As mentioned in Chapter 3.3.1, Carter and Kulhawy (1988) suggested the empirical bearing capacity equation for shaft resistance based on the work of Rowe and Armitage (1984, 1987). And Carter and Kulhawy equation (1988) are based on lower value and Rowe and Armitage equation (1987) are based on mean value of relationship between shaft resistance and unconfined compressive strength of rock core. Because two equations were suggested using same load test results, Carter and Kulhawy (1988) equation was selected for lower-bound of resistance. Applying the unconfined compressive strength of rock mass from Equation (5.1) to Carter & Kulhawy (1988) equation, lower-bound of shaft resistance for Carter and Kulhawy equation (1988) and Rowe and Armitage equation (1987) were calculated.

Figure 5.1 shows the relationship between measured shaft resistance and unconfined compressive strength (UCS) of rock mass. Every measured resistance versus UCS of rock mass points was placed above Carter & Kulhawy bearing capacity equation (dotted line). This result means that lower-bound of shaft resistance for Carter and Kulhawy (1988) and Rowe and Armitage equation (1987) can be estimated by applying the UCS of rock mass into Carter and Kulhawy equation (1988).

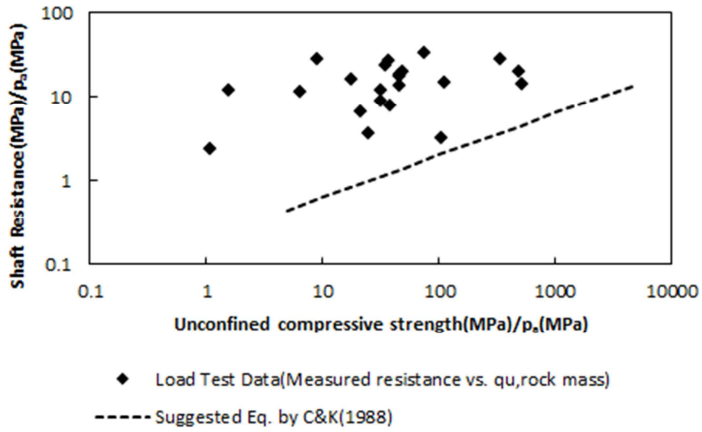

Figure 5.1 Relationship between measured shaft resistance and UCS of rock mass for Carter & Kulhawy (1988) equation

■ **Horvath & Kenney (1979)**

Likewise in case of Carter and Kulhawy equations, unconfined compressive strength of rock mass from Equation (5.1) were applied to Horvath & Kenney (1979) equation, and lower-bound of shaft resistance were calculated. The relationship between measured shaft resistance and unconfined compressive strength (UCS) of rock mass are shown in Figure 5.2.

Most of measured resistance versus UCS of rock mass points was placed above Horvath and Kenney bearing capacity equation (dotted line). However, one point, highlighted by circle, was located below the bearing capacity equation line. This point means that the calculated resistance using UCS of rock mass was smaller than measured resistance at same location. The concept of lower-bound is the physical limit to the smallest possible capacity, however,

this point shows that there is a probability of smaller resistance than resistance calculated from Horvath and Kenney equation with UCS of rock mass. Therefore, it was concluded that replacing the UCS of rock core with that of rock mass could not simulate the lower-bound resistance of this equation.

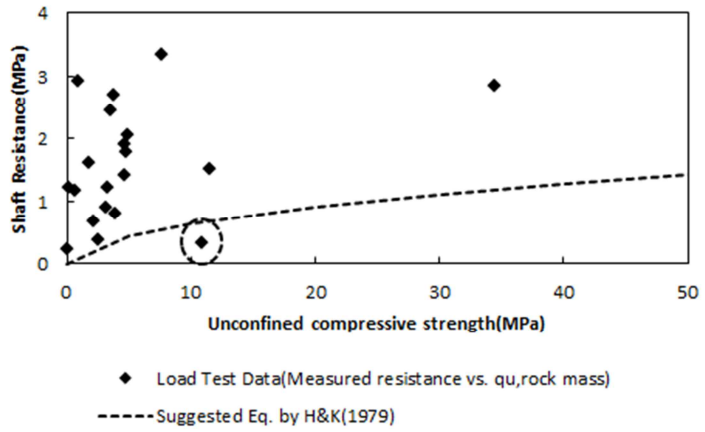

Figure 5.2 Relationship between measured shaft resistance and UCS of rock mass for Horvath & Kenney (1988) equation

■ **FHWA (1999)**

For lower-bound of resistance using FHWA method, additional consideration was adopted. According to Turner (2006), unit side resistance determined strictly by empirical correlations with uniaxial compressive strength does not account explicitly for the degree of jointing in the rock mass. Therefore, values of unit side resistance calculated by FHWA should be modified to account for rock mass behavior in terms of RQD, modulus ratio

(E_m/E_i), and joint condition using the factor α as defined in Table 5.1.

Table 5.1 Estimation of α (Turner, 2006; O'Neill and Reese, 1999)

E_m/E_i	α
1.0	1.0
0.5	0.8
0.3	0.7
0.1	0.55
0.05	0.45

Where, E_m: rock mass modulus, E_i: intact rock modulus

To determine the reduction factor, α, the ratio of rock mass modulus to intact rock modulus (E_m/E_i)are calculated using GSI by Equation (5.5) suggested by Liang and Yang (2006).

$$E_M = \frac{E_R}{100} e^{GSI/21.7} \tag{5.5}$$

Therefore, equation for lower-bound of resistance for FHWA (1999) defined as follow.

$$f_{s,LB} = 0.65\alpha p_a [q_u/p_a]^{0.5} (\text{kPa}) \tag{5.6}$$

Figure 5.3 shows the measured and predicted shaft resistances with

unconfined compressive strength (UCS) of rock mass. Reduction factors, α, were different for each data point and lower-than one, predicted resistances were placed below FHWA (1999) bearing capacity lined. Most of measured resistance versus UCS of rock mass points was placed above predicted resistance. However, one point, highlighted by circle, was located intermediate of predicted resistance. Considering this point, it was concluded that the lower-bound resistance using Equation (5.6) could not simulate the lower-bound resistance of this equation.

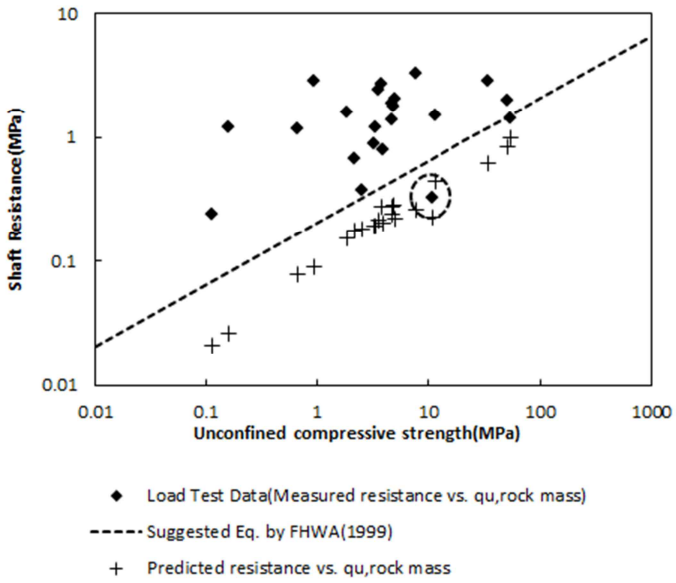

Figure 5.3 Measured and predicted shaft resistance with UCS of rock mass for FHWA (1999) equation

5.2.1.2 Lower-bound of base resistance

- **Carter & Kulhawy (1988)**

As mentioned in Chapter 3.3.2, Carter and Kulhawy (1988) bearing capacity equation for base resistance was already imply the concept of Hoek-Brown (2002) failure criteria. Mass properties by Hoek-Brown (2002) failure criteria were used for determination of base resistance as follow Equation (5.9). So, applying UCS of rock mass for estimation of lower-bound had danger of duplication of Hoek- Brown failure criteria.

$$\mathrm{m_b} = m_i \exp\left(\frac{GSI-100}{28}\right) \tag{5.7}$$

$$s = exp\ \left(\frac{GSI-100}{9}\right) \tag{5.8}$$

$$q_b = [s^{0.5} + (m \cdot s^{0.5} + s)^{0.5})]q_u \tag{5.9}$$

According to Hoek and Brown (1997), in recently blasted faces, new discontinuity surfaces will have been created by the blast and these will give a GSI value which may be as much as 10 points lower than that for undisturbed rock mass. Generally, drilled shafts were constructed after boring. Therefore, it was assumed that rock-drilled shaft interface were similar with recently blasted faces. So, GSI values were downgraded much as 10 points lower to

estimate the lower-bound of base resistance for Carter and Kulhawy equation in this thesis. When GSI values decreased, material constant, m and s, were also decreased, and consequently, lower-bound of base resistance were estimated.

Figure 5.4 shows the measured and predicted base resistances with unconfined compressive strength (UCS) of rock mass. Most of measured resistances were bigger than predicted resistance. However, two points, highlighted by circle, were smaller than predicted resistances. These points show that there is a probability of smaller measured resistance than calculated resistance by this method. Therefore, it was concluded that downgrading 10 point of GSI could not simulate the lower-bound resistance of this equation.

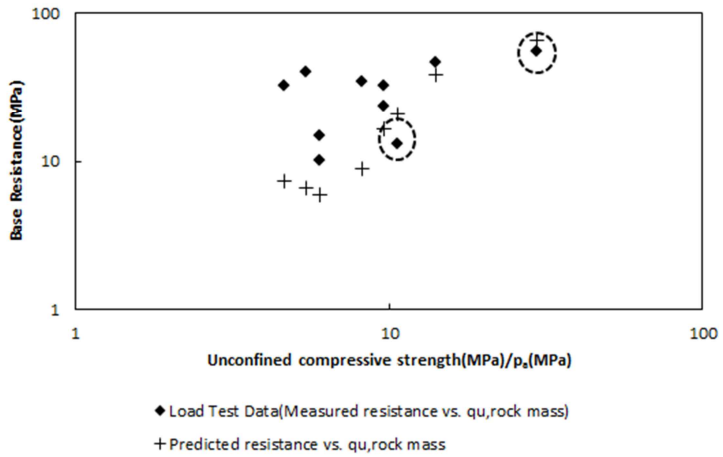

Figure 5.4 Measured and predicted base resistance with UCS of rock mass for Carter & Kulhawy (1988) equation

■ **FHWA (1999)**

FHWA (1999) recommends the use of Equation (5.10) for base resistance where the rock is sedimentary jointed and where the joints are primarily horizontal.

$$q_b = 3K_{sp}\theta q_u (\text{kPa}) \tag{5.10}$$

$$K_{sp} = \frac{3+\frac{c}{B_s}}{10\sqrt{\left(1+\frac{300\ \delta}{c}\right)}} \tag{5.11}$$

$$\theta = 1 + 0.4\frac{L_s}{B_s} \tag{5.12}$$

where, K_{sp} is bearing capacity factor based on vertical joint spacing and quality, θ is depth factor. c is vertical spacing between joints, δ is thickness, or "aperture" of joints (open joints or joints filled with debris), B_s is diameter of the base of the drilled shaft, and L_s is the depth of the drilled shaft socket.

This bearing capacity equation considered the presence and condition of discontinuities like spacing and aperture. However, FHWA (Brown et al., 2010) mentioned that highly fractured rock describes a rock mass intersected by multiple sets of intersecting joints such that the strength is controlled by the overall mass response and not by failure along pre-existing structural discontinuities. Also, GSI provides an improved correlation for rock mass

engineering properties and should be used as the basis for estimating strength parameters. Therefore, like procedure of estimation of lower-bound resistance of shaft resistance, lower-bound of base resistance are estimated by applying of UCS of rock mass.

Figure 5.5 shows the measured and predicted base resistances with unconfined compressive strength (UCS) of rock mass. Every measured resistance versus UCS of rock mass points was placed above predicted resistance. This result means that lower-bound of base resistance for FHWA (1999) can be estimated by applying the UCS of rock mass into Equation (5.10).

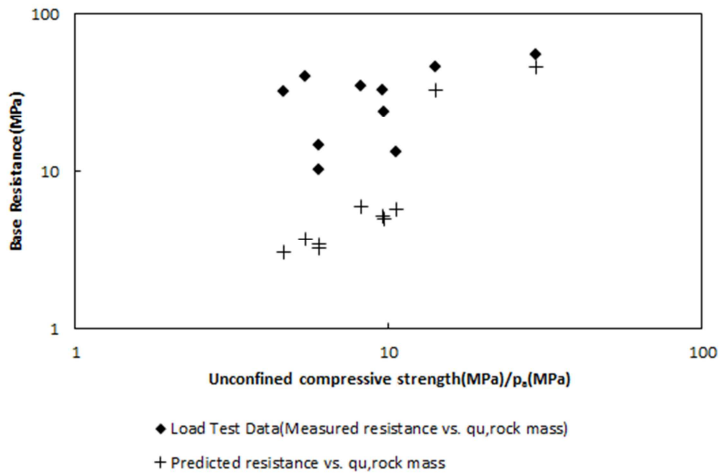

Figure 5.5 Measured and predicted base resistance with UCS of rock mass for FHWA (1999) equation

■ **Zhang & Einstein (1998)**

Zhang and Einstein bearing capacity equation was empirical equation based on mean value of load test results, and lower-bound equation was separately suggested as shown in Figure 5.6. The lower-bound equation was defined as Equation (5.13)

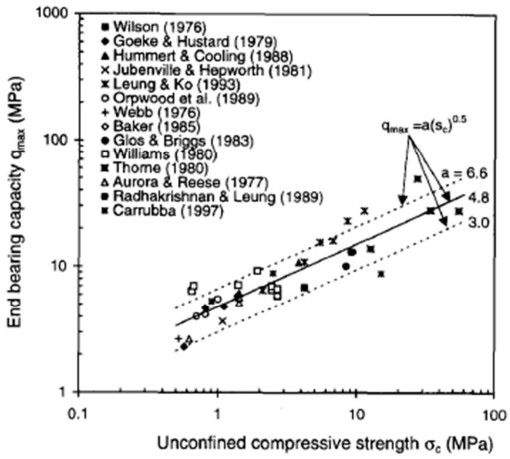

Figure 5.6 Design curves for q_{max} versus σ_c (Zhang and Einstein, 1998)

$$q_b = 3.0 q_u^{0.51} \text{(kPa)} \quad (5.13)$$

Also, unconfined compressive strength was only variable for base resistance in Zhang and Einstein (1998) bearing capacity equation. Therefore, likewise in case of shaft resistances, unconfined compressive strength of rock mass from Equation (5.1) were applied to lower-bound equation defined as

Equation (5.12), and lower-bound of base resistance were calculated. The relationship between measured base resistance and unconfined compressive strength (UCS) of rock mass are shown in Figure 5.7.

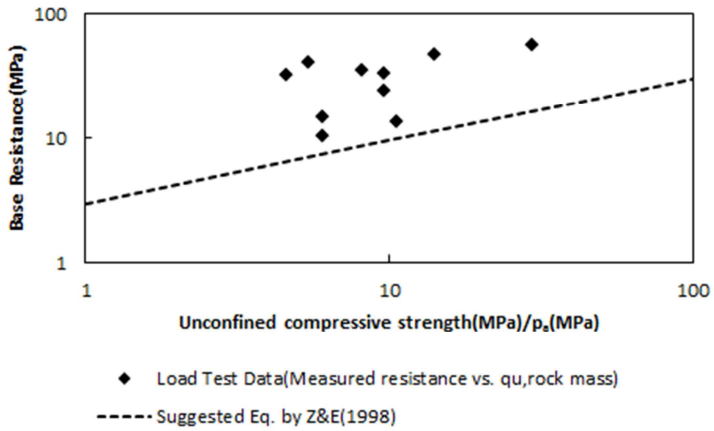

Figure 5.7 Relationship between measured base resistance and UCS of rock mass for Zhang & Einstein (1998) equation

Every measured base resistance versus UCS of rock mass points was placed above lower-bound equation (dotted line). This result means that lower-bound of base resistance can be estimated by applying the UCS of rock mass into lower-bound equation suggested by Zhang & Einstein (1998).

5.2.2 Geological strength index (GSI)

In previous Chapter 5.2.1, Hoek-Brown failure criteria (1988, 2002) were adopted for determination of lower-bound resistance. According to Hoek-Brown failure criteria (1988, 2002), unconfined compressive strength of rock mass were calculated and adopted to bearing capacity equation replacing the unconfined compressive strength of rock core. However, only applying UCS of rock mass could not determine the lower-bound resistance in some bearing capacity equation including Horvath and Kenney (1979), and FHWA (1999) for shaft resistance and Carter and Kulhawy (1988) for base resistance. It means that just applications of UCS of rock mass are not sufficient to describe the critical state of bedrock.

Therefore, as well as Hoek-Brown failure criteria (2002), geological strength index (GSI) also downgraded for lower-bound resistance. As shown in Equation (5.1) to Equation (5.4), GSI is the important factor to determine the unconfined compressive strength of rock mass. The GSI provides a system for estimating the reduction in rock mass strength for different geological conditions, and it is recommended that GSI should be estimated directly by means of the chart presented in Figure 5.8. From borehole cores of test pile construction sites, GSI at each depth are determined using Figure 5.8. However, the concept of lower-bound is physical limit to the smallest possible capacity for a deep foundation. Considering this concept, GSI were downgraded much as 10 points lower corresponding to one-category downgrading of rock structure in y-axis of Figure 5.8. When GSI values decreased, material constant, m and s, were also decreased, and consequently,

unconfined compressive strength of rock mass by Equation (5.1) were additionally decreased. In this chapter, lower-bound using downgraded GSI were estimated, the results were compared with results of non-downgraded GSI, which were shown in above chapter.

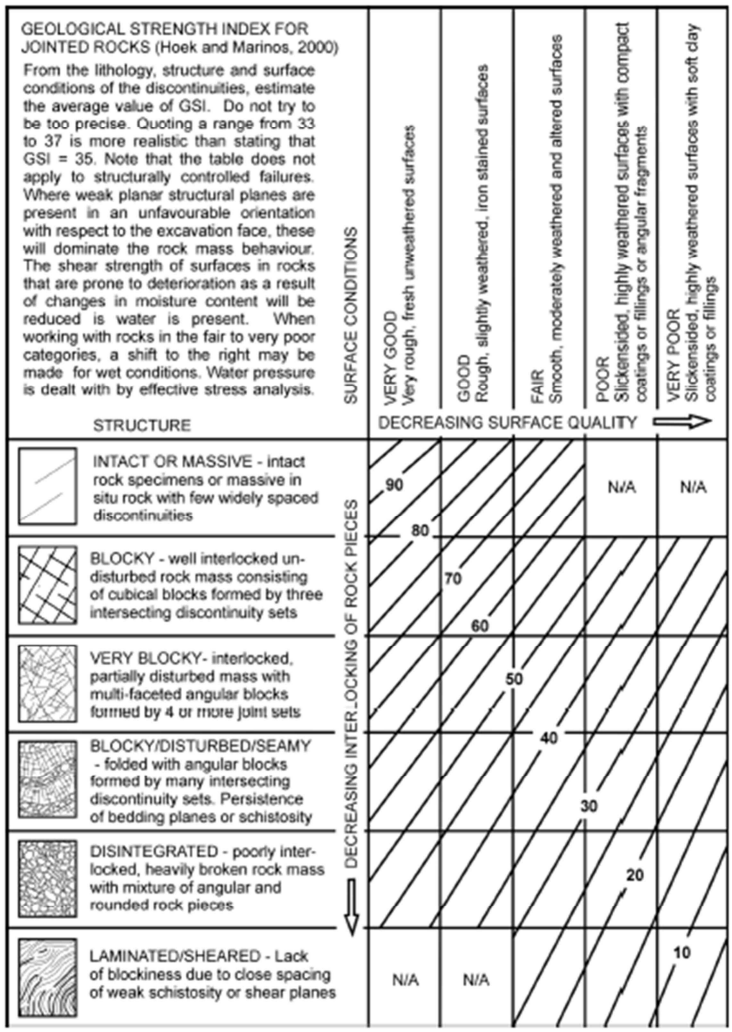

Figure 5.8 Estimate of Geological Strength index (GSI) based on deological descriptions (Hoek et al., 2002)

5.2.2.1 Lower-bound of shaft resistance

Figure 5.9, Figure 5.10, and Figure 5.11 shows the results of application of GSI downgrading with unconfined compressive strength (UCS) of rock mass. The methods for determination of lower-bound with downgraded GSI were same with the procedure explained in above chapter. The newly determined UCSs of rock mass with downgraded GSI were applied into each bearing capacity equations, and lower-bound of shaft resistances were calculated.

Figure 5.9 shows the result of shaft lower-bound resistance with downgraded GSI for Carter and Kulhawy (1988) method. Similar with the results of shaft lower-bound without GSI downgrading (Figure 5.1), every measured resistance versus UCS of rock mass points was placed above Carter & Kulhawy bearing capacity equation (dotted line). Also, the margin between measured with predicted resistances were increased because of the effects of GSI downgrading. This result means that lower-bound of shaft resistance for Carter and Kulhawy (1988) and Rowe and Armitage equation (1987) can be estimated by applying the UCS of rock mass with downgraded GSI into Carter and Kulhawy equation (1988). Also, lower-bounds using downgraded GSI were more confident than lower-bound using only UCS of rock mass.

In case of shaft lower-bound resistance with only UCS of rock mass for Horvath and Kenney (1979) method (Figure 5.2), a point was places below the predicted resistance, and because of this point, it was concluded that replacing the UCS of rock core with that of rock mass could not simulate the

lower-bound resistance of this equation. Figure 5.10 shows the result of shaft lower-bound resistance with downgraded GSI. Even though GSI downgrading was considered, the point placed below the predicted point in Figure (5.2) did not exceed the predicted resistance. It means that, it was impossible to calculate the physical smallest resistance, defined as lower-bound, by replacing the UCS of rock core with that of rock mass and downgrading of GSI. Therefore, it was concluded that the lower-bound of shaft resistance for Horvath and Kenney equation (1979) could not determine in this thesis.

In case of FHWA (1999) shaft bearing capacity equation in Figure 5.3, one point was located intermediate predicted resistance, and it was not sure of shaft lower-bound resistance using only UCS of rock mass. The results with downgraded GSI were shown in Figure 5.11. The point, which was placed intermediate predicted resistance in Figure 5.3, was moved and placed above predicted resistance, and the difference between measured with predicted resistance was increased due to effects of GSI downgrading. This result means that lower-bound of shaft resistance for FHWA (1999) can be estimated by applying the UCS of rock mass with downgraded GSI into conventional FHWA (1999) equation. Also, lower-bounds using downgraded GSI were more confident than lower-bound using only UCS of rock mass.

Consequently, lower-bound of shaft resistances were determined using each bearing capacity equations except the Horvarth and Kenney (1979) equation. The determined shaft lower-bound resistances, and the ratios of the lower-bound resistance to the predicted resistance for each bearing capacity equations were summarized in Table 5.2.

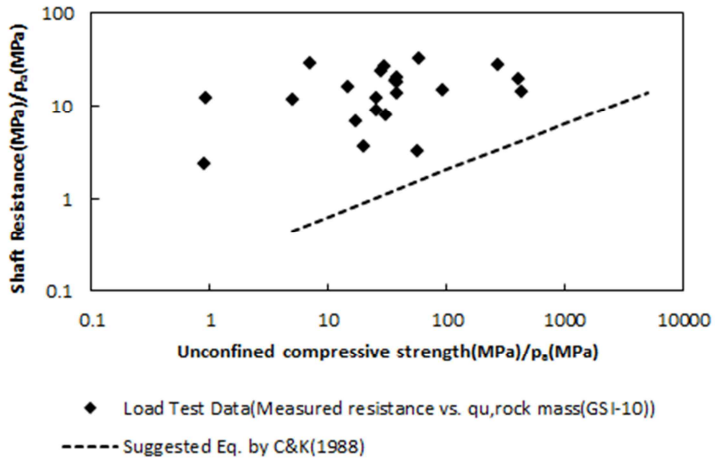

Figure 5.9 Relationship between measured shaft resistance and UCS of rock mass with downgraded GSI for Carter & Kulhawy (1988) equation

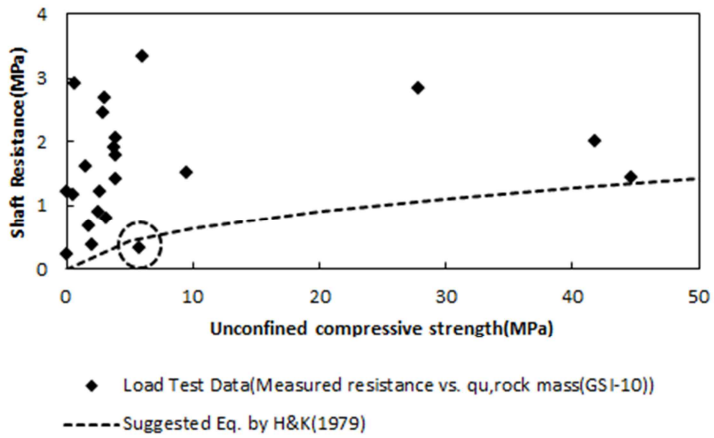

Figure 5.10 Relationship between measured shaft resistance and UCS of rock mass with downgraded GSI for Horvath & Kenney (1979) equation

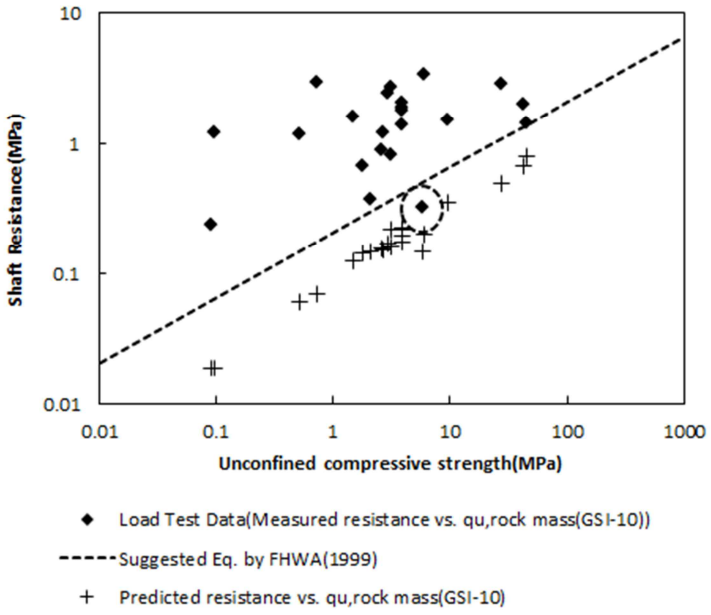

Figure 5.11 Measured and predicted shaft resistance with UCS of rock mass and downgraded GSI for FHWA (1999) equation

Table 5.2 Lower-bound of shaft resistances, and the ratios of the lower-bound resistance to the predicted resistance

	Depth(m)	Carter & Kulhawy (1988)			FHWA (1999)			Rowe & Armitage (1987)		
		Predicted resistance (kPa)	LB of resistance (kPa)	Ratio of LB/Predicted resistance	Predicted resistance (kPa)	LB of resistance (kPa)	Ratio of LB/Predicted resistance	Predicted resistance (kPa)	LB of resistance (kPa)	Ratio of LB/Predicted resistance
TP1	32.0-34.0	471.02	173.50	0.37	475.57	70.19	0.15	1084.01	173.50	0.16
	35.0-36.0	360.23	332.97	0.42	363.71	151.70	0.19	829.04	332.97	0.18
	36.0-37.0	797.68	347.80	0.45	805.37	173.22	0.22	1835.76	347.80	0.20
	37.0-38.7	768.27	401.47	0.44	775.68	194.10	0.21	1768.09	401.47	0.19
TP2	28.8-32.9	894.17	362.60	0.41	902.80	160.35	0.18	2057.84	362.60	0.18
	32.9-33.9	769.63	330.35	0.43	777.06	155.04	0.20	1771.22	330.35	0.19
	33.9-35.3	1031.15	405.66	0.39	1041.10	174.15	0.17	2373.08	405.66	0.17
TP3	26.9-28.0	571.41	272.19	0.48	576.93	143.87	0.25	1315.05	272.19	0.21
	28.0-29.0	650.23	294.37	0.45	656.50	146.61	0.22	1496.43	294.37	0.20
	29.0-30.0	823.50	402.15	0.49	831.44	218.96	0.26	1895.19	402.15	0.21
	30.0-31.0	809.40	405.10	0.50	817.21	227.22	0.28	1862.74	405.10	0.22

Table 5.2 Lower-bound of shaft resistances, and the ratios of the lower-bound resistance to the predicted resistance (continued)

	Depth(m)	Carter & Kulhawy (1988)			FHWA (1999)			Rowe & Armitage (1987)		
		Predicted resistance (kPa)	LB of resistance (kPa)	Ratio of LB/Predicted resistance	Predicted resistance (kPa)	LB of resistance (kPa)	Ratio of LB/Predicted resistance	Predicted resistance (kPa)	LB of resistance (kPa)	Ratio of LB/Predicted resistance
TP3	31.0-33.1	669.26	360.32	0.54	675.72	220.95	0.33	1540.23	360.32	0.23
TP4	24.0-30.5	274.50	61.89	0.23	277.15	18.60	0.07	631.73	61.89	0.10
TP5	44.0-45.85	2177.81	491.04	0.23	2198.82	147.58	0.07	5011.98	491.04	0.10
	46.5-48.5	2584.52	1078.86	0.42	2609.45	491.50	0.19	5947.99	1078.86	0.18
	48.5-50.5	2849.74	1323.67	0.46	2877.23	679.14	0.24	6558.36	1323.67	0.20
	50.5-52.5	2667.65	1368.15	0.51	2693.39	790.54	0.29	6139.30	1368.15	0.22
	52.5-54.5	1261.24	631.25	0.50	1273.40	354.07	0.28	2902.60	631.25	0.22
TP7	45.5-50.2	1361.47	501.50	0.37	1374.60	202.87	0.15	3133.27	501.50	0.16
TP8	46.26-48.26	279.04	62.92	0.23	281.73	18.91	0.07	642.17	62.92	0.10
	48.26-49.76	384.41	146.48	0.38	388.12	61.04	0.16	884.67	146.48	0.17
	49.76-51.35	552.80	250.26	0.45	558.13	124.64	0.22	1272.20	250.26	0.20

5.2.2.2 Lower-bound of base resistance

Likewise lower-bound of shaft resistance, the newly determined UCSs of rock mass with downgraded GSI were applied into each bearing capacity equations, and lower-bound of base resistances were calculated.

In case of Carter and Kulhawy (1988) for determination of the lower-bound of base resistance in previous chapter, the GSI values were downgraded much as 10 points lower to avoid the danger of duplication of Hoek-Brown (2002) failure criteria. This reduction of GSI was based on assumption that rock-drilled shaft interface were similar with recently blasted faces, therefore GSI were reduced much as 10 points lower corresponding to one-category downgrading of rock surface quality in x-axis of Figure 5.8. Additional GSI of downgrading in this part were based on one-category downgrading of rock structure in y-axis of Figure 5.8, and there were no duplications of downgrading of GSI.

In Figure 5.4 which shows the results of base lower-bound resistance, two points were smaller than lower-bound base resistances. These points show that there is a probability of smaller measured resistance than calculated resistance by this method. However, after application of downgraded GSI, these two points were placed above lower-bound base resistance. The results of measured and predicted base resistance with UCS of rock mass for Carter & Kulhawy (1988) equation were shown in Figure 5.12. Also, differences between measured with predicted resistances were increased due to effects of GSI downgrading. This result means that lower-bound of base resistance for

Carter and Kulhawy (1988) equation can be estimated by applying the UCS of rock mass with downgraded GSI. Also, lower-bounds using downgraded GSI were more confident than lower-bound using only UCS of rock mass.

Figure 5.13 and Figure 5.14 show the result of base lower-bound resistance with downgraded GSI for FHWA (1999) and Zhang and Einstein (1988) method. Similar with the results of base lower-bound without GSI downgrading (Figure 5.5 and Figure 5.7), every measured resistance versus UCS of rock mass points was placed above predicted resistance. Also, the margin between measured with predicted resistances were increased because of the effects of GSI downgrading. These results mean that lower-bound of base resistance for FHWA (1999) and Zhang and Einstein (1998) can be estimated by applying the UCS of rock mass with downgraded GSI into each lower-bound bearing capacity equations (Equations (5.10) and Equation (5.13)). Also, lower-bounds using downgraded GSI were more confident than lower-bound using only UCS of rock mass.

The determined base lower-bound resistances, and the ratios of the lower-bound resistance to the predicted resistance for each bearing capacity equations were summarized in Table 5.3.

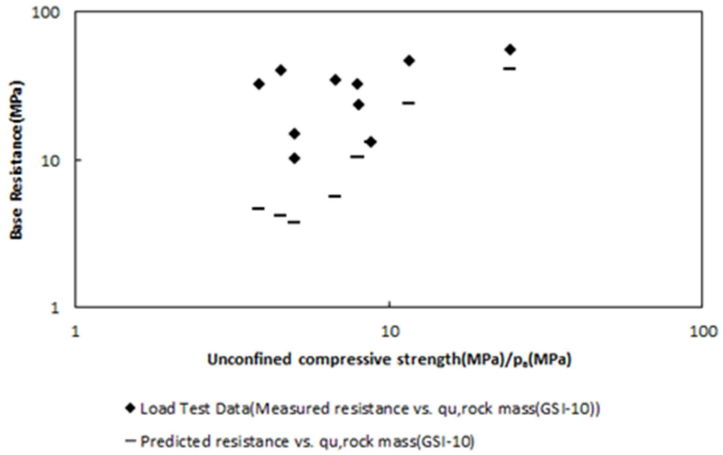

Figure 5.12 Measured and predicted base resistance with UCS of rock mass and downgraded GSI for Carter & Kulhawy (1988) equation

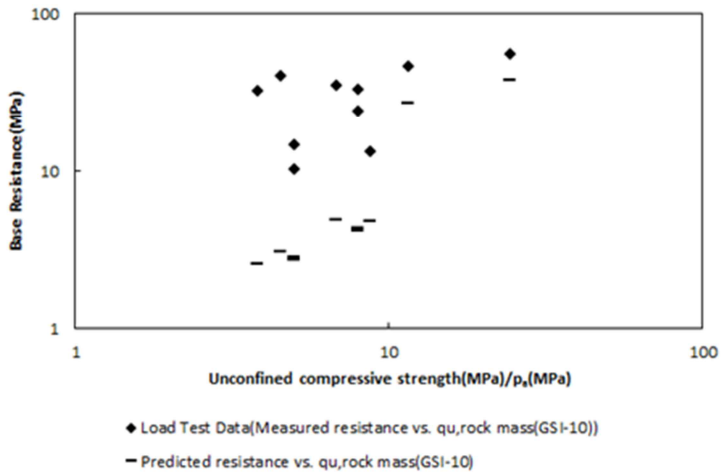

Figure 5.13 Measured and predicted base resistance with UCS of rock mass and downgraded GSI for FHWA (1999) equation

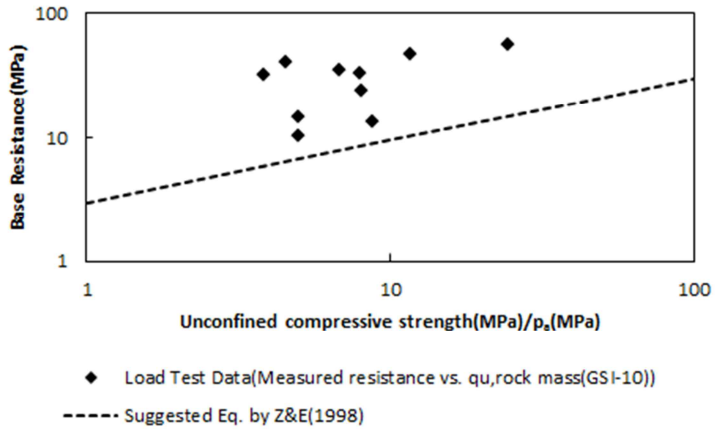

Figure 5.14 Relationship between measured base resistance and UCS of rock mass with downgraded GSI for Zhang & Einstein (1998) equation

Table 5.3 Lower-bound of base resistances, and the ratios of the lower-bound resistance to the predicted resistance

	Depth(m)	Carter & Kulhawy (1988)			FHWA (1999)			Zhang & Einstein(1998)		
		Predicted resistance (MPa)	LB of resistance (MPa)	Ratio of LB/Predicted resistance	Predicted resistance (MPa)	LB of resistance (MPa)	Ratio of LB/Predicted resistance	Predicted resistance (MPa)	LB of resistance (MPa)	Ratio of LB/Predicted resistance
TP 1	38.96	11.76	4.62	0.39	12.71	2.52	0.20	21.91	5.89	0.27
TP 2	36.21	10.64	4.19	0.39	18.92	3.06	0.16	26.42	6.38	0.24
TP 3	33.41	61.92	24.24	0.39	93.65	27.26	0.29	31.70	10.24	0.32
TP 5	55.42	105.72	41.46	0.39	151.32	38.20	0.25	49.83	14.86	0.30
TP 7	51.2	14.15	5.58	0.39	34.17	4.95	0.14	34.42	7.83	0.23
TP 8	52.26	26.30	10.34	0.39	19.94	4.16	0.21	31.12	8.51	0.27
TP 10	13.5	9.49	3.74	0.39	20.52	2.70	0.13	30.88	6.71	0.22
TP 11	13.5	9.49	3.74	0.39	21.43	2.82	0.13	30.88	6.71	0.22
TP 12	13.5	26.50	10.41	0.39	20.52	4.32	0.21	30.88	8.48	0.27
TP 13	13.5	33.49	13.15	0.39	20.52	4.76	0.23	30.88	8.90	0.29

5.2.2.3 Lower-bound of total resistance

In this study, predicted total resistances for each test piles are calculated as the sum of shaft and base resistances as mentioned in Chapter 3.3.3. It is because that f-w curves of this study from Figure 3.14 to 3. 30 showed the ductile behavior and there were not deflection softening. Therefore, predicted total resistances for each test piles are calculated as the sum of shaft and base resistances in this study according to AASHTO (2010)

Likewise predicted resistances, lower-bounds of total resistances were determined as the sum of shaft and base lower-bound resistance. The results of lower-bound of total resistance and the ratios of the lower-bound resistance to the predicted resistance for each bearing capacity equations were summarized in Table 5.4.

Table 5.4 Lower-bound of total resistances, and the ratios of the lower-bound resistance to the predicted resistance

	Depth(m)	Carter & Kulhawy (1988)			FHWA (1999)		
		Predicted resistance (MN)	LB of resistance (MN)	Ratio of LB/Predicted resistance	Predicted resistance (MN)	LB of resistance (MN)	Ratio of LB/Predicted resistance
TP 1	38.96	83.60	32.68	0.39	88.07	16.82	0.19
TP 2	36.21	64.49	25.83	0.40	87.09	14.67	0.17
TP 3	33.41	107.23	43.99	0.41	152.83	44.25	0.29
TP 5	55.42	854.78	346.20	0.41	1147.41	286.01	0.25
TP 7	51.2	101.48	38.84	0.38	181.52	26.41	0.15
TP 8	52.26	118.79	46.35	0.39	93.65	18.84	0.20

5.3 Calibration of Resistance Factor considering Lower-Bound Resistance

5.3.1 Incorporating lower-bound resistance into LRFD

As mentioned in Chapter 2.2, lower-bound of resistance have a significant effect on reliability of a design. Therefore, a reliability-based LRFD design code should include information on the lower-bound resistance. Incorporating the effect of a lower-bound resistance, design checking equation is defined as follows.

$$\phi_{R(LB)} \cdot r_{nominal} \geq \gamma_S \cdot s_{nominal} \tag{5.14}$$

where, $\phi_{R(LB)}$ indicate the resistance factor expressed as the function of the lower-bound capacity, $r_{nominal}$ is nominal resistance calculated using a bearing capacity equations, γ_S is load factor, and $s_{nominal}$ is nominal load for design. When there is no lower bound and when the load and the resistance follow conventional lognormal distributions, the reliability and resistance factor are calculated from Equation (5.15) and Equation (5.16) suggested by Najjar (2009).

$$Reliability = \Phi\left(\frac{\ln(FS_{median})}{\sqrt{[(1+\delta_S^2)(1+\delta_R^2)]}}\right) \quad \text{if LB} = 0 \tag{5.15}$$

$$\phi_R = \frac{\gamma_S}{e^{\beta_{target}\sqrt{[(1+\delta_S^2)(1+\delta_R^2)]}}}\left(\frac{\lambda_R}{\lambda_S}\right)\sqrt{\frac{(1+\delta_S^2)}{(1+\delta_R^2)}} \quad \text{if LB} = 0 \tag{5.16}$$

Also, for a nonzero lower-bound capacity, reliability index is linearly increased when the ratio of lower-bound to predicted capacity exceed the certain value, and consequently, the resistance factor is increased due to an increase of reliability. The lower-bound resistance, $\phi_{R(LB)}$, can be expressed in terms of the conventional case as follows.

$$\phi_{R(LB)} = \left(\frac{FS_{median(LB=0)}}{FS_{median(LB)}}\right)\phi_R \tag{5.17}$$

In Figure 5.15 and Figure 5.16, effects of lower-bound resistance on reliability and resistance factor were shown, repeatedly.

In this chapter, lower-bound information calculated in previous part will be applied for calibration of resistance and the calibrated resistance factors incorporating lower-bound resistance will be given.

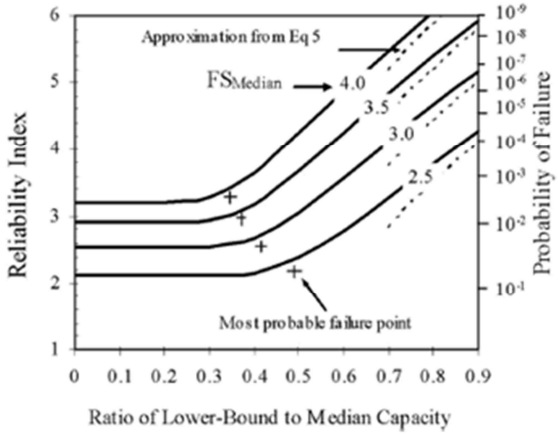

Figure 5.15 Effect of lower-bound resistance on reliability (Najjar, 2009)

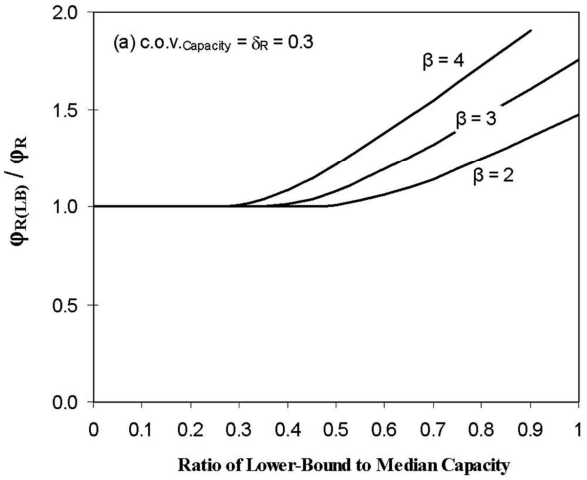

Figure 5.16 Variation of increase in resistance factor with lower-bound resistance (Najjar, 2009)

In previous research by Najjar (2009), a simple approximation was proposed to relate the reliability to the lower-bound resistance. The model was defined by three points and these points were determined based on Equation (5.15) and Equation (5.16). Also, he assumed that load and resistance bias were equal to one, which means load and resistance were unbiased.

Contrary to research by Najjar (2009), statistical characteristics were not unbiased and already calculated in Chapter 4.2, and load statistics were divided for live load and dead load. Therefore, additional statistical characteristics were applied into mathematical formulations suggested by Najjar (2009). Resistance factor used by Najjar (2009) were shown in Equation (5.16), repeatedly. And, reliability index considering dead load, live load, and biased resistance characteristics were defined as Equation (5.19). Considering additional statistical characteristics, Equation (5.18) was modified as Equation (5.20). In this thesis, resistance factors were calibrated using Equation (5.20).

$$\phi_R = \frac{\gamma_S}{e^{\beta_{target}\sqrt{[(1+\delta_S^2)(1+\delta_R^2)]}}}\left(\frac{\lambda_R}{\lambda_S}\right)\sqrt{\frac{(1+\delta_S^2)}{(1+\delta_R^2)}} = \frac{\gamma_S}{FS}\left(\frac{\lambda_R}{\lambda_S}\right)\sqrt{\frac{(1+\delta_S^2)}{(1+\delta_R^2)}} \quad \text{if LB} = 0 \qquad (5.18)$$

$$\beta = \frac{\ln\left[\left(\frac{\lambda_R/\phi(\gamma_{QL}+\gamma_{QD}QD/QL)}{(\lambda_{QL}+\lambda_{QD}QD/QL)}\right)\sqrt{(1+\delta_{QL}^2+\delta_{QD}^2)/(1+\delta_R^2)}\right]}{\sqrt{\ln(1+\delta_R^2)(1+\delta_{QL}^2+\delta_{QD}^2)}} \qquad (5.19)$$

$$\emptyset_R = \frac{\gamma_S \cdot \ln\left(1+\frac{QD}{QL}\right)}{e^{\beta_{target}\sqrt{\ln\left[\left(1+\delta_R{}^2\right)\left(1+\delta_{QL}{}^2+\delta_{QD}{}^2\right)\right]}}}\left(\frac{\lambda_R\times\left(1+\frac{QD}{QL}\right)}{\lambda_{QL}+\lambda_{QD}\times\frac{QD}{QL}}\right)\sqrt{\frac{1+\delta_{QL}{}^2+\delta_{QD}{}^2}{1+\delta_R{}^2}} \qquad (5.20)$$

After considering the additional statistical characteristics, threshold value in simplified bilinear reliability model were calculated. A proposed approximation for this threshold is the “most probable failure point” for the capacity in the case where there is no lower-bound, which is given as below Equation (5.21). And then, effects of lower-bound resistance on reliability and resistance factor were analyzed by newly estimation of relationship between lower-bound ratio with reliability index and resistance factor.

$$\frac{LB_{threshold}}{r_{median}} \equiv \frac{r_{MPP,LB=0}}{r_{median}} e^{-\left(\ln\left[(1+\delta_R{}^2)/\sqrt{\ln\left[(1+\delta_{QL}{}^2+\delta_{QD}{}^2)\right]}\right]\right)\beta} \quad (5.21)$$

5.3.2 Calibration results of resistance factor considering lower-bound resistance

Using the lower-bound resistance determined in Chapter 5.2, resistance factors were calibrated considering lower-bound for each resistances (shaft, base, and total resistance) and bearing capacity equations. For each bearing capacity equations, relationship between the ratio of lower-bound to predicted capacity with reliability index and resistance factor ratio were newly drawn. Figure 5.17 to Figure 5.22 show the relationship between lower-bound with the reliability index and the resistance factor ratio for shaft resistances. As mentioned above chapter, Horvath and Kenney (1979) method could not

determine the lower-bounds, therefore, calibration of resistance factor did not performed. In Figure 5.23 to Figure 5.28, the relationship between lower-bound with the reliability index and the resistance factor ratio for base resistance were summarized, and the relationship between lower-bound with the reliability index and the resistance factor ratio for total resistance were shown in Figure 5.29 to Figure 5.32. As shown in figures, threshold values of ratio of lower-bound to predicted resistances were decreased with target reliability index increasing.

And then, the resistance factors considering lower-bound resistance were determined based on below figures and the ratio of resistance factors. Lower-bound information were determined in previous part, Chapter 5.2 and the resistance factors without lower-bound information were summarized in Table 4.10 for shaft resistance, Table 4.11 for base resistance, and Table 4.12 for total resistance. The determined lower-bound and calibration results of resistance factors considering lower-bound resistance were summarized in Table 5.5.

As summarized in Table 5.5, lower-bound resistance ranged from 18~42% of predicted resistance for shaft resistance, 20~39% for base resistance, and 21~40% for total resistance. Consequently, resistance factors were increased with consideration of the lower-bound resistance about 0~8% for shaft resistance factor, 0~13% for base resistance factor, and 0~2% for total resistance factor.

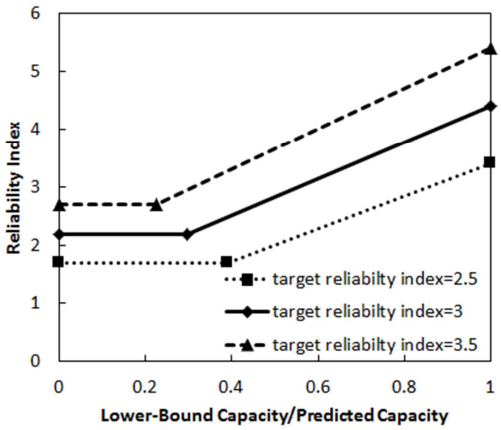

Figure 5.17 the relationship between lower-bound ratio with reliability index for Carter and Kulhawy (1988) shaft resistance equation

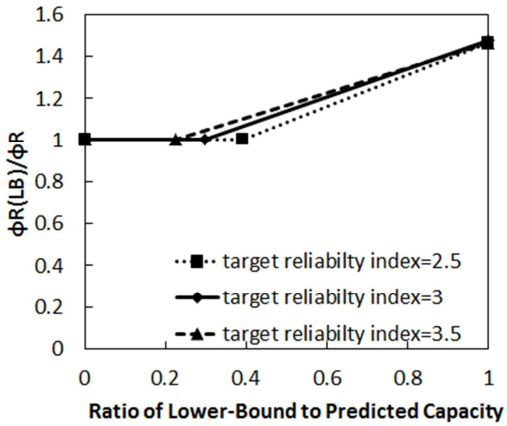

Figure 5.18 the relationship between lower-bound ratio with resistance factor ratio for Carter and Kulhawy (1988) shaft resistance equation

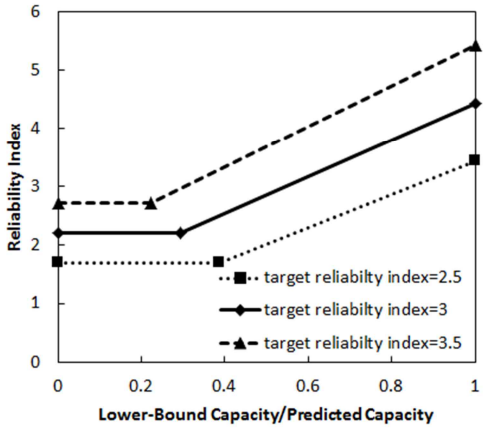

Figure 5.19 the relationship between lower-bound ratio with reliability index for FHWA (1999) shaft resistance equation

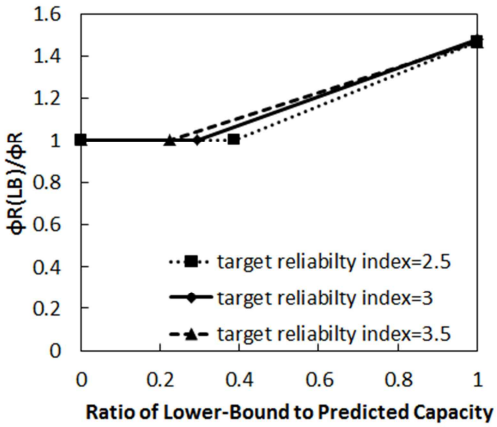

Figure 5.20 the relationship between lower-bound ratio with resistance factor ratio for FHWA (1999) shaft resistance equation

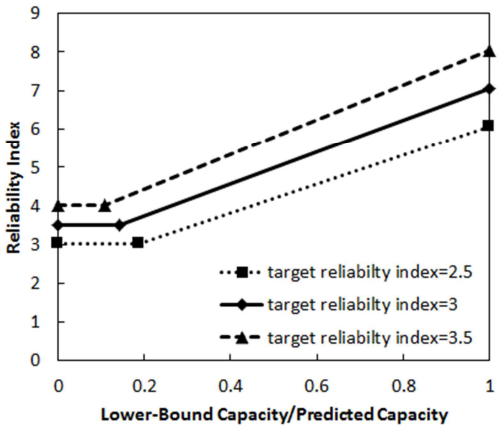

Figure 5.21 the relationship between lower-bound ratio with reliability index for Rowe and Armitage (1987) shaft resistance equation

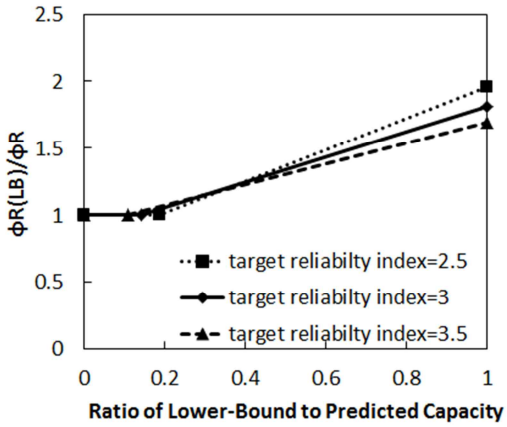

Figure 5.22 the relationship between lower-bound ratio with resistance factor ratio for Rowe and Armitage (1987) shaft resistance equation

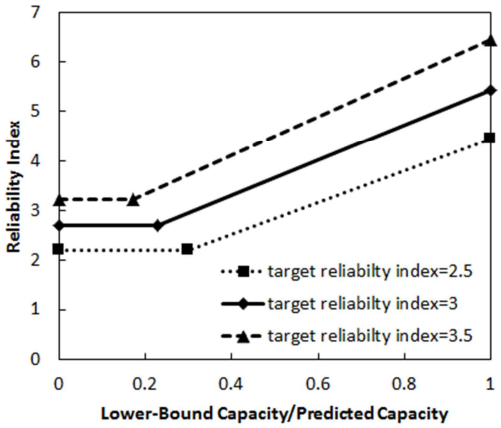

Figure 5.23 the relationship between lower-bound ratio with reliability index for Carter and Kulhawy (1988) base resistance equation

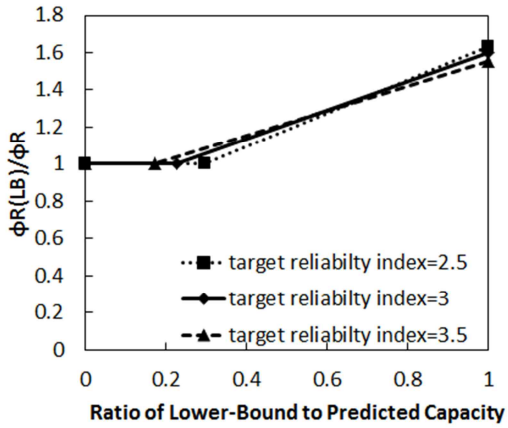

Figure 5.24 the relationship between lower-bound ratio with resistance factor ratio for Carter and Kulhawy (1988) base resistance equation

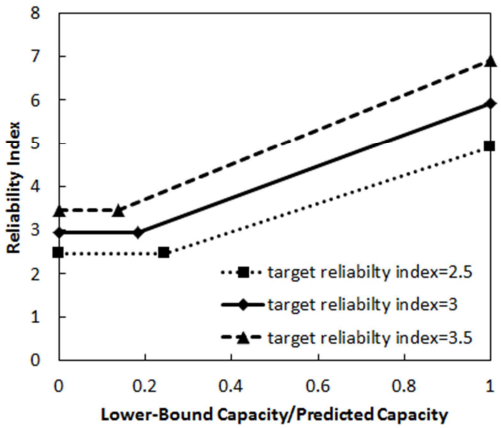

Figure 5.25 the relationship between lower-bound ratio with reliability index for FHWA (1999) base resistance equation

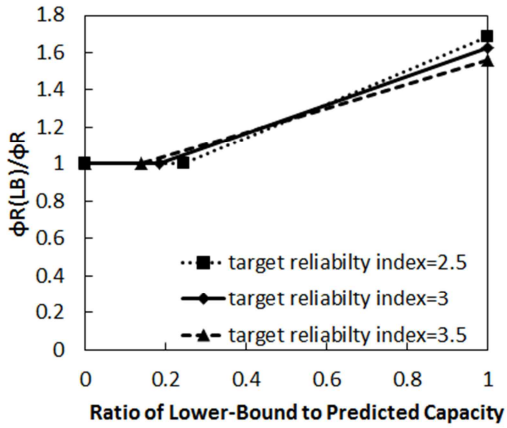

Figure 5.26 the relationship between lower-bound ratio with resistance factor ratio for FHWA (1999) base resistance equation

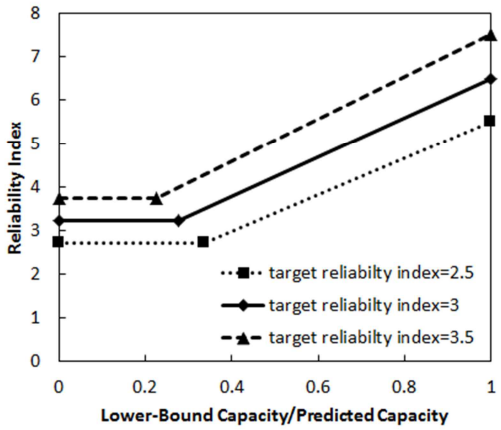

Figure 5.27 the relationship between lower-bound ratio with reliability index for Zhang and Einstein (1998) base resistance equation

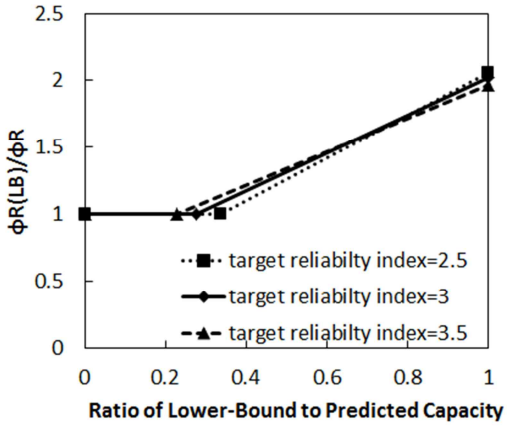

Figure 5.28 the relationship between lower-bound ratio with resistance factor ratio for Zhang and Einstein (1998) base resistance equation

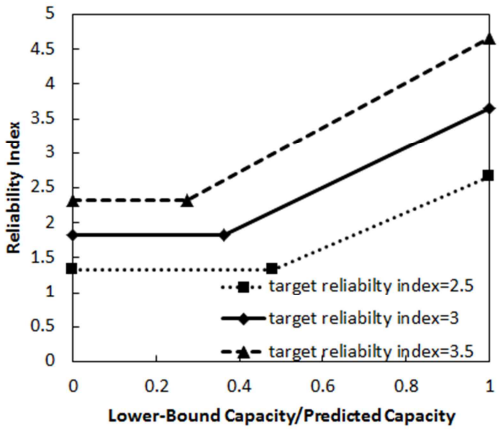

Figure 5.29 the relationship between lower-bound ratio with reliability index for Carter and Kulhawy (1988) total resistance equation

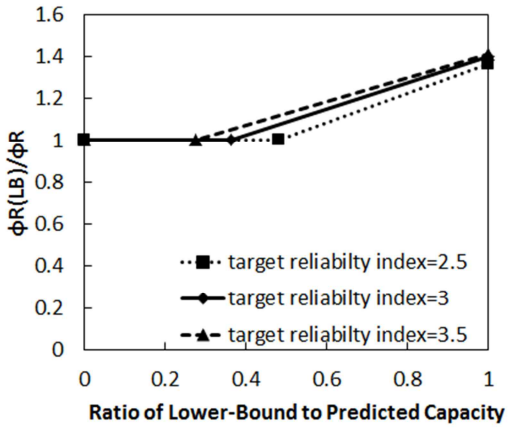

Figure 5.30 the relationship between lower-bound ratio with resistance factor ratio for Carter and Kulhawy (1988) total resistance equation

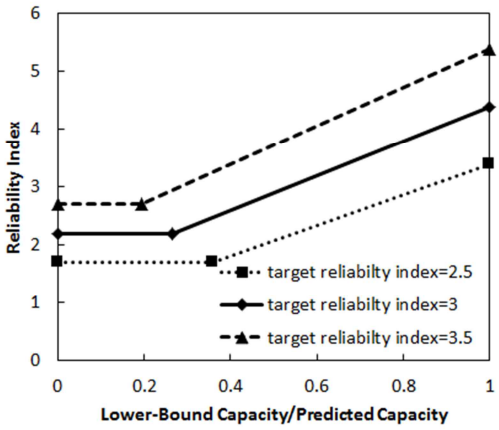

Figure 5.31 the relationship between lower-bound ratio with reliability index for FHWA (1999) total resistance equation

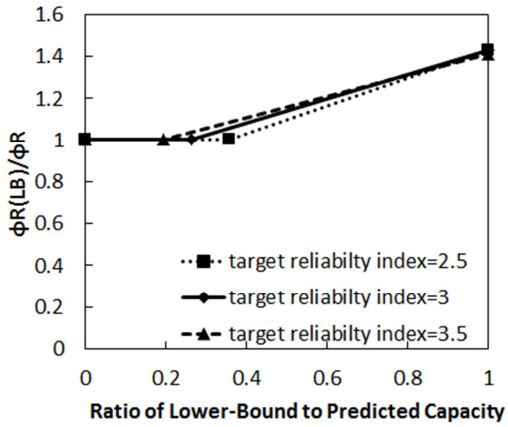

Figure 5.32 the relationship between lower-bound ratio with resistance factor ratio for FHWA (1999) total resistance equation

Table 5.5 Summary of determined lower-bound and calibration results of resistance factors considering lower-bound resistance

Bearing capacity Equation		Lower-bound /Predicted Resistance	Resistance factor						Note [2]
			β_T=2.5		β_T=3.0		β_T=3.5		β_T=3.0
			Before calibration	Lower-bound Calibration	Before calibration	Lower-bound Calibration	Before calibration	Lower-bound Calibration	AASHTO (2010)
Shaft resistance	Carter & Kulhawy (1988)	42%	0.45	0.49 (8% ↑)	0.32	0.35 (8% ↑)	0.24	0.26 (8% ↑)	0.5
	Horvath & Kenney (1979)	- [1]	0.42	0.42 (-)	0.30	0.30 (-)	0.22	0.30 (-)	0.55
	FHWA (1999)	20%	0.44	0.44 (-)	0.32	0.32 (-)	0.24	0.24 (-)	0.55
	Rowe & Armitage (1987)	18%	0.19	0.20 (4% ↑)	0.13	0.13 (4% ↑)	0.11	0.11 (4% ↑)	-
Base resistance	Carter & Kulhawy (1988)	39%	0.32	0.36 (13% ↑)	0.24	0.27 (13% ↑)	0.21	0.24 (13% ↑)	0.5
	FHWA (1999)	20%	0.25	0.25 (1% ↑)	0.19	0.19 (1% ↑)	0.17	0.17 (1% ↑)	0.5
	Zhang & Einstein (1998)	26%	0.37	0.37 (-)	0.29	0.29 (-)	0.24	0.24 (-)	
Total resistance	Carter & Kulhawy (1988)	40%	0.57	0.58 (2% ↑)	0.42	0.43 (2% ↑)	0.30	0.31 (2% ↑)	
	FHWA (1999)	21%	0.40	0.40 (-)	0.28	0.28 (-)	0.22	0.22 (-)	

1) Horvath and Kenney (1979) equation method could not determine the lower-bounds, therefore, calibration of resistance factor did not performed
2) Resistance factors suggested by AASHTO LRFD (2010)

5.4 Summary

The purpose of this chapter was to determine the lower-bound resistance and calibrate the resistance factors considering lower-bound information. The summary of this chapter were presented below.

1. To determine the lower-bound of resistances, Hoek-Brown failure criteria (1988, 2002) were adopted to calculate the unconfined compressive strength of rock mass. And determined UCSs of rock mass were applied into bearing capacity equations to calculate the lower-bound resistance. However, in case of some bearing capacity equations including Horvath and Kenney (1979), FHWA (1999) method for shaft resistance and Carter and Kulhawy (1988) method for base resistance, replacing the UCS of rock core with that of rock mass could not simulate the lower-bound resistance of this equation.

2. In addition to Hoek- Brown failure criteria (1988, 2002), geological strength index (GSI) also downgraded much as 10 points corresponding to one-category downgrading of rock structure. Consequently, lower-bound could be calculated from applying the UCS of rock mass with downgraded GSI into bearing capacity equations, except for Horvath and Kenney (1979) method for shaft resistance. Also, lower-bounds using downgraded GSI were more confident than lower-bound using only UCS

of rock mass. In case of Horvath and Kenney (1979) method for shaft resistance, even though GSI downgrading was considered, it was impossible to calculate the physical smallest resistance by replacing the UCS of rock core with that of rock mass and downgrading of GSI. The determined lower-bound resistance ranged from 18~42% of predicted resistance for shaft resistance, 20~39% for base resistance, and 21~40% for total resistance.

3. Using the determined lower-bound resistance, resistance factors were calibrated considering lower-bound for each resistances (shaft, base, and total resistance) and bearing capacity equations. For each bearing capacity equations, relationship between the ratio of lower-bound to predicted capacity with reliability index and resistance factor ratio were newly drawn. Consequently, resistance factors were increased with consideration of the lower-bound resistance about 0~8% for shaft resistance factor, 0~13% for base resistance factor, and 0~2% for total resistance factor. The calibrated resistance factors considering lower-bound resistance were determined as following.

Resistance	Bearing capacity Equation	Resistance factor			Note
		β_T=2.5	β_T=3.0	β_T=3.5	AASHTO (2010)
Shaft resistance	Carter & Kulhawy (1988)	0.49 (8% ↑)	0.35 (8% ↑)	0.26 (8% ↑)	0.5
	Horvath & Kenney (1979)	0.42 (-)	0.30 (-)	0.30 (-)	0.55
	FHWA (1999)	0.44 (-)	0.32 (-)	0.24 (-)	0.55
	Rowe & Armitage (1987)	0.20 (4% ↑)	0.13 (4% ↑)	0.11 (4% ↑)	-
Base resistance	Carter & Kulhawy (1988)	0.36 (13% ↑)	0.27 (13% ↑)	0.24 (13% ↑)	0.5
	FHWA (1999)	0.25 (1% ↑)	0.19 (1% ↑)	0.17 (1% ↑)	0.5
	Zhang & Einstein (1998)	0.37 (-)	0.29 (-)	0.24 (-)	-
Total resistance	Carter & Kulhawy (1988)	0.58 (2% ↑)	0.43 (2% ↑)	0.31 (2% ↑)	-
	FHWA (1999)	0.40 (-)	0.28 (-)	0.22 (-)	-

6. Summary and Conclusions

6.1 Summary

Recently, the Load Resistance Factor Design (LRFD) has been substituted for the Allowable Stress Design (ASD) or Working Stress Design (WSD), for the design of foundations around the world. The Load Resistance Factor Design (LRFD) method was introduced into Korea about a decade ago. However, the resistance factors suggested by AASHTO (2007, 2010) should represent the characteristics of bedrocks defined in the US, which may differ from the bedrocks in Korea. Considering the discrepancies in rock conditions between the US and Korea, direct application of the AASHTO resistance factors for domestic design is not appropriate. Therefore, it is necessary to determine accurate resistance factors for drilled shafts based on reliable load test results, considering the discrepancies of rock between the US and Korea.

Also, there is a general belief that the calculated probabilities of failure from conventional reliability analyses are not realistic, because of the conservative bias used when predicting the resistance and tails of probability distributions for load and resistance. There is a physical limit to the smallest possible capacity for a pile foundation. This limit is greater than zero, and is defined as the lower bound for resistance. The existence of a lower bound of resistance affects the reliability and resistance factors, even though the lower bound of resistance is small. Therefore, it is necessary to calibrate the

resistance factors considering the lower bound resistance.

In this thesis, the main objectives are to determine accurate resistance factors for drilled shafts based on load test results in Korea, and to calibrate the determined resistance factors considering the lower bound of resistance. Thirteen sets of drilled shaft load test data with strain gauges were collected, and load transfer analysis was performed, to determine accurate shaft and base resistances. After the determination of resistances, reliability analysis was performed for the determination of target reliability index and resistance factors using the AFOSM (Advanced First Order Second Moment reliability method). After that, the lower bound of resistance for each resistance (shaft, base and total) and different bearing capacity equation were determined. Finally, the resistance factors were calibrated considering the lower bound of resistance. The conclusions of this thesis are presented in the following.

6.2 Conclusions and Recommendations

- **Evaluation of Resistance for Drilled Shaft**

The resistances of test piles were evaluated to determine the measured and predicted resistance. Calibration for measured resistances, and the review of bearing capacity equations were performed.

1. For this study, load test data were reviewed. First, target pile foundation

types for this thesis were selected as drilled shafts. Second, bi-directional load tests for drilled shafts were mainly selected. Also, load test data with strain gauges in test piles were collected for accurate measurements of shaft and base resistances. With the overall considerations, 13 sets of load test results of drilled shafts were collected for this study.

2. When the measured resistances were determined from pile-load tests, some calibrations were performed, to determine more accurate and realistic resistances. In load transfer analysis steps for shaft and base resistances, reduction of the elastic modulus of drilled shafts was considered, using the method suggested by Fellenius (1989). Also when plotting the equivalent load-displacement curve for total resistances, the modified method for equivalent load-displacement curve suggested by Kwon (2006) was adopted. Based on the calibrated results, f-w curves, q-w curves, and equivalent load-displacement curves for each test pile were obtained. From these results and the extrapolation method suggested by Jung (2010), measured shaft, base, and total resistances were determined.

3. Predicted resistances were calculated by the bearing capacity equation, using the unconfined compressive strengths of rock cores: shaft resistance (Carter and Kulhawy 1988; Horvath and Kenney 1979; FHWA 1999; Rowe and Armitage 1987); base resistance (Carter and Kulhawy 1988; FHWA 1999; Zhang and Einstein 1987); and total resistance (Carter and Kulhawy 1988; FHWA 1999).

■ **Determination of Resistance Factor**

The target reliability index was determined, and the resistance factors for the shaft, base, and total resistances for drilled shafts were calibrated, using reliability analysis.

4. To perform reliability analysis, load and resistance statistical characteristics are needed. In contrast to resistance statistics, load statistics are known to be negligible for regional variations. Therefore, in this thesis, the load statistical characteristics from the current AASHTO LRFD Specifications (2010) were used. Resistance statistics were evaluated, using the ratio of the measured to the predicted resistance. According to Paikowsky (2004), extreme outlying data points that were outside the boundary defined by the mean plus two times the standard deviation were omitted.

5. To consider a transitional period from the Allowable Stress Design (ASD) to the Load Resistance Factor Design (LRFD), reliability analysis was performed, and the reliability index of the ASD was estimated. When the factor of safety is 3, the reliability analysis results for each resistance and bearing capacity equation with the AFOSM are summarized as 1.01~2.40 for the shaft resistance, 1.41~1.97 for the base resistance, and 2.24~2.80 for the total resistance. Furthermore, the reliability indices implicit in the existing global factor of safety designs lie in the range of approximately

2.6 to 3.7. Thus, the target reliability indices of 2.5, 3.0 and 3.5 were selected in this thesis for the determination of resistance factors.

6. In this thesis, the AFOSM method is used for the determination of resistance factors. For the target reliability index of 3.0 (AASHTO recommended value), resistance factors for each bearing capacity equation were determined as the following. Compared to the AASHTO (2010) suggested resistance factors, the determined resistance factors were about 30~60% for the shaft resistance, and 40~60% for the base resistance. These differences of resistance factors between AASHTO and this study were induced because of the discrepancy of the target rock.

Resistance	Bearing capacity Equation	Resistance factor			Note
		β_T=2.5	β_T=3.0	β_T=3.5	AASHTO (2010)
Shaft resistance	Carter & Kulhawy (1988)	0.45	0.32	0.24	0.5
	Horvath & Kenney (1979)	0.42	0.30	0.22	0.55
	FHWA (1999)	0.44	0.32	0.24	0.55
	Rowe & Armitage (1987)	0.19	0.13	0.11	-
Base resistance	Carter & Kulhawy (1988)	0.32	0.24	0.21	0.5
	FHWA (1999)	0.25	0.19	0.17	0.5
	Zhang & Einstein (1998)	0.37	0.29	0.24	-
Total resistance	Carter & Kulhawy (1988)	0.57	0.42	0.30	-
	FHWA (1999)	0.40	0.28	0.22	-

■ **Calibration of Resistance Factor considering Lower-Bound Resistance**

The lower bound resistances were determined and the resistance factors were calibrated considering the lower bound information.

7. To determine the lower bound of resistances, the Hoek-Brown failure criteria (1988, 2002) were adopted to calculate the unconfined compressive strengths of rock masses. Determined UCSs of rock masses were applied to the bearing capacity equations, to calculate the lower bound resistance. However, in some cases of bearing capacity equations, including the Horvath and Kenney (1979) and FHWA (1999) methods for shaft resistance, and Carter and Kulhawy (1988) method for base resistance, replacing the UCS of rock core with that of rock mass could not simulate the lower bound resistance of this equation.

8. In addition to the Hoek-Brown failure criteria (1988, 2002), the geological strength index (GSI) was also downgraded by 10 points, corresponding to a one-category downgrade of rock structure. Consequently, the lower bound could be calculated from application of the UCS of rock mass with the downgraded GSI to the bearing capacity equations, except for the Horvath and Kenney (1979) method for shaft resistance. Also, lower bounds using the downgraded GSI were more reasonable than lower bounds using only the UCS of rock mass. In the case of the Horvath and Kenney (1979) method for the shaft resistance,

even though the GSI downgrade was considered, it was impossible to calculate the physical lower bound of resistance by replacing the UCS of rock core with that of rock mass, and downgrading the GSI. The determined lower bound resistance ranged from 18~42% of the predicted resistance for the shaft resistance, 20~39% for the base resistance, and 21~40% for the total resistance.

9. Using the determined lower bound resistance, resistance factors were calibrated considering the lower bound for each resistance (shaft, base, and total resistance), and the bearing capacity equations. For each bearing capacity equation, the relationship between the ratio of lower bound to the predicted capacity with reliability index and resistance factor ratio were newly plotted. Consequently, resistance factors were increased by about 0~8% for the shaft resistance factor, 0~13% for the base resistance factor, and 0~2% for the total resistance factor. The calibrated resistance factors considering the lower bound resistance were determined as the following.

Resistance	Bearing capacity Equation	Resistance factor			Note
		β_T=2.5	β_T=3.0	β_T=3.5	AASHTO (2010)
Shaft resistance	Carter & Kulhawy (1988)	0.49 (8% ↑)	0.35 (8% ↑)	0.26 (8% ↑)	0.5
	Horvath & Kenney (1979)	0.42 (-)	0.30 (-)	0.30 (-)	0.55
	FHWA (1999)	0.44 (-)	0.32 (-)	0.24 (-)	0.55
	Rowe & Armitage (1987)	0.20 (4% ↑)	0.13 (4% ↑)	0.11 (4% ↑)	-
Base resistance	Carter & Kulhawy (1988)	0.36 (13% ↑)	0.27 (13% ↑)	0.24 (13% ↑)	0.5
	FHWA (1999)	0.25 (1% ↑)	0.19 (1% ↑)	0.17 (1% ↑)	0.5
	Zhang & Einstein (1998)	0.37 (-)	0.29 (-)	0.24 (-)	-
Total resistance	Carter & Kulhawy (1988)	0.58 (2% ↑)	0.43 (2% ↑)	0.31 (2% ↑)	-
	FHWA (1999)	0.40 (-)	0.28 (-)	0.22 (-)	-

References

AASHTO (1997), *AASHTO Standard Specifications for Highway Bridges,* 16th Edition (1996 with 1997 interim), AASHTO, Washington, DC.

AASHTO (2004), *AASHTO LRFD Bridge Design Specifications*, 3rd Edition, AASHTO, Washington, DC.

AASHTO (2007), *AASHTO LRFD Bridge Design Specifications*, 4th Edition, AASHTO, Washington, DC.

AASHTO (2010), *AASHTO LRFD Bridge Design Specifications*, 5th Edition, AASHTO, Washington, DC.

American Concrete Institute(ACI)(1996), *Building code requirements for structural concrete. ACI Manual of Concrete Practice Part 3: Use of concrete in Buildings – Design, Specifications, and Related Topics(ACI 318-95)*, ACI, Detroit.

ASCE (1997), *Standard Guidelines for the Design and Installation of Pile Foundations*, ASCE 20-96, ASCE

AUSTROADS (1992), *AUSTROADS Bridge Design Code*, National Office, AUSTROADS, Surry Hills, NSW, Australia

Barker, R. M., Duncan, J. M., Rojiani, K. B., Ooi, P. S. K., Tan, C. K., and Kim, S. G. (1991), *NCHRP Report 343: Manual for the Design of Bridge Foundations,* Transportation Research Board, Washington, D.C.

Brown, D. A., Turner, J. P., and Castelli, R. J. (2010), *Drilled Shafts: Construction Procedures and LRFD Design Methods, FHWA-NHI-10-01625*, Department of Transportation, Federal Highway Administration, U.S.

Canadian Geotechnical Society (2006), *Canadian Foundation Engineering Manual*, 4th edition, Bi-Tech Publishers, Ltd.

Canadian Standards Association (CAS) (2006), *Canadian Highway Bridge Design Code (CHBDC)*, CSA Standard S6-00, Rexdale, Ontario

Carter, J. P., and Kulhawy, F. H. (1988), *Analysis and design of drilled shaft foundations socketed into rock*, Report EL-5918, Electric Power Research Institute, Palo Alto, California

Fellenius, B. H. (1989), "Tangent modulus of piles determined from strain data", Foundation Engineering: Current Principles and Practices (GSP 22), ASCE, pp.500～510.

Fellenius, B. H. (2001), "From strain measurements to load in an instrumented

pile", Geotechnical News Magazine, Vol. 19, No. 1, pp.35～38.

Gilbert, R. B., S. S. Najjar, and Y. J. Choi (2005), "Incorporating lower-bound capacities into LRFD codes for pile foundations", Contemporary Issues in Foundation Engineering (GSP 22), ASCE, pp.1-17

Haldar, A. and Mahadevan, S. (2000), *Probability, Reliability and Statistical Methods in Engineering Design*, John Wiley & Sons, New York, NY.

Haldar, A. and Mahadevan, S. (2000), *Reliability Assessment using Stochastic Finite Element Analysis*, John Wiley & Sons, New York, NY.

Haldar, S. and Babu, G. L. S., (2008). "Load Resistance Factor Design of Axially Loaded Pile Based on Load Test Results" Journal of Geotechnical and Geonenvironmental Engineering,ASCE, Vol.134, No.8, pp.1106-1117.

Hansell, W. C. and Viest, I. M. (1971), "Load factor design for steel highway bridges", Engineering Journal, American Institute of Steel Construction, Vol.8, No.4, pp.113-123

Horvath, R. G. and Kenney, T. C. (1979), "Shaft resistance of rock-socketed drilled piers", Drilled shaft design and construction in Florida, Department of Civil Engineering, University of Florida, Gainesville.

Hoek, E. (1983), "Strength of jointed rock masses – 23rd Ranking Lecture",

Geotechnique, Vol. 33, No. 3, pp. 187-223

Hoek, E. and Brown, E. T. (1988), "The Hoek-Brown Failure Criterion – a 1988 Update", Proceeding of 15th Canadian Rock Mechanics Symposium, Toronto, Dept. Civil Engineering, University of Toronto, pp. 31-38.

Hoek, E. and Brown, E. T. (1997), "Practical estimates of rock mass strength" International Journal of Rock Mechanics and Mining Sciences, Vol. 34, No. 8, pp. 1165-1186.

Hoek, E., Carranza-Torres, C., and Corkum, B. (2002), "Hoek-Brown failure criterion-2002 edition", Proceedings of NARMS-Tac, pp. 267-273.

Jung, S. J. (2010), "Calibration of Resistance Factors of Load and Resistance Factor Design for Drilled Shafts Embedded in Weathered Rock", Ph. D. thesis, Seoul National University, Seoul, Korea.

Korean Geotechnical Society (2003), *Korea structure and foundation structure design specification* (in Korean)

Korea Institute of Construction Technology (KICT) (2008), *Determination of Resistance Factors for Foundation Structure Design by LRFD*, Research Policy/Infrastructure Development Program, Ministry of Land, Transport and Maritime Affairs, South Korea, 2008

Kulhawy, F. H, and Phoon, K. K (1996), “Engineering judgment in the evolution from deterministic to reliability base foundation design”, Proceedings of Uncertainty ’96, Uncertainty in the Geologic Environment - From Theory to Practice (GSP 58), ASCE, pp.29-48

Kwon, O. S (2004), “Effect of Rock Mass Weathering on Resistant Behavior of Drilled Shaft Socketed into Weathered Rock”, Ph. D. thesis, Seoul National University, Seoul, Korea.

Kwon, O. S., Choi, Y.K., Kwon, O.K., and Kim, M. M. (2005), “Comparison of the bidirectional load test with the top-down load test.” Transportation Research Record 1936, Transportation Research Board, Washington, DC, 108–116

Kwon, O. S., Choi, Y.K., Kwon, O. K., and Kim, M. M. (2006), “Method of Estimating Pile Load-displacement Curve Using Bi-directional Load Test”, Journal of the Korean Geotechnical Society, KSCE, Vol. 22, No.4, pp. 11-19.

Mcvay, M. C., Kuo, C. L. and Guisinger, A. L. (2003), “Calibration Resistance Factor in the Load and Resistance Factor Design of Statnamic Loading Test”, University of Florida

Ministry of Transportation (MOT) (1992), *Ontario Highway Bridge Design Code and Commentary*, Third edition, Ministry of Transportation Ontario, Downsview, Ontario.

Najjar, S. S. (2005), "The importance of lower-bound capacities in geotechnical reliability assessments", Ph. D. thesis, Univ. of Texas at Austin, Austin, Tex, U.S.

Najjar, S. S. (2009) , "Importance of Lower-Bound Capacities in the Design of Deep Foundations", Journal of Geotechnical and Geoenvironmental Engineering, ASCE, Vol.135, No. 7, pp. 890-900

Nowak, A. S.(1999), *NCHRP Report 368: Calibration of LRFD Bridge Design Code*, Transportation Research Board, Washington, D.C.

National Research Council of Canada (NRC) (2010), National Building Code of Canada, NRC, Ottawa, Canada.

Osterberg, J. O. (1998), "The Osterberg Load Test Method for Drilled Shafts and Driven Piles-The First Ten Years", Proceedings 7th International Conference on Deep Foundations, Vienna, pp. 1-11

O'Neill, M. W., and Reese, L. C. (1999), *Drilled Shafts: Construction Procedures and Design Methods, FHWA-IF-99-025*, Department of Transportation, Federal Highway Administration, U.S.

Paikowsky, S. G. (2004), *Load and Resistance Factor Design (LRFD) for Deep Foundations, NCHRP Report 24-17,* Transportation Research Board,

Washington, D.C.

Park, J. H. (2011), “Resistance Factor Calibration and Bayesian Implementation for LRFD of Axially-Loaded Driven Steel Pipe Piles”, Ph. D. thesis, Seoul National University, Seoul, Korea.

Rowe, R. K., and Armitage, H. H. (1984), “The design of piles socketed into weak rock”, Report GEOT-11-84, University of Western Ontario, London, 1984, pp.366

Rowe, R. K., and Armitage, H. H. (1987), “A design method for drilled piers in soft rock”, Canadian Geotechnical Journal, CGS, Vol.24, No.1, pp. 126-142.

Standard Association of Australia (SAA) (1995), *Australian Standard 2159: Piling-Design and Installation*, Homebysh, NSW

Turner, J. P (2006), *NCHRP Report 360: Rock-socketed shafts for highway structure foundations,* Transportation Research Board, Washington, D.C.

Withiam, J. L., E. P. Voytko, R. M. Barker, J. M. Duncan, B. C. Kelly, S. C. Musser and V. Elias (1998). *Load and Resistance Factor Design (LRFD) of Highway Bridge Sunstructures. FHWA Publication No. FHWA-HI-98-032*, Federal Highway Administration, Washington, D. C.

Wu, T., et al. (1989), “Reliability of Offshore Foundations-State of the Art”, Journal of Geotechnical Engineering, Vol.115, No.2, pp. 57-178

Yoon, H. J., Jung, S. J, and Kim, M. M.(2007). “Resistance Factors for Drilled Shafts Embedded in Weathered Rock”, Journal of the Korea Geotechnical Society, KSCE, Vol.23, No.8, pp.107-116.

Zhang, L., and Einstein, H. H. (1998), “End bearing capacity of drilled shafts in rock”, Journal of Geotechnical and Geoenvironmental Engineering, Vol.124, No.7, pp. 574-584.

초 록

최근 전세계적으로 지반구조물의 설계에 있어 하중저항계수설계법 (LRFD)이 허용응력설계법(ASD)을 대체하고 있는 추세이며, 이미 국내에서도 그 사용이 증가하고 있다. 하지만 AASHTO (2007, 2010)에서 제안하고 있는 저항계수는 기반암이 무결암인 북미의 실정에 적합하게 제안된 값이며, 기반암이 대부분 풍화암 또는 연암인 국내에 적용하는 것은 부적합하다. 또한, 저항계수 산정에 있어 사용되는 신뢰성 분석법으로 산정한 파괴확률은 지지력의 하한을 고려하지 않고 산정되었기 때문에 비현실적인 것으로 알려져 있다.

본 연구에서는 국내에서 수행된 13개의 하중전이 분석이 가능한 재하시험을 바탕으로 국내의 실정에 맞는 보다 정확한 저항계수를 산정하였다. 목표신뢰도지수는 AFOSM 방법을 이용하여 산정한 결과와 선행연구의 제안 값을 종합하여 2.5, 3.0, 그리고 3.5로 결정되었다. AASHTO (2010)에서 제안하고 있는 현장타설말뚝의 목표신뢰도지수인 3.0인 경우, 지지력 공식에 따라

주면 저항계수는 0.13-0.32, 선단 저항계수는 0.19-0.29, 그리고 전체 저항계수는 0.28-0.42의 범위를 가지는 것으로 산정되었다.

또한, 하한지지력을 고려하여 산정된 저항계수를 보정하였다. Hoek-Brown (2002) 파괴기준과 GSI를 감소시키는 방법을 통해 하한지지력을 산정하였으며, 이를 저항계수 보정에 사용하였다. 그 결과, 주면 저항계수는 약 0-8%, 선단 저항계수는 약 0-13%, 그리고 전체 저항계수는 0-2% 가량 증가하였다.

주요어: 하중저항계수설계법, 현장타설말뚝, 하중전이분석, 저항계수, 하한지지력

학 번: 2008-22974